University of Alberta

A critical role for Nup53 in the biogenesis of the nuclear pore complex and the nuclear envelope

by

Lisa Anne Hawryluk-Gara ©

A thesis submitted to the Faculty of Graduate Studies and Research
in partial fulfillment of the requirements for the degree of

Doctor of Philosophy

Department of Cell Biology

Edmonton, Alberta
Spring, 2008

Library and
Archives Canada

Published Heritage
Branch

395 Wellington Street
Ottawa ON K1A 0N4
Canada

Bibliothèque et
Archives Canada

Direction du
Patrimoine de l'édition

395, rue Wellington
Ottawa ON K1A 0N4
Canada

Your file Votre référence
ISBN: 978-0-494-45442-8
Our file Notre référence
ISBN: 978-0-494-45442-8

NOTICE:
The author has granted a non-exclusive license allowing Library and Archives Canada to reproduce, publish, archive, preserve, conserve, communicate to the public by telecommunication or on the Internet, loan, distribute and sell theses worldwide, for commercial or non-commercial purposes, in microform, paper, electronic and/or any other formats.

The author retains copyright ownership and moral rights in this thesis. Neither the thesis nor substantial extracts from it may be printed or otherwise reproduced without the author's permission.

AVIS:
L'auteur a accordé une licence non exclusive permettant à la Bibliothèque et Archives Canada de reproduire, publier, archiver, sauvegarder, conserver, transmettre au public par télécommunication ou par l'Internet, prêter, distribuer et vendre des thèses partout dans le monde, à des fins commerciales ou autres, sur support microforme, papier, électronique et/ou autres formats.

L'auteur conserve la propriété du droit d'auteur et des droits moraux qui protège cette thèse. Ni la thèse ni des extraits substantiels de celle-ci ne doivent être imprimés ou autrement reproduits sans son autorisation.

In compliance with the Canadian Privacy Act some supporting forms may have been removed from this thesis.

While these forms may be included in the document page count, their removal does not represent any loss of content from the thesis.

Conformément à la loi canadienne sur la protection de la vie privée, quelques formulaires secondaires ont été enlevés de cette thèse.

Bien que ces formulaires aient inclus dans la pagination, il n'y aura aucun contenu manquant.

Canada

Abstract

Nuclear pore complexes (NPCs) form channels across the otherwise impermeable nuclear envelope (NE) and provide the sole sites of macromolecular traffic between the nucleoplasm and the cytoplasm. NPCs are evolutionarily conserved, elaborate structures comprised of approximately 30 proteins termed nucleoporins (nups) that are each present in multiple copies and organized into sub-complexes of interacting nups. We have investigated the function of the conserved nup Nup53. Fractionation data suggest that Nup53 tightly associates with the NE membrane and the nuclear lamina. *In vitro* binding data demonstrate that Nup53 physically interacts with the nuclear lamina protein lamin B, a group of nups including Nup93, Nup155, and Nup205, and the transmembrane nup NDC1. Moreover, depletion of Nup53 using RNA interference causes a decrease in the cellular levels of Nup93, Nup155, and Nup205 strongly suggesting that Nup53 plays a critical role in NPC assembly. Our data are consistent with a model in which Nup53 may function as a bridge point between the NPC core and the pore membrane, a strategic location to influence NE and NPC biogenesis. In an effort to further understand the function of Nup53 in NE formation, we investigated the role of various regions of Nup53 in mediating its assembly into the NPC and interactions with neighboring nups, namely Nup93, Nup155, Nup205, and NDC1. We showed that Nup53 interacts with these nups through mutually exclusive regions and that each of these binding regions are sufficient to target Nup53 to the nuclear rim *in vivo*. Using this information, we employed the *Xenopus laevis* nuclear reconstitution assay to first determine the role of Nup53 in NPC formation, and then further to define the region of Nup53 and which of its interacting partners are required for this function. We found that Nup53 is required for both NPC

and NE assembly *in vivo* and that formation of a Nup53-Nup155 complex is critical for these processes. These data provide further evidence for the existence of a previously proposed NE and NPC assembly checkpoint that functions to inhibit NE vesicle fusion until NPC assembly occurs.

Dedication

Per la mia famiglia

Acknowledgements

I am deeply indebted to several individuals for their integral contributions to my research and the preparation of this thesis. Foremost of these is my supervisor, Rick Wozniak. Rick, I cannot begin to express my gratitude for your patience, guidance, and encouragement from my humble beginnings as an undergraduate student in your laboratory. In these past years, I have learned volumes about scientific theory and principles, research, and writing, and this is in no small part a result of your mentoring and dedication to science. I will greatly miss interacting with you and being a part of your research group, but look forward to our future correspondence.

It has been my pleasure to strive to a common goal with a group of budding young scientists who have been extraordinary characters, comrades, and friends. I would like to extend the most sincere thanks to Patrick Lusk, Andrea Anderson, Dave Van de Vosse, Jana Mitchell, and, of course, Rob Scott - I will never forget the science or the shenanigans. Patrick, thank you for recruiting me to this laboratory and contributing to my transformation into a "universal student", and for instilling the importance of broadening my horizons. Andrea Anderson, my fellow small town girl and "soul sister of science", many thanks for being a major contributor to the famous Wozniak lab photo wall that documents many memories which I will cherish always. Rob, thank you for the afternoon coffees and life/science talks, and for endorsing my "it's not where you live, it's how you live" philosophy. You all have truly been a second family to me. I thank you for your friendship and wish you continued success in the paths that you have chosen.

I would also like to thank my husband, Lorne Gara, my parents, Earl and Gabriella Hawryluk, and the remainder of my family for being an unwavering cheering section and source of inspiration all these many years of my education marathon. This accomplishment truly would not have been possible without you.

Finally, I acknowledge our collaborators cited in the body of this thesis and financial support from both the Alberta Heritage Foundation for Medical Research and the Canadian Institutes of Health Research.

Table of Contents

Chapter I: *Introduction* 1
1.1 Preface 2
1.2 The Nuclear Envelope 2
1.3 The Nuclear Pore Complex 4
1.3.1 Nucleoporins 6
1.4 Movement of molecules through the NPC 15
1.4.1 Karyopherins and signal sequences 15
1.4.2 Ran 17
1.4.3 Transport Models 19
1.5 NE Dynamics: Nuclear Disassembly 22
1.5.1 NEBD: The Vesiculation Model 25
1.5.2 NEBD: The Reabsorption Model 26
1.5.3 NEBD: Model Integration 26
1.5.4 Processes influencing NEBD 27
1.5.5 Mitotic fates of NE constituents 32
1.6 NE Dynamics: NE and NPC Formation 33
1.6.1 NE membrane formation 33
1.6.2 Post-mitotic NPC assembly 36
1.6.3 The Role of Ran in NE and NPC biogenesis 41
1.6.4 NPC assembly in intact membranes 42
1.7 Thesis Focus 43

Chapter II: *Experimental procedures* 45
2.1 *Xenopus* Nup53 antibody production 46
2.2 Nup93 and Nup53 plasmid construction 46
2.3 Purification of rat liver nuclei and nuclear envelopes 47
2.4 Extraction of purified nuclear envelopes 49
2.5 Purification of nup and nuclear lamina enriched fractions 49
2.6 Protein purification for pulldown and *in vitro* binding studies 50
2.7 GST-pulldown assays 51
2.8 Direct *in vitro* binding experiments 52
2.9 Protein staining procedures 52
2.10 Mass spectrometry identification 53
2.11 Sucrose gradient sedimentation 53
2.12 Transfections and isolation of stable lines 53
2.13 Isolation of HeLa cell extracts 54
2.14 Immunofluorescence 55
2.15 siRNAs for depletion of nups 56
2.16 RT-PCR 57
2.17 Western blotting 57
2.18 Cell cycle analysis in Nup53 depleted HeLa cells 58
2.19 *Xenopus* egg extract preparation 59

2.20 Depletion of Nup53 from *Xenopus* oocytes 60
2.21 Transmission Electron Microscopy 61
2.22 Analysis of Nup53 phosphorylation 62
2.23 *In vitro* binding experiments with ss- and dsDNA cellulose 64

Chapter III: *Vertebrate Nup53 interacts with the nuclear lamina and is required for the assembly of a Nup93-containing complex* 65
- 3.1 Overview 66
- 3.2 Results 67
  - 3.2.1 Characterization of a vertebrate counterpart to the yeast nucleoporin Nup53p 67
  - 3.2.2 Nup53 is tightly associated with the nuclear membrane and lamina 69
  - 3.2.3 Nup53 interacts with Nup93, Nup155, and Nup205 73
  - 3.2.4 Depletion of Nup53 inhibits the assembly of interacting nups and the spindle checkpoint protein Mad1 into the NPC 76
  - 3.2.5 Depletion of Nup53 or Nup93 leads to aberrant nuclear morphology 83
- 3.3 Discussion 83

Chapter IV: *Nup53 interacts with the transmembrane nup NDC1 and is required for nuclear envelope and nuclear pore complex assembly* 96
- 4.1 Overview 97
- 4.2 Results 98
  - 4.2.1 A Link between NDC1 and Nup53 Complex 98
  - 4.2.2 Mapping the interactions between Nup53 and neighbouring nups 101
  - 4.2.3 *In vivo* localization of Nup53 truncations 106
  - 4.2.4 Removal of Nup53 leads to a block in NPC formation and NE membrane fusion 110
  - 4.2.5 The Nup53-Nup155 interaction is required for nuclear envelope formation. 118
- 4.3 Discussion 124

Chapter V: *Perspectives* 131
- 5.1 Synopsis 132
- 5.2 Alternative NPC functions 132
- 5.3 Crystal structure of the NPC 134
- 5.4 Organization of Nup53 within the NE 135
- 5.5 The phosphorylation of Nup53 138
- 5.6 The conserved RNA recognition motif (RRM) of Nup53 140
- 5.7 Nup53 and the NE/NPC assembly checkpoint 141

Chapter VI: *References* 146
Chapter VII: *Appendix* 170

List of Figures

Figure 1-1. Schematic representation of a vertebrate NPC. 3

Figure 1-2. Schematic of NPC architecture 7

Figure 1-3. Schematic representation of nup subcomplex organization in yeast and metazoans. 13

Figure 1-4. Nucleocytoplasmic transport. 18

Figure 1-5. Nuclear envelope breakdown (NEBD). 24

Figure 3-1. Localization of endogenous Nup53 to the NPC. 68

Figure 3-2. Nup53 interacts tightly with the nuclear envelope membrane and lamina. .. 71

Figure 3-3. Identification of Nup53 interacting partners using *in vitro* binding assays. . 75

Figure 3-4. *In vivo* depletion of Nup53 using small interfering RNAs 77

Figure 3-5. HeLa cells depleted of Nup53 exhibit a growth delay 80

Figure 3-6. *In vivo* depletion of Nup53 leads to co-depletion of a subset of interacting nups and the mitotic checkpoint protein Mad1. 82

Figure 3-7. *In vivo* depletion of Nup93 and the identification Nup93 interacting partners using *in vitro* binding assays. 85

Figure 3-8. Sucrose gradient analysis of rat liver NE extracts. 89

Figure 3-9. Nup53 is accessible to specific antibodies in the presence and absence of the NE membrane. 90

Figure 4-1. NDC1 interacts with the Nup53 complex 100

Figure 4-2. Summary of human Nup53 truncation characterization 102

Figure 4-3. Nup53 domain interaction analysis using GST-pulldown assays 104

Figure 4-4. *In vivo* localization of EGFP-Nup53 truncations 108

Figure 4-5. Depletion of Nup53 from cytosol blocks formation of a closed NE 113

Figure 4-6. Depletion of Nup53 from cytosol blocks NPC assembly 116

Figure 4-7. Characterization of *in vitro* assembled nuclei 117

Figure 4-8. Nup53 fragments that interact with NDC1 or Nup93 alone are not sufficient to restore NE formation. 120

Figure 4-9. A Nup53 fragment that interacts with Nup155 is sufficient to restore NE formation 123

Figure 4-10. Analysis of Nup53-interacting nucleoporins.. 127

Figure 5-1. Model of conserved yeast and vertebrate Nup53 complexes. 136

Figure 5-2. Model representing the critical players linking NE and NPC assembly...... 142

Figure 5-3. Model for the Nup53-Nup155 interaction function in NE and NPC assembly. 145

Figure 7-1. The phosphorylation of human Nup53 173

Figure 7-2. Nup53 interacts with ss- and dsDNA... 175

Figure 7-3. Characterization of the Nup53 RRM. 177

List of Abbreviations

ATP	adenosine triphosphate
Da	Dalton
CIP	calf intestinal phosphatase
DMSO	dimethylsulphoxide
DNA	deoxyribonucleic acid
DNase	deoxyribonuclease
DTT	dithiothreitol
ECL	enhanced chemiluminescence
EM	electron microscopy
FEISEM	field emmision in lens scanning electron microscopy
Fig	Figure
FG	phenylalanine, glycine
g	gram
g	gravitational force
GAP	GTPase activating protein
GDP	guanosine diphosphate
GEF	guanosyl exchange factor
GFP	green fluorescent protein
GST	glutathione-S-transferase
GT	glutathione
GTP	guanosine triphosphate
GTPase	guanosine triphosphatase
h	hour(s)
HRP	horse radish peroxidase
INM	inner nuclear membrane
IPTG	isopropyl-β-D-thiogalactopyransoside
Kap	karyopherin
min	minute(s)
μ	micro
m	milli
M	Mitotic phase, moles per litre, Mega (1 x 10^6)
mRNA	messenger RNA
MT	microtubule
NE	nuclear envelope
NEBD	nuclear envelope breakdown
NEM	N-ethylmaleimide
NES	nuclear export signal
NLS	nuclear localization signal
Noc	nocodazole
NPC	nuclear pore complex
NSF	N-ethylmaleimide-sensitive factor
nup	nucleoporin
OD	optical density

ONM	outer nuclear membrane
ORF	open reading frame
PAGE	polyacrylamide gel electrophoresis
PCR	polymerase chain reaction
pH	-log[H+]
PM	pore membrane
PMSF	phenymethyl sulfonyl fluoride
Pom	pore membrane protein
RNA	ribonucleic acid
RNase	ribonuclease
RNAi	RNA interference
RNP	ribonucleoprotein
RT-PCR	reverse transcriptase polymerase chain reaction
SAC	spindle assembly checkpoint
SEM	scanning electron microscopy
siRNA	small interfering RNA
SDS	sodium dodecyl sulphate
snRNP	small nuclear RNP
SNARE	soluble NSF attachment protein receptor
TCA	trichoroacetic acid
TEA	triethanolamine
TEM	transmission electron microscopy
tRNA	transfer RNA
WGA	wheat germ agglutinin

Chapter I: *Introduction*

1.1 Preface

Eukaryotic cells contain a specialized membrane system termed the nuclear envelope (NE) that functions to provide a physical barrier between the nucleus and cytoplasm and compartmentalize their unique metabolic tasks. This separation of the chromatin and transcription machinery from the cytoplasmic translational machinery necessitates an intricate transport system that allows for both constitutive and regulated trafficking of macromolecules across the NE. Nuclear pore complexes (NPCs), together with soluble transport factors including a group of proteins termed karyopherins, provide the molecular tools for this transport system.

NPCs are the only known gateways across the NE. Apart from directly mediating macromolecular transport across the NE, these elaborate protein assemblies participate in a myriad of additional cellular functions, including the regulation of gene expression and chromosome segregration. Therefore, understanding how these structures are organized within the NE and how their assembly is coordinated with other cellular events is essential to broaden our understanding of how the NPC contributes to processes such as cell cycle progression and disease states linked to abnormal NPC function such as cancer and viral infection.

1.2 The Nuclear Envelope

The nuclear envelope (NE) is one of the defining characteristics of eukaryotic cells. It consists of two membrane bilayers and is defined by three morphologically distinct membrane regions (Fig. 1-1). The outer nuclear membrane (ONM) is continuous with the rough endoplasmic reticulum (ER) membrane system. Both contain a similar set of

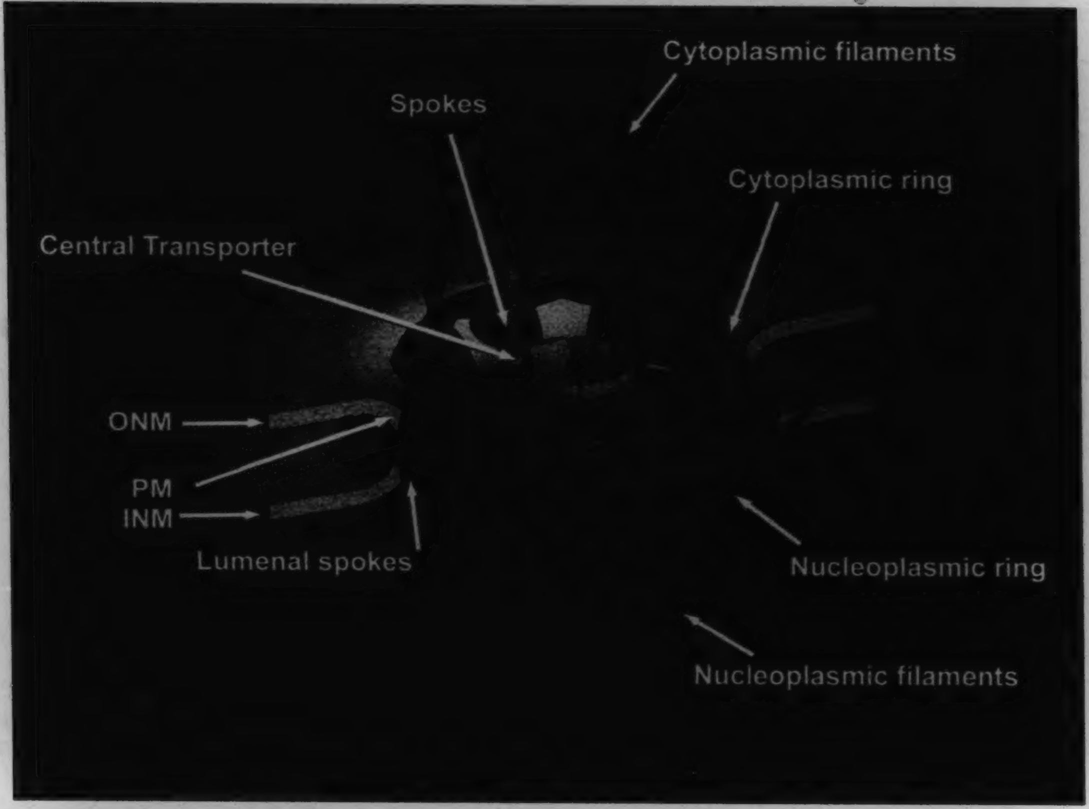
Cytoplasmic filaments
Spokes
Cytoplasmic ring
Central Transporter
ONM
PM
INM
Lumenal spokes
Nucleoplasmic ring
Nucleoplasmic filaments

Figure 1-1. Schematic representation of a vertebrate NPC.

A model of the NPC embedded in the nuclear envelope (NE, grey). Outer nuclear membrane (ONM), inner nuclear membrane (INM) and pore membrane (PM) are denoted. The NPC consists of a central core scaffold (light blue, magenta) on which the other NPC components are assembled. Extending from the core into the nucleus and cytosol are nucleoplasmic filaments (dark blue) and cytoplasmic filaments (red) where the latter surround a central transporter (pink). Modified from Rout and Aitchison, 2001.

proteins and are decorated with ribosomes (reviewed in Mattaj, 2004). The inner nuclear membrane (INM) lies adjacent to the nucleoplasm and contains integral membrane proteins unique to this membrane. In metazoans, it is these membrane proteins that, in part, mediate the interaction between the INM and chromatin. INM proteins also interact with a network of proteins termed lamins. This family of proteins can be divided into two classes, Lamin A/C and Lamin B. The lamin proteins are structurally related to the intermediate filament family of proteins and like their cytoplasmic counterparts, they form filaments. These filaments form a fibrous protein meshwork that is largely localized adjacent to the INM. Together with INM proteins, the nuclear lamina proteins are believed to mediate interactions between the INM and chromatin (Bridger et al., 2007; Foisner, 2001; Goldberg et al., 1999; Gruenbaum et al., 2003; 2005; Holmer and Worman, 2001; Worman and Courvalin, 2000; 2005). Finally, at numerous locations along the NE, the ONM and INM are interrupted by pores where the INM and the ONM are bridged by a connecting membrane termed the pore membrane domain (POM). Within these transcisternal pores reside the nuclear pore complexes (NPCs) (Fig. 1-1).

1.3 The Nuclear Pore Complex

NPCs are the sole sites of both passive diffusion of small ions and metabolites and selective or active transport of large macromolecules across an otherwise impermeable NE. The NPC is a massive structure. Early studies have estimated that these supramolecular protein assemblies are approximately 72 MDa in vertebrates and yeast (Reichelt et al., 1990; Rout et al., 2000). These size estimates are based both on ultrastructural analysis (see below) and recent proteomic and comparative analyses of the relative abundance of NPC components, referred to as nucleoporins, or nups (Cronshaw et al., 2002; Rout et al., 2000). The extent of our current understanding of NPC three-dimensional architecture is a direct result of various ultrastructural analyses of NEs derived from yeast, *Xenopus* oocytes, and, in case of the slime mould *Dictyostelium,* intact and transport-competent nuclei (Akey and Radermacher, 1993; Beck et al., 2004; Hinshaw et al., 1992; Jarnik and Aebi, 1991; Kiseleva et al., 2001; Reichelt et al., 1990; Stoffler et al., 2003; Yang et al., 1998). From these studies, a picture has emerged revealing a central core that is embedded in the NE membrane. The central core structure bears striking two-fold symmetry in a plane that is parellel to the NE and eight-fold rotational symmetry about an axis perpendicular to the NE and passing through the center of the NPC. Cytoplasmic and nuclear rings, together with the luminal spoke ring comprise the membrane-spanning central framework thought to anchor the NPC in the NE. This structure encircles a central channel. Interestingly, using cryoelectron tomography techniques that allow for visualization of NPCs at 8 nm resolution, Beck and colleagues (2004) were able to observe cargo in transit through the central channel. Extending into both the nucleoplasm and cytoplasm are an ornate arrangement of peripheral fibrils that are anchored to the core. Emanating from the central core into the cytoplasm are the flexible cytoplasmic fibrils that are believed to serve as docking sites for import cargoes. In contrast, extending into the nuclear interior from the central core, the nuclear filaments culminate in a more structured basket-like conformation, terminating at the distal ring.

1.3.1 Nucleoporins

The building blocks of NPCs are proteins termed nucleoporins, or nups. Proteomic analyses of both yeast and rat NPC-enriched fractions have revealed that, given its apparent molecular mass, an NPC is comprised of relatively few nups (~30), (Cronshaw et al., 2002; Rout et al., 2000). In many cases these nups are organized into modules of interacting nups that are well conserved in both composition and function (reviewed in Tran and Wente, 2006 and 1.3.1.4). Recent computational and biochemical approaches aimed at understanding the structure of nups have lead to their broad classification into three categories (Devos et al., 2006 and Fig. 1-2). The first consists of those nups that span the pore membrane and are referred to as pore membrane proteins, or poms. A more peripherally localized set of nups that contain a repetitive motif consisting of phenylalanine (F) and glycine (G) amino acid residues (termed FG-nups), comprise the second group. Finally, the third group consists of those nups that largely lack FG-repeats (termed non-FG nups) and form the central scaffold, or core structure of the NPC.

1.3.1.1 Transmembrane nups/Poms

The transmembrane nups, also referred to as poms, contain transmembrane helical stretches of fifteen to thirty residues that anchor them into the membrane (Devos et al., 2006; Mansfeld et al., 2006; Rout et al., 2000; Winey et al., 1993; Wozniak et al., 1989; 1992; 1994). To date, there are three poms that have been identified in association with NPCs: Pom152p, Ndc1p, and Pom34p in yeast, and POM121, NDC1, and gp210 in

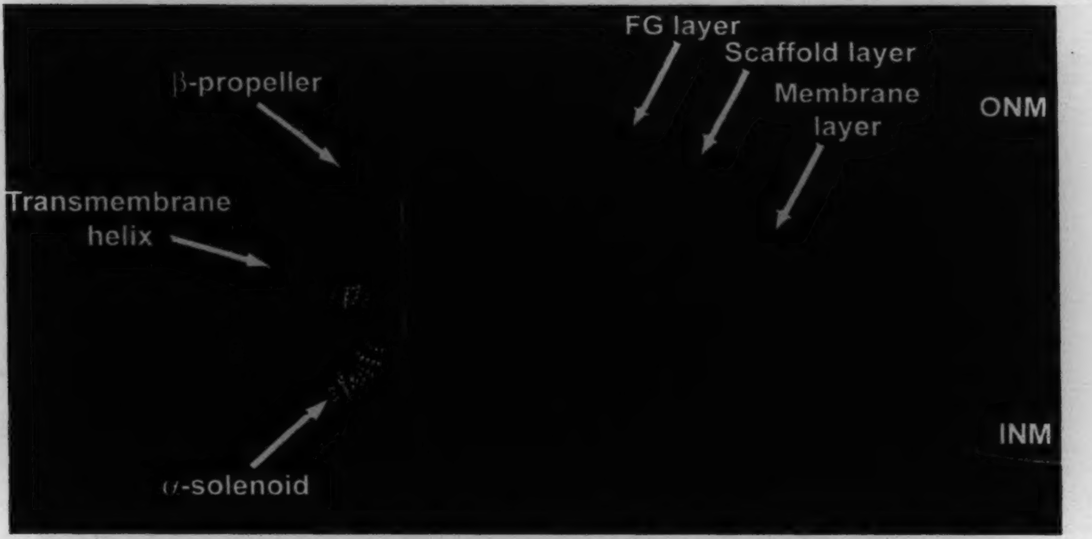
FG layer
Scaffold layer
β-propeller
Membrane layer
ONM
Transmembrane helix
INM
α-solenoid

Figure 1-2. Schematic of NPC architecture.

Summary of computational and biochemical characterization of yeast and vertebrate nup structure. Folds were assigned for ~95% of all nup polypeptides. Viewed in the plane of the NE, nups are segregated into one of the following groups; the membrane (red), scaffold (blue), and FG (green) layers. Examples of domain fold types assigned to the membrane (transmembrane helix) and scaffold (β-propeller, α-solenoid) groups are indicated on the left. The remaining fold types characterized in this analysis are not depicted. Adapted from Devos et al., 2006.

metazoans (Chial et al., 1998; Gerace et al., 1982; Hallberg et al., 1993; Mansfeld et al., 2006; Rout et al., 2000; Wozniak et al., 1989). While a majority of the peripheral nups are conserved in either structure or function (see 1.3.1.4), evolutionary relationships between the poms are, for the most part, less clear. For example, Pom152p and the known vertebrate poms share no significant sequence homology with the exception of a twenty one amino acid stretch of Pom152p that shares fourty three percent similarity to POM121 (Wozniak et al., 1994). However, there have been proposed structural similarities between the luminal domain of gp210 and Pom152p (Devos et al., 2004). Likewise, vertebrate and yeast NDC1 are only marginally similar in the primary sequence of their carboxy termini but share a similar topology (Mansfeld et al., 2006). Finally, homology searches have failed to uncover orthologs of Pom34 (Miao et al., 2006; Rout et al., 2000).

Regardless of the perplexing lack of clear evolutionary similarity between the poms, their ability to traverse the NE membrane has long been viewed to reflect roles for these proteins in anchoring the NPC to the pore membrane. The poms have been proposed to perform essential roles in the process of NPC and NE biogenesis (Gerace et al., 1982; Wozniak et al., 1989). This will be discussed in greater detail in section 1.6.2.3.

1.3.1.2 FG nups

Approximately one third of all the nups contain FG repeats (Cronshaw et al., 2002; Rout et al., 2000). This motif is generally present within the context of four amino acid residue stretches with sequences of FxFG, GLFG, SxFG, or PxFG. Individual FG-nups have between four and fourty eight different FG repeats (Zeitler and Weis, 2004). Moreover, the FG-nups believed to adopt natively unfolded conformations (Denning et al., 2003; Denning et al., 2002).

Several groups have previously reported a differential localization of FG nups within the NPC, and further classified them into three groups: those that are associated largely with either the nuclear or cytoplasmic faces of the NPC, and those symmetrically positioned on both faces of the NPC. Of note, it appears that the cytoplasmic fibrils and nuclear basket are comprised of FG-nups (Rout et al., 2000; Stoffler et al., 1999; Suntharalingam and Wente, 2003; Vasu and Forbes, 2001). In vertebrates, the FG-nups CAN/Nup214 and Nup358/RANBP2 localize exclusively to the cytoplasmic fibrils (Fornerod et al., 1997; Wu et al., 1995) while Nup153 is localized at the nuclear basket (Krull et al., 2004; Sukegawa and Blobel, 1993). In contrast, several FG-nups including the Nup62, Nup58, Nup45, and Nup54 are detected on both sides of the NPC in close proximity to the mid-plane of the NPC (Guan et al., 1995). This has lead to the hypothesis that the FG-nups line the entire translocation channel where they would be positioned to mediate translocation of transport factor-cargo complexes through the NPC. Consistent with this idea, the FG-repeats have been shown to provide specific interaction interfaces for transport factors both *in vitro* and *in vivo* (reviewed in Ryan and Wente, 2000). This is exemplified by X-ray crystallography analysis that mapped direct contact points between the FG-repeats of FxFG and GLFG peptides and the Kap-β1 backbone (Bayliss et al., 2000; Bayliss et al., 2002).

The FG-repeats of the FG-nups provide multiple potential binding sites for kap-cargo complexes per NPC (Rout et al., 2000; Strawn et al., 2004). Earlier work in yeast has revealed a degree of functional redundancy between the FG-nups in transport (Fabre et al., 1995; Iovine and Wente, 1997). More recently, a systematic analysis aimed at understanding relationships between the FG-nups yielded surprising findings (Strawn et al., 2004). Surprisingly, deletion of up to half of the total mass of FG-repeats was tolerable without significantly impairing nuclear import or cell viability. Furthermore, FG-repeats mapping to those FG-nups that were asymmetrically localized were found to be dispensible for essential transport pathways. These data shed new light on interpretations of the previously suggested nuclear transport models described in 1.4.3.

1.3.1.3 Non-FG-Nups

As their name implies, the non-FG-nups lack the amino acid residue repeats found in the FG-nups. However, many members of this group are predicted to share structural features. These include the presence of NH_2-terminal β-propeller and COOH-terminal α-solenoid domains, either singly or in combination (Berke et al., 2004; Devos et al., 2004; 2006). In certain cases, these proposed structural features have been confirmed by X-ray crystallography. For example, the solved crystal structure of the NH_2-terminus of Nup133, a member of the Nup107-160 complex, revealed the presence of a seven-blade β-propeller (Berke et al., 2004). In addition, Nup155, a member of the Nup53 complex (Chapter III), has also been predicted to contain both β-propeller and α-solenoid domains. Intriguingly, the structural features of these nups are similar to those found in proteins comprising the major types of vesicle coating complexes utilized in the secretory pathway, including members the clathrin complex, which forms coat-like structures on membranes (reviewed in Kirchhausen, 2000a; 2000b; Boehm and Bonifacino 2001;

Bonifacino and Lippincott-Schwartz, 2003; Lippincott-Schwartz and Liu 2003). This led to the proposal that non-FG nups may function like coat proteins at the pore membrane and contribute to the stabilization of membrane curvature (Devos et al., 2004; 2006).

Consistent with this notion, the non-FG nups have further been proposed to act as a structural scaffold, serving as anchoring points between the transmembrane nups and the FG-nups lining the central channel (Berke et al., 2004; Devos et al., 2006; Suntharalingam and Wente, 2003; see Fig.1-3). In further support of a key structural role of these nups are data from Rabut et al. (2004) examining NPC residence times of several GFP-labelled nups. In this study, members of the Nup107-160 complex were very stably associated with the NPC compared to others. In light of these observations, it is not surprising that this subcomplex of nups, together with others, have been implicated in having central roles in NPC assembly. This will be discussed at greater length in 1.6.2.1.

1.3.1.4 Organization and conservation of the NPC

Much of our understanding of nup organization within the NPC originated from immunolocalization analysis of isolated yeast NEs (Hurwitz et al., 1998; Kraemer et al., 1995; Marelli et al., 1998; Nehrbass et al., 1996; Rout et al., 2000; Strambio-de-Castillia et al., 1999; Wente et al., 1992; 1993; 1994). Nups were found to be either symmetrically distributed on both sides of the NPC, or preferentially associated with either the nuclear or cytoplasmic face of the NPC. It is noteworthy that a similar comprehensive list of spatial NPC localization of vertebrate nups has not been compiled. Only certain nups have been localized by immunoelectron microscopy (Krull et al., 2004;

Pante et al., 1994; Radu et al., 1993; 1994) but the remainder of the localizations have been inferred based on nup homology. This differential localization of nups within the NPC, together with the idea they exist in multiple copies per NPC, is consistent with a model in which nups or subcomplexes of nups contribute to distinct structural components of the NPC. For example, both the yeast Nup159p/Nup82p and its vertebrate counterpart the Nup214/Nup88 complex are preferentially localized to the cytoplasmic face indicating that they are components of the cytoplasmic fibrils (Bastos et al., 1997; Kraemer et al., 1994; Pante et al., 1994, Rout et al., 2000). The central scaffold of the NPC predominantly consists of two conserved nup complexes. The first is the Nup53 complex. In yeast this complex of nups consists of Nup53p, Nup59p, Nup170p, and Nup157p (Marelli et al., 1998) and in metazoans it is comprised of Nup53, Nup155, Nup93, and Nup205 (Chapter III). The second is the homologous yeast Nup84p and vertebrate Nup107-160 complexes (Krull et al., 2004; Pante et al., 1994; Rout et al., 2000). Finally Nup153 and Tpr contribute to the nucleoplasmic ring and fibrils in vertebrate cells (Krull et al., 2004) and an analogous contribution is made by Nup1p, Nup60p and Mlp1p/Mlp2p in yeast (Rout et al., 2000).

Approximately two thirds of the nups have a remarkably high degree of either structural or functional conservation between yeast and vertebrates (Tran and Wente, 2006 and Fig. 1-3). In many cases the protein sequences have varying levels of identity or similarity between the species (Cronshaw et al., 2002; Stoffler et al., 1999; Suntharalingam and Wente, 2003; Vasu and Forbes, 2001). Regardless of this variability, orthologs have been defined based on spatial NPC localization, commonality of subcomplex interactions, or, in a few cases, cross-species functional complementation.

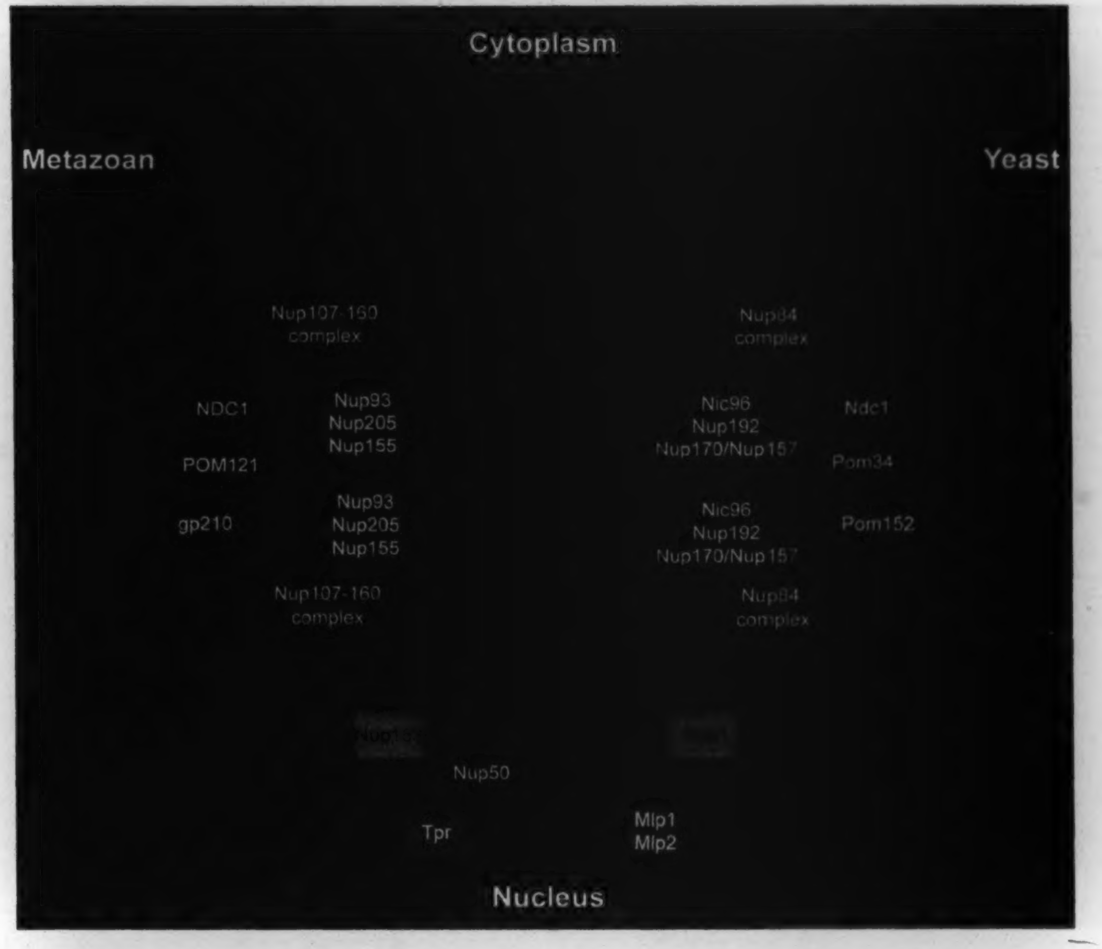
Cytoplasm
Metazoan
Yeast
Nup107-160 complex
Nup84 complex
NDC1
Nup93
Nup205
Nup155
Nic96
Nup192
Nup170/Nup157
Ndc1
POM121
Pom34
gp210
Nup93
Nup205
Nup155
Nic96
Nup192
Nup170/Nup157
Pom152
Nup107-160 complex
Nup84 complex
Nup50
Tpr
Mlp1
Mlp2
Nucleus

Figure 1-3. Schematic representation of nup subcomplex organization in yeast and metazoans.

Cross-sectional model of the NPC perpendicular to the plane of the nuclear envelope. Nups and, in certain cases, nup subcomplexes that are either symmetrically or asymmetrically localized are denoted by colored boxes. Transmembrane nups are depicted as red spheres. Blue and green rectangles denote nups or nup subcomplexes that comprise the scaffold and FG layers, respectively. Based on either primary sequence similiarity or functional relationships, orthologous nups/subcomplexes are represented in matching colors. FG-nups are indicated in black text. Note that not all nups are represented and localizations are based on estimations. Adapted from Powers and Dasso, 2003; Schwartz, 2005.

For example, all three of these criteria have established yeast Nup170p as the homolog of vertebrate Nup155 (Aitchison et al., 1995).

In both yeast and vertebrates, most nups belong to subcomplexes of interacting nups. These interacting modules construct the NPC, contributing to its characteristic eight-fold symmetry (Vasu and Forbes, 2001; Cronshaw et al., 2002; Suntharalingam and Wente, 2003). A notable example of subcomplex conservation is the *S. cerevisiae* Nup84p complex comprised of Seh1p, Sec13p, Nup84p, Nup85p, Nup120p, Nup133p, and Nup145Cp whose vertebrate counterparts comprising the corresponding Nup107-160 complex are Sec131, Sec13R, Nup107, Nup75, Nup160, Nup133, and Nup96 respectively (Siniossoglou et al., 1996; Fontoura et al., 1999; Siniossoglou et al., 2000; Cronshaw et al., 2002; Lutzmann et al., 2002; Boehmer et al., 2003; Harel et al., 2003; Walther et al., 2003). In vertebrates, the complex also contains Nup37 and Nup43, which appear to be specific to higher eukaryotes (Loiodice et al., 2004). Interestingly, the yeast Nup84p complex has been reconstituted *in vitro* from purified recombinant proteins and was imaged in a "Y" configuration by EM (Siniossoglou et al., 2000; Lutzmann et al., 2002). The similarity in the composition of the Nup84p/Nup107-160 complexes suggests that they have conserved functional roles. Indeed, both the Nup84p and vertebrate Nup107-160 complexes are believed to contribute to the central scaffold of the NPC (Alber et al., 2007; Allen et al., 2002; Belgareh et al., 2001; Harel et al., 2003 and section 1.3.1.4) and are essential for proper NPC assembly (Siniossoglou et al., 1996; 2000; Boehmer et al., 2003; Walther et al., 2003; Harel et al., 2003 and 1.6.2.1). Another example of structural and functional conservation of a nup subcomplex is detailed in

Chapters III and IV where the functional characterization of the conserved nup Nup53 is presented.

1.4 Movement of molecules through the NPC

The NPC acts as an aqueous diffusion channel for molecules that are less than 9 nm in diameter, including ions, metabolites, and other small molecules. However, most macromolecules such as mRNAs, tRNAs, ribosomal subunits, snRNPs, and most soluble proteins are transported through the NPC using an intricate transport system. This process requires a nuclear localization signal (NLS) or nuclear export signal (NES) on the cargo molecule, soluble transport factors that facilitate cargo movement through the NPC, and energy. Those molecules that recognize the NLS and NES also interact with the NPC to mediate the movement of the cargo/carrier complex through the NPC. Many of these carrier proteins are members of a family of structurally related proteins, termed karyopherins. Karyopherin-mediated bi-directional translocation of cargoes has been extensively studied over the years and will be reviewed in the following sections.

1.4.1 Karyopherins and signal sequences

Karyopherins, or kaps, also termed importins and exportins, belong to a family of structurally related proteins. There are 14 members of this family in yeast, and upwards of 20 in metazoans that function as either importers or exporters, or, in one observed case, bidirectionally (Wozniak et al., 1988, Gorlich and Kutay, 1999, Strom and Weis, 2001; Macara, 2001; Fried and Kutay, 2003; Yoshida and Blobel, 2001). This family is further categorized into two groups known as α-kaps (or α-importins) and β-kaps (or β-importins). Fundamentally, the difference between these two groups lies in their mode of interaction with signal-containing cargoes. The α-kaps can be considered as adaptor molecules that bridge interactions between a β-kap and cargo. Cargoes are recognized and bound directly by β-kaps, and this mode of transport can account for the majority of traffic across the NPC (Macara, 2001; Fried and Kutay, 2003).

Members of the β-kap family have relatively low similarity at the sequence level, with the exception of their NH_2-terminal regions responsible for interacting with the small GTPase, Ran (see 1.4.2). Nonetheless, they appear to adopt a similar overall structure (Wozniak et al., 1998; Gorlich and Kutay, 1999; Fried and Kutay, 2003), that include the presence of HEAT repeats, which are ~40 amino acids stretches that arrange into two α-helices and are adjoined by a short linker region (Fried and Kutay, 2003; Conti et al., 2006). Highlighting the structural similari[illegible] are elegant X-ray crystallography studies of Kap-β1 and Kap-β2 alone (Lee et al., 2000), in complex with cargo (Cingolani et al., 1999), with Ran-GTP (Chook and Blobel, 1999), and with an FG-repeat peptide (Bayliss et al., 2000). Overall, these analyses revealed that Ran and cargo binding surfaces were positioned at the interior binding pocket created by the tertiary structure of the HEAT repeats, while the FG-repeat binding interfaces lied on the outer surface (references above and Weis, 2003). Moreover, they imply a significant degree of flexibility of these molecules perhaps indicative of the ability of kaps to interact with multiple components of the transport machinery (Fried and Kutay, 2003).

Karyopherins identify their substrates through their recognition of signal sequences present within the cargoes. These are categorized based on their final cellular locale and referred to as nuclear localization or nuclear export signals (NLS, NES respectively). Whereas the bulk of these signals do not conform to a specific consensus sequence, the classical NLS binding specifically to Kapβ1/Kapα serves as an example of unique signal sequences binding to unique kaps (Fried and Kutay, 2003). This not only appears to reflect an extent of functional redundancy between the kaps, but also hints that there are distinct transport pathways across the pore.

1.4.2 Ran

Together with Kaps and NPCs, certain transport processes require the activity of the small GTPase Ran, a member of the Ras-superfamily (Gorlich and Kutay, 1999; Macara, 2001; Weis, 2003; Fried and Kutay, 2003). Similar to other members of this group, Ran switches between GDP- and GTP-bound states and this cycling provides the only known source of energy for transport (see below). Initial clues to the role of Ran in transport were provided by the observed compartmentalization of its regulators. Ran is a predominantly nuclear protein. Here it is maintained in a GTP-bound state by the chromatin associated guanine-nucleotide-exchange factor (GEF) termed RCC1 (Ohtsubo et al., 1989; Bishoff and Ponstingl, 1991; Nemergut et al., 2001). Conversely, Ran which enters the cytoplasm is converted to the GDP-bound form through the action of its GTPase-activating protein, RanGAP, which is present both in the cytoplasm and in association with the NPC through its interaction with Nup358/RanBP2 (Matunis et al., 1996; Mahajan et al., 1997; Saitoh et al., 1997).

The distribution of RanGAP and RCC1 in the cytoplasm and nucleoplasm, respectively, results in a gradient of RanGTP across the NPC offering an attractive model that would explain the directionality of transport. There is compelling evidence that this

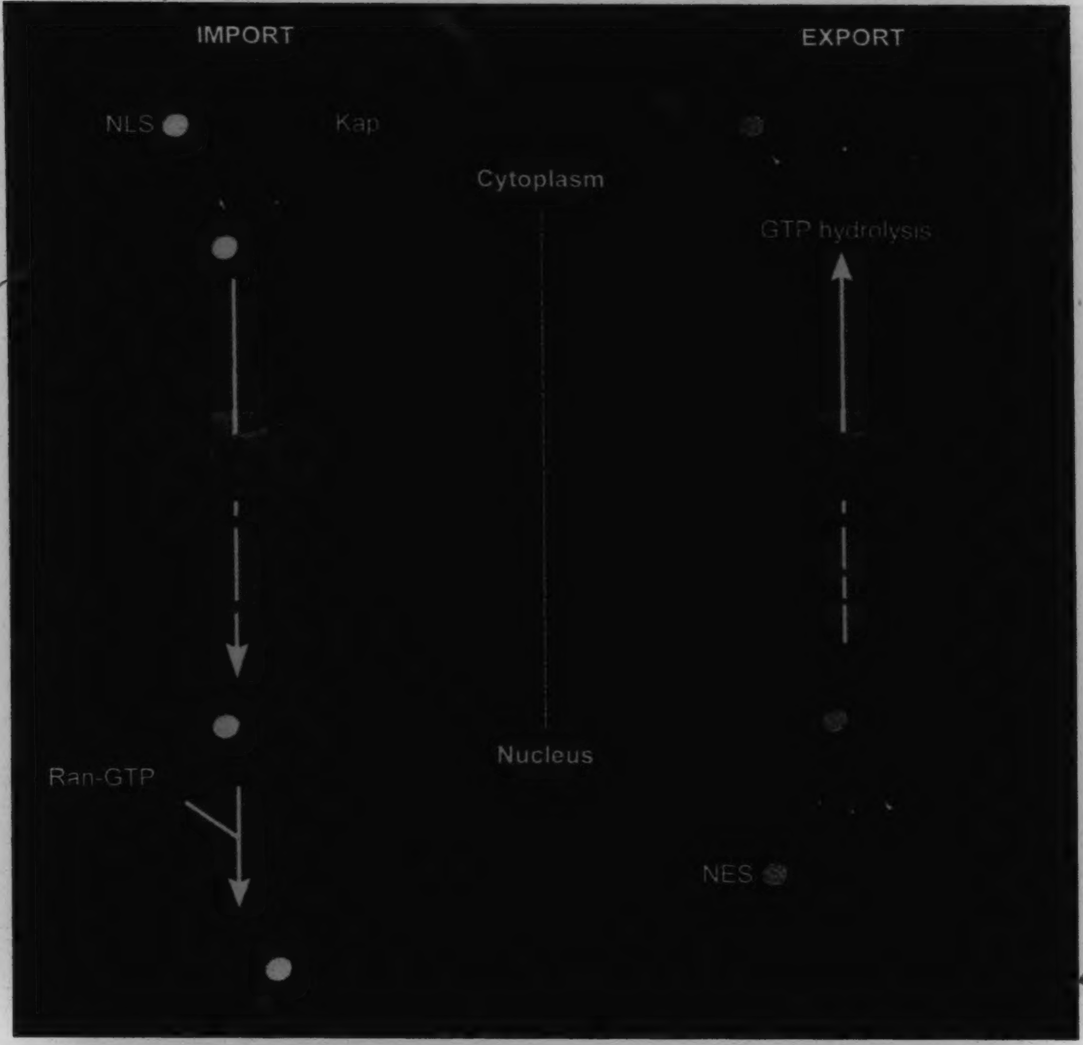
IMPORT
EXPORT
NLS
Kap
Cytoplasm
GTP hydrolysis
Nucleus
Ran-GTP
NES

Figure 1-4. Nucleocytoplasmic transport.

Representation of the steps of karyopherin-mediated nuclear transport. In import, a NLS-containing cargo (yellow) is recognized by an import karyopherin (green) in the cytoplasm. This complex docks at the NPC, and translocates to the nucleoplasm. Ran-GTP, which is present in high concentrations in this compartment, binds to the kap and releases the cargo. An export kap (grey) binds to an export cargo containing an NES (pink) in the presence of Ran-GTP. Following translocation to the cytoplasm, GTP hydrolysis results in dissociation of the cargo from the kap.

gradient functions by mediating either the assembly or disassembly of transport complexes in the correct compartments (Gorlich and Kutay, 1999; Macara, 2001; Weis, 2003; Fried and Kutay, 2003 and Fig. 1-4). For example, stable interactions between a kap and NLS-containing cargo are favoured in the Ran-GDP rich environment of the cytoplasm. Once this import complex reaches the Ran-GTP rich nucleoplasm upon nuclear import, Ran-GTP itself binds to the kap and displaces the cargo in its destination compartment (Gorlich and Kutay, 1999; Macara, 2001; Weis, 2003; Fried and Kutay, 2003 and Fig.1-4). Correspondingly, an export complex consisting of a kap, NES-containing cargo, and Ran-GTP would be disassembled upon encountering Ran-GAP on the cytoplasmic face of the NPC. Experiments aimed at understanding energy requirements of transport steps have revealed that a single import event is not dependent on GTP hydrolysis (Schwoebel et al.,1998; Englmeier et al., 1999; Ribbeck et al., 1999). Regardless, nuclear transport requires energy. Kap recycling to the cytoplasm for subsequent rounds of import and export events results in this energy requirement (Kose et al., 1997; 1999; Schwoebel et al., 2002).

It is noteworthy that, apart from nuclear transport, Ran has been implicated in other key cellular processes. As an example, the role of Ran in NE and NPC biogenesis will be discussed in section 1.6.3.

1.4.3 Transport Models

The nuclear transport machinery has been well characterized. From this body of work, a basic framework has emerged and there are generally accepted principles for mechanisms governing nucleocytoplasmic exchange. Among these are the ideas that the

FG-nups, through their ability to bind kaps both directly and specifically, and their tendency to be highly unstructured or natively unfolded, play a central role in translocation through the NPC. Precisely how these FG-nups contribute to the selective permeability of the NPC and a detailed explanation of how they mediate this movement have been a manner of intense debate. In this regard, a number of models have been proposed that will next be described.

1.4.2.1 The Selective Phase

Ribbeck and Gorlich (2001, 2002) proposed the selective phase model which predicts that the FG nups, through their enrichment at the interior of the central channel and by nature of their natively unfolded state, form a hydrophobic FG-interaction meshwork. A prediction of this model is that the central channel acts as a molecular sieve where the size of the holes in the meshwork imparts an exclusion limit. Diffusion of small molecules is suggested to occur through these holes. Conversely, large molecules are excluded. Kaps, through their unique ability to interact with FG-repeats, would locally disrupt this hydrophobic meshwork of interactions and partition into the channel. Compelling evidence for the existence of this meshwork was provided in a study by Frey et al. (2006) who found that the yeast Nsp1p FG domain was capable of forming an elastic hydrogel *in vitro*. Importantly, this gel was shown to recapitulate the permeability barrier properties, providing evidence for this model (Frey et al., 2007). This model does not explain, however, how Kap-cargo complexes would progressively traverse the channel once it was able to partition into it (Bickel and Bruinsma, 2002).

Along the same lines as the selective phase model is the oily spaghetti model (Macara, 2001) in which it is thought that NPC is in fact an open structure where the FG-repeats of nups surround and extend into the diffusion channel. Upon entry into the transport channel, these FG-repeats would effectively be displaced by transport complexes. Indeed, atomic force microscopy studies have recently shown that FG-repeats can extend or collapse (Lim et al., 2006), providing evidence for previous suggestions that FG-nups act like polymer brushes.

1.4.2.2 The Virtual Gate

This model relies on the previously reported distribution of the FG nups along with their natively unfolded disordered states (Denning et al., 2003; Denning et al., 2002; Patel et al., 2007; Rout et al., 2000). It proposes that asymmetric FG nups filaments effectively sweep away molecules that cannot interact with them and symmetric FG nups block the opening to the channel. Together, the FG nups impart an entropic barrier nature to the NPC. This barrier is overcome by FG-nup mediated tethering of Kap-cargo complexes to the NPC and subsequent movement through the NPC would involve Brownian motion (Rout et al., 2000, Rout et al., 2003).

1.4.2.3 The Affinity Gradient

Unlike the previous models, the affinity gradient model attempts to explain how kap-cargo complexes would move through the NPC once they dock there. It is also based largely on the asymmetrical distribution of FG-nups on the nuclear and cytoplasmic faces of the NPC (Rout et al., 2000), in combination with observations that the affinity of kaps with particular FG-nups increases from the cytoplasmic filaments to the nuclear basket (Ben-Efraim and Gerace, 2001; Pyhtila and Rexach, 2003). The filamentous extensions serve as initial docking sites for Kap-cargo complexes in transit. It is these initial interactions that would increase the residence time of transport complexes, thereby increasing the probability that they would enter the channel. Once in the channel, transport complex are pulled through by an increasing affinity of the kaps for the nups along the way.

1.5 NE Dynamics: Nuclear Disassembly

While critical for the maintenance of nuclear integrity, normal cell physiology dictates that the NE is also highly dynamic. In higher eukaryotes, during cell division, the mitotic spindle must gain access to the duplicated and condensed chromosomes. To overcome the physical barrier provided by the NE, the NE becomes completely dispersed in pro-metaphase of the cell cycle, through a process termed nuclear envelope breakdown (NEBD) (Fig. 1-5). During telophase, the dispersed NE components are then recycled to form a nucleus within each daughter cell. Nuclear growth, which occurs throughout interphase of metazoan and yeast cells, demands that the NE is continually remodelled. These complex NE dynamics are under spatial and temporal control and involve interactions with microtubules, chromatin, and a variety of cell-cycle regulatory molecules (Aitchison and Rout, 2002; Burke and Ellenberg, 2002; Hetzer et al., 2005; Salina et al., 2001).

Figure 1-5. Nuclear envelope breakdown (NEBD).
Cross-sectional representation of a mammalian cell nucleus depicting chromosomes (purple), nuclear lamina (green), nuclear membranes (yellow), microtubules (red), and centrosomes (orange). During interphase, chromosomes are decondensed and surrounded by the nuclear lamina and a continuous NE. In prophase, in close proximity to the centrosomes, folds in the NE may be observed along with chromosome condensation. Microtubule motor protein generated pulling forces result in NE stretching opposite the centrosome. As NEBD continues, NE tension results in a tear of the lamina and NE (white oval) and structural collapse of the nucleus. In prometaphase, fragments of the NE are observed, and remain attached to condensed chromosomes. During metaphase, chromosomes position and align along an axis between the mitotic centrosomes known as the metaphase plate. Adapted from Burke and Ellenberg, 2002.

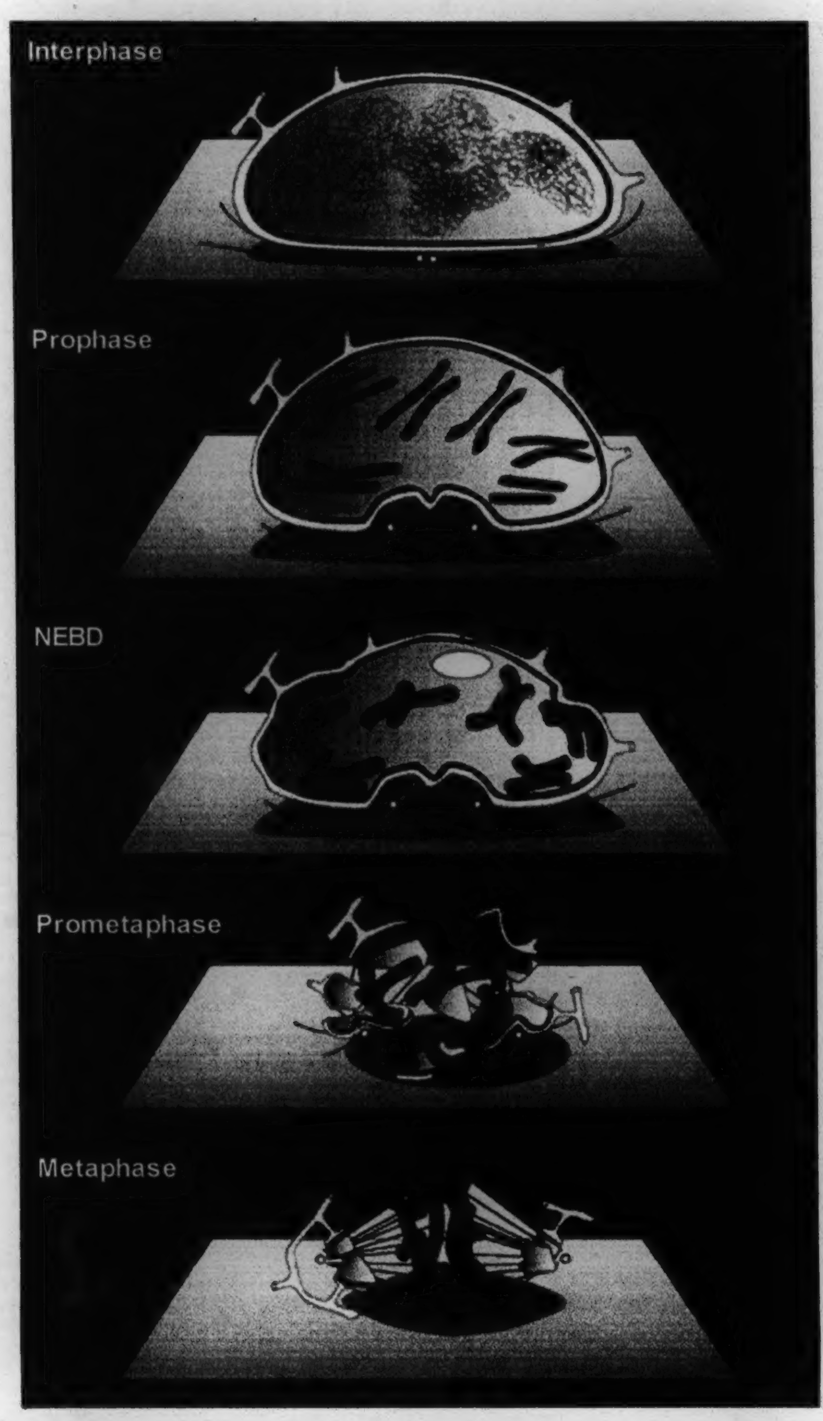
Interphase
Prophase
NEBD
Prometaphase
Metaphase

Figure 1-5. Nuclear envelope breakdown (NEBD).

1.5.1 NEBD: The Vesiculation Model

As early as 1973, transmission electron microscopy studies by Roos and colleagues revealed the highly dynamic nature of the metazoan NE (Roos, 1973). Since then, three models have been proposed to explain the mechanisms that control NEBD (reviewed in Hetzer et al., 2005). In this first model, the NE membrane reversibly disassembles into vesicles that are distinct from the intact mitotic ER network. Evidence lending support to this hypothesis arose from several observations. Firstly, early ultrastructural analyses of rat epithelial cells hinted that at the onset of mitosis, the NE underwent a continual fragmentation process presumably indicative of random scission events (Zeligs and Wollman, 1979). Secondly, separate studies in both mitotic HeLa cells and embryonic *Xenopus* extracts demonstrated that vesicles enriched in the NE proteins could be isolated (Buendia and Courvalin, 1997; Chaudhary and Courvalin, 1993; Sasagawa et al., 1999; Vigers and Lohka, 1991). Finally, when the recruitment of NE constituents to the chromatin was observed during reassembly of the NE, markers of the INM (LBR and LAP2) and the pore membrane (gp210) were observed binding to chromatin in anaphase and telophase, respectively, suggesting that they were present in distinct vesicle populations (Chaudhary and Courvalin, 1993). However, critics of this model have pointed out that it relies on seemingly circumstantial evidence, as round and membranous structures visualized by electron microscopy may represent either vesicles or tubules, and that apparently different vesicle populations may be artifacts resulting from cell homogenization procedures (Collas and Courvalin, 2000). Furthermore, similar experiments comparing the post-mitotic nuclear periphery localization of gp210 and POM121, revealed that their recruitment differed temporally, suggesting that vesicles enriched in NPC membrane constituents likely did not exist (Bodoor et al., 1999). Despite these criticisms, however, it is difficult to completely discount vesiculation as at least a contributing factor to NEBD given recent reports described above implicating the COPI machinery in this process (Liu et al., 2003) along with observations that Brefeldin A, a coat protein assembly inhibitor that blocks vesicle formation, also inhibits NEBD (Cotter et al., 2007).

1.5.2 NEBD: The Reabsorption Model

The reabsorption model proposes that NE membranes and their protein constituents that are transmembrane in nature distribute into the ER. Evidence in support of this model stems from observations made in studies of somatic cultured cells aimed at examining the mitosis-specific localization of markers of all NE membrane. LAP1, LAP2, and the pore membrane POM121 and gp210 were shown to colocalize with ER markers in mitosis (Daigle et al., 2001; Yang et al., 1997). Furthermore, Ellenburg and colleagues utilized a GFP-tagged Lamin B receptor (LBR) and FRAP/FLIP techniques to uncover that this inner nuclear membrane component was indeed present and highly mobile within the mitotic ER network (Ellenberg et al., 1997).

1.5.3 NEBD: Model Integration

The random diffusion and domain models, while speculative, attempt to amalgamate the vesiculation and absorption models (Collas and Courvalin, 2000; Mattaj, 2004). They reason that the NE membrane proteins are distributed throughout the ER during mitosis in one of two plausible scenarios (Collas and Courvalin, 2000; Mattaj, 2004). In the random diffusion model, the integrity of the nuclear membrane domains is lost during NEBD and all NE proteins randomly diffuse throughout the ER. In contrast, the domain model predicts that nuclear membrane domains partition from the remainder of the ER components as either multiprotein complexes or membrane microdomains (Collas and Courvalin, 2000; Mattaj, 2004). If this were the case, subcellular fractionation would potentially yield microsomal vesicles enriched in NE components. The domain model further implies that connections between the NE and ER membrane systems are maintained in mitosis thereby allowing for free and rapid diffusion of NE integral membrane proteins once the nuclear membrane disassembles. Presumably, these NE proteins would become mobilized as a result of their dissociation from anchoring ligands such as chromatin, the lamina, or NPCs. Indeed, the observation that LBR-GFP immobilizes in anaphase at ER-chromatin contact sites corroborates this idea (Ellenberg et al., 1997).

1.5.4 Processes influencing NEBD

During interphase, nuclear and NE stability are maintained through a complex interaction network consisting of the chromatin, the nuclear lamina, INM proteins, and NPCs (Foisner, 2001; Holmer and Worman, 2001). These interactions must be at least partially dissociated to allow for progression through mitosis. Over the years, there have been numerous examples of a variety of factors that facilitate the intricate process of nuclear disassembly. These include post-translational modification of proteins, as well as the involvement of microtubules, and vesicle trafficking machinery.

1.5.4.1 Phosphorylation of NE proteins

Several independent biochemical analyses have uncovered that many NE constituents undergo phosphorylation by cyclin B/p34^{cdc2}, or Cdk1 in vertebrates during mitosis. In the case of nuclear lamina components, phosphorylation has been directly implicated in their depolymerization and disperal throughout the cytoplasm of mitotic cells (Collas, 1999; Gerace and Blobel, 1980; Nigg, 1992; Stick et al., 1988). Integral INM constituents LBR, LAP2, and emerin have similarly been shown to become phosphorylated suggesting that this modification may be involved in the initial detachment of the INM from chromatin (Burke and Ellenberg, 2002; Courvalin et al., 1992; Ellis et al., 1998; Foisner and Gerace, 1993; Nikolakaki et al., 1997; Worman and Courvalin, 2000). In addition, phosphorylation of a number of NPC proteins has been observed. Nup358, Nup214, and Nup153 are phosphorylated in all phases of the cell cycle, where, interestingly, a two-fold increase in phosphorylation was observed in both S- and M-phase (Favreau et al., 1996). M-phase specific phosphorylation, on the other hand, has been detected for Nup107, Nup133, Nup160, Nup96 (Glavy et al., 2007), all of which are members of the Nup107-160 complex and Nup53 (L.A. Hawryluk-Gara and R.W. Wozniak, unpublished. See Appendix Fig. 7-1). Of the known pore membrane nups of the vertebrate NPC, only gp210 appears to be phosphorylated in M-phase (Favreau et al., 1996).

The precise mechanism explaining how mitotic phosphorylation would trigger NEBD has currently not been established. From an historical perspective, however, it has been classically believed likely that this modification would potentially disrupt structurally significant protein-protein interactions necessary for NE integrity, thereby resulting in disassembly. As an extension of this concept, it then follows that dephosphorylation may be a critical step in post-mitotic reassembly of NE components. Indeed, in a study examining NPC assembly in *Drosophila* embryos, authors demonstrated that Cdk1, a mitotic kinase, was indeed required for maintaining NPCs in a dissociated state during mitosis and that phosphatase activity appeared to be involved in reassembly of NPCs (Onischenko et al., 2005).

1.5.4.2 Proposed roles of microtubules

The concept of microtubule involvement in the initiation of NEBD has stemmed largely from classic EM studies in which intimate connections between spindle and the NE were observed in late G2/early prophase HeLa cells (Paweletz and Lang, 1988; Robbins and Gonatas, 1964) where deep NE invaginations were noted in the centrosomal regions (Robbins and Gonatas, 1964). For three decades the functional relevance of these associations remained elusive until Georgatos and colleagues, who detected MTs and centrosomes within the deep NE invaginations, proposed that NEBD was initiated by microtubules physically piercing the NE resulting in membrane permeability (Georgatos et al., 1997).

A more in depth understanding of the mechanism of MT-mediated NEBD was provided by two independent detailed studies that, using slightly different methodologies, visualized the process of NEBD at unprecedented resolution (Beaudouin et al., 2002; Salina et al., 2002). Utilizing a more traditional approach of immunofluorescence and state-of-the-art quantitative 4D imaging techniques, both groups demonstrated that, at the onset of mitosis, the NE develops two invaginations that each contain the newly duplicated centrosomes. Projections of MTs could be visualized emanating from the pockets that also contain nups along with markers of both the nuclear lamina and the INM. Importantly, and contrary to what was previously proposed (Georgatos et al., 1997), rupture of the NE did not appear to occur at the sites of these invaginations, but rather at distal locations, leading to the suggestion that NEBD was initiated as a result of mechanical tension generated by the MTs. This possibility was further exemplified by the observation that NEBD was significantly impaired, albeit not completely inhibited, when cells were treated with the MT-destabilizing drug, nocodazole (Beaudouin et al., 2002; Salina et al., 2002).

With the goal in mind of identifying a specific motor protein required for the generation of this MT-driven tension, Salina and colleagues revisited earlier reports that the minus end microtubule motor protein dynein, together with its regulatory complex dynactin, was capable of associating with the NE in a variety of cell types (Busson et al., 1998; Gonczy et al., 1999; Reinsch and Karsenti, 1997; Robinson et al., 1999). They not only confirmed this observation, but went on to demonstrate that dynein/dynactin were recruited to the NE in late G2, notably prior to any detectable changes in NE morphology (Salina et al., 2002). In a series of related experiments that further implicated dynein in NEBD, the effect of overexpression of p62, a subunit of the dynactin complex, on NE dynamics during mitosis was explored. Importantly, overexpression of p62 had previously had been shown to result in dissociation of dynein from membrane cargo without impairing the ability of MTs to organize at centrosomes (Quintyne et al., 1999). Remarkably, BHK cells overexpressing p62 displayed a decrease in NE associated dynein and a corresponding delay in NEBD. In the aggregate, these data provided compelling evidence that dynein was indeed the molecular motor complex responsible for MT-mediated NE tension. However, the observation that NEBD was not completely abolished in cells that had depolymerized microtubules as a result of nocodazole treatment suggested that while MTs facilitate NEBD, the generation of tension on the NE is not absolutely required, suggesting that other processes are involved.

1.5.4.3 The COP1 Connection

Because NPCs are embedded in the NE membrane, they are strategically positioned to actively participate in nuclear disassembly. As a case in point, a role for Nup153 in NEBD has recently been described (Liu et al., 2003). In this report, authors first found that a central domain of Nup153, containing a zinc finger, exerted a dominant negative effect on NEBD in *Xenopus* oocytes. Upon further investigation into the cause of this inhibition, they demonstrated that this region of Nup153 was able to physically interact with several members of the COPI coatomer complex involved in Golgi to ER retrograde transport (Lee et al., 2004). Furthermore, *in vivo* depletion of β-coatomer, a member of the COPI complex, also results in NEBD inhibition. Taken together with its observed recruitment to the NE prior to NEBD in HeLa cells, it was proposed that Nup153 recruits the coatomer complex to the NE, where it participates in vesiculation of the NE.

1.5.5 Mitotic fates of NE constituents

The dispersal of the lamina, INM, and nups resulting from disassembly of the NE marks a critical event during cell cycle progression. Once disassembled, NE components have been detected at several cellular locations. As previously discussed, integral membrane proteins, of both the pore membrane (PM) and INM alike, are redistributed throughout the mitotic ER network (Daigle et al., 2001; Yang et al., 1997) and the disassembled lamins disperse throughout the cytoplasm (Collas, 1999; Gerace and Blobel, 1980; Nigg, 1992; Stick et al., 1988). Similar to the lamin proteins, the majority of nups are also distributed in the cytoplasm but there are intriguing exceptions. For example, Nup107-160 complex members have been shown to associate with kinetochores, spindle poles, and microtubules during mitosis (Belgareh et al., 2001; Loiodice et al., 2004; Orjalo et al., 2006). Subsequent functional analyses to this initial observation have reported that once targeted there, this subcomplex may actively participate in chromosome segregation. Indeed, siRNA mediated depletion of members of this complex resulted in striking kinetochore-MT attachment defects resulting in spindle assembly checkpoint (SAC)-mediated mitotic delay (Zuccolo et al., 2007). Another example of nup-kinetochore relocation in mitosis was noted for Nup358/RanBP2 and its binding partner RanGAP1, which are also detected along specific regions of the mitotic spindle (Joseph et al., 2002; Salina et al., 2003). Here, like the Nup107-160 complex, it has been implicated in maintaining stable kinetochore-MT associations (Joseph et al., 2004). These NPC constituents that localize to the mitotic kinetochores and spindle have not been classified as SAC proteins per se. Rather, they have been proposed to participate in a pathway that signals from the newly disassembled NE to the kinetochore indicating that NEBD has occurred at mitotic onset (Salina et al., 2003).

1.6 NE Dynamics: NE and NPC Formation

A necessary event for the completion of the cell cycle is the reassembly of the NE and its associated structures around the duplicated and segregated chromosomes. Nuclear formation in higher eukaryotes involves the recruitment and fusion of NE membrane vesicles to the chromatin surface coupled with the assembly of NPCs and nuclear lamina. Mechanisms underlying NPC subcomplex assembly and organization and coordination with NE formation have, until recently, been largely undefined. Furthermore, how different nups and NPC subcomplexes interact during NPC assembly is largely unclear. Combinations of RNAi interference studies and nuclear reconstitution assays in *Xenopus* have been instrumental in furthering our understanding of the complex interplay between these processes.

1.6.1 NE membrane formation

Critical aspects of reformation of the NE membrane include the initial targeting of the membrane vesicles to chromatin, membrane fusion to form a continuous bilayer, and the incorporation of NPCs. *In vitro* NE assembly was first visualized in a landmark study by Lohka and Masui (1983) using *Xenopus* ooctye extracts and sperm chromatin. Since then, this assay has been used extensively to study NE assembly *in vitro*. Using this approach, NE assembly has been shown to require cytosolic factors and be inhibited by non-hydrolyzable forms of both GTP and ATP, *N*-ethylmaleimide, and the calcium chelator BAPTA (Macaulay and Forbes, 1996). From more recent studies using this assay, it is clear that there are distinct populations of vesicles that are capable of binding to chromatin and contributing to NE formation (Antonin et al., 2005; Vigers and Lohka, 1991). Reformation of the NE membrane is initiated by the binding of these vesicles to the chromatin surface in an energy- and cytosol-independent manner (Newport and Dunphy, 1992; Vigers and Lohka, 1991). Moreover, vesicle binding does not appear to be dependent on specific DNA or chromatin structures (Forbes et al., 1983; Newport, 1987). An important determinant of membrane vesicle recruitment, however, is nucleoplasmin, a protein that has been shown to be critical for the deposition of histones onto chromatin and decondensation (Philpott and Leno, 1992; Ulbert et al., 2006). Presumably, this chromatin decondensation exposes sites for vesicle docking.

It has long been believed that transmembrane proteins mediate the interaction between membrane vesicles and chromatin (Beundia and Courvalin, 1997; Burke and Ellenberg, 2002; Chaudhary and Courvalin, 1993; Collas and Courvalin, 2000; Holmer and Worman, 2001; Wilson and Newport, 1988; Foisner and Gerace, 1993). For example, direct interactions between LBR and Lap2β with chromatin associated proteins heterochromatin protein one (HP1) and barrier-to-autointegration factor (BAF), respectively, have been detected (Ye et al., 1997; Dechat et al., 2000). Furthermore, LBR and two pore membrane proteins POM121 and NDC1 are capable of directly interacting with chromatin and naked DNA *in vitro* (Ulbert et al., 2006). The basic cytosolic domains of these transmembrane proteins were predicted to confer affinity to chromatin, through interactions with DNA. Interestingly, NDC1 and POM121 were found to be enriched in the same chromatin binding vesicle population (Antonin et al., 2005;

Mansfeld et al., 2006; Section 1.6.2.2). Collectively, these data provide evidence for a general mechanism in which these proteins are responsible for the initial docking of NE membrane vesicles to chromatin.

Subsequent to the initial vesicle docking are membrane fusion steps resulting in a closed and continuous NE. Elegant studies following this process in *Xenopus* egg extracts have allowed for the visualization of distinct phases of this process (Hetzer et al., 2001). Initially, a tubular membrane network on the sperm chromatin surface is formed and this process is dependent on GTP hydrolysis by Ran (Hetzer et al., 2000; 2001). Secondly, a sealed NE is constructed through the action of p97, an AAA-ATPase that has been implicated in the regulation of membrane fusion events and vesicle trafficking (Miyachi et al., 2004; Patel and Latterich, 1998 and references therein), and GTP hydrolysis by Ran (Boman et al., 1992; D'Angelo et al., 2006, Hetzer et al., 2000; 2001; Macaulay and Forbes, 1996). Finally, nuclear growth dictates both significant NE expansion to accommodate decondensation of the chromatin and nucleoctytoplasmic transport (Benavente at al., 1989; Macaulay and Forbes, 1996; Newport et al., 1990). Whereas the *in vitro* NE sealing step involves p97 and adaptor proteins Ufd1 and Npl4 (Hetzer et al., 2001; Meyer et al., 2000), the final expansion stage appears to be mediated by a distinct complex between p97 and a different adaptor, p47 (Hetzer et al., 2001).

Precisely how the p97/Ufd1/Npl4 and p97/p47 complexes mediate NE sealing and growth is unclear, but the observation that distinct complexes are involved has been suggested to reflect the requirement of distinct fusion mechanisms (Burke, 2001; Burke and Ellenberg, 2002). Specifically, p97/Ufd1/Npl4 have been proposed to mediate annular fusion that would close gaps in the membranes and, in doing so, seal the NE. In contrast, the expansion step, which involves point fusion of vesicles with the ONM, would be mediated by p97/p47 (Burke, 2001), in a manner equivalent to how this complex mediates homotypic membrane fusion in the Golgi apparatus (Rabouille et al., 1998). Interestingly, very recent data has also implicated NSF- and SNARE-dependent membrane fusion steps early in NE assembly (Baur et al., 2007).

1.6.2 Post-mitotic NPC assembly

Concomitant with NE membrane vesicle binding to the chromatin are the initial steps in NPC formation. Experiments examining cultured cells and using *in vitro Xenopus* NE assembly assays have established a general ordering of events that lead to NPC assembly. An early step in this process is recruitment of the core Nup107-160 complex to chromatin in late anaphase, thereby potentially serving as seeding sites for recruitment of subsequent nups (Belgareh et al., 2001; Harel et al., 2003; Walther et al., 2003). Following Nup107-160 complex recruitment to the chromatin, a sequential targeting of distinct nups has been noted. Nup153 and POM121 are recruited, followed by the Nup62 complex, and Nup214, a component of the cytoplasmic fibrils. Arriving at the NPC relatively late in assembly, are the pore membrane nup gp210 and the nuclear basket associated TPR where the latter appears to be incorporated following formation of a sealed NE around the chromatin (Bodoor et al., 1999). This late recruitment of gp210 compared to POM121, suggests that POM121 is required for early NE membrane/NPC association events.

The ordered temporal association of various nups with the chromatin is consistent with the idea that the presence of certain NPC subcomplexes on the chromatin is necessary for subsequent nup incorporation as NPC assembly progresses through telophase and early G1. Furthermore, the sequential recruitment of nups lent support to the notion of the presence of discrete structural assembly intermediates visualized on the surface of NEs (Gant et al., 1998; Goldberg et al., 1997; Kiseleva et al., 2001) suggesting that NPCs are built in a stepwise manner.

1.6.2.1 The Nup107-160 complex

As alluded to above, key players implicated in NPC assembly were nups belonging to the Nup107-160 complex that were shown to be recruited to chromatin early during NPC assembly (Belgareh et al., 2001; Bodoor et al., 1999; Boehmer et al., 2003). Boehmer and colleagues (2003) built on previous observations by utilizing an RNAi strategy to assess the function of individual components of the Nup107-160 complex in NPC assembly. They demonstrated that siRNA mediated depletion of Nup107 resulted in an inability of other complex members and the mAb414 reactive nups Nup358, Nup215, and Nup153 to incorporate into NPCs, resulting in their degradation. The apparent requirement of chromatin associated Nup107-160 complex for progression of NPC assembly was further explored using the *Xenopus* nuclear reconstitution assay. Similar to previous observations in mitotic HeLa cells, ordered recruitment to sperm chromatin was also visualized, where the Nup107-160 complex members were associated early, in the absence of membranes. Immunodepletion of the Nup107-160 complex resulted in nuclei that lacked detectable NPCs (Harel et al., 2003; Walther et al., 2003). However, NE vesicles remained competent to dock to chromatin and fuse to form a closed NE indicating that the processes of NPC and NE assembly are distinct, separable events. When the Nup107-160 complex was added to preassembled nuclei devoid of NPCs but with a closed NE, new NPCs were not inserted (Walther et al., 2003). These observations lead to a model in which the Nup107-160 complex associates with chromatin where it forms a "pre-pore" structure that forms seeding sites for subsequent nup recruitment to assemble complete NPCs.

1.6.2.2 POM121, Nup155, and NDC1

Further clues as to how the coordination of NPC assembly and NE membrane vesicle docking and fusion may be regulated arose from immunodepletion studies of the integral membrane nup POM121 from *Xenopus* extracts (Antonin et al., 2005). Like the Nup107-160 complex, POM121 is recruited early during post-mitotic nuclear assembly (Bodoor et al., 1999; Daigle et al., 2001). Nuclei assembled with reconstituted membrane vesicles devoid of POM121, were found to have chromatin docked but unfused vesicles thereby blocking closed NE formation. Interestingly, observation of this vesicle fusion defect was dependent on the presence of the Nup107-160 complex as depletion of both POM121 and the Nup107-160 complex removed this block in vesicle fusion and resulting nuclei contained a closed NE lacking NPCs. Importantly, this result suggests that POM121 is not involved in the fusion process itself but rather functions in a pathway that signals the fusion machinery. Moreover, it highlights a role for POM121 in coordinating three essential aspects of NE assembly: the assembly of soluble nups, the anchoring of these nups to the NE, and fusion of membrane resulting in a sealed NE. These observations lead to a mod[illegible] which a checkpoint functions to monitor NE and NPC formation. In the NE/NPC assembly checkpoint, progression of NE vesicle fusion is inhibited until such time as the presence of POM121, presumably through interactions with the "pre-pore" Nup107-160 complex on the surface of chromatin, is detected (Antonin et al., 2005).

Other players participating in the proposed NE/NPC assembly checkpoint have also recently been uncovered. For example, Nup155 depletion from *in vitro* nuclear assembly reactions not only resulted in a loss of mAb414 nup accumulation at the nuclear periphery, indicative of a block in NPC assembly, but also prevented the formation of a closed NE, halting the process at the vesicle docking stage (Franz et al., 2005). This phenotype was reminiscent of that observed for depletion of POM121, and served as the first example of a soluble nup having a role in both assembly of the NPC and the NE. It further suggested that Nup155, like POM121 and the Nup107-160 complex, plays a critical role both in NE and NPC assembly. Notably, Nup155 was recruited to chromatin later than the Nup107-160 complex and POM121 but did not affect their ability to associate with chromatin thus defining a role for Nup155 in later events of NE/NPC formation (Franz et al., 2005).

A strikingly similar depletion phenotype has also been observed for both *in vivo* and *in vitro* depletion of the conserved transmembrane Nup, NDC1. Upon depletion of NDC1 in HeLa cells using RNAi, a reduction in incorporation of mAb414 nups was observed indicative of severe NPC assembly defects (Mansfeld et al., 2006; Stavru et al., 2006a). Like depletion of the Nup107-160 complex, POM121, and Nup155, NDC1 depletion resulted in membrane vesicles docking to the chromatin but no fusion

(Mansfeld et al., 2006). Further investigation of the function of NDC1 is described in detail in Chapter IV.

1.6.2.3. The role of transmembrane nups in NE/NPC biogenesis

While the mechanistic roles remain unclear, several studies, apart from those already described, have lead to further proposals of how both yeast and vertebrate POMs function in NE formation. For example, these proteins may contribute to the induction of membrane curvature resulting in the transcisternal pores which NPCs reside in. The overproduction of yeast Nup53p, for example, leads to a massive intranuclear proliferation of the NE that contains transcisteneral pores but lack NPCs (Marelli et al., 2001). Apart from Nup53p, both of the yeast POMs, Pom152p and Ndc1p, were detected on these membranes, suggesting that they may be involved in the formation of these pores that were devoid of NPCs. More recent work investigating the interphase NPC assembly function of the yeast POMs has offered more clues. Madrid and colleagues (2006) reported that nups normally localized to the cytoplasmic fibrils, the central core, and nuclear basket were all mislocalized in cells lacking either Ndc1p and Pom152p. A more dramatic mislocalization of these nups was noted in cells where both Ndc1p and Pom152p were removed. TEM analysis also revealed abnormal NPC morphology in these mutant cells. These pores appeared to lack significant protein content of the central channel and, in many cases, were abnormally wide. In contrast, cells lacking Pom34p showed no such defects, demonstrating that it is dispensible for NPC formation. Taken together, these studies provide compelling evidence that, in yeast, Pom152p and Ndc1p may be functionally redundant. Furthermore, they lend further support to previous models in which POMs are required to recruit soluble nup subcomplexes to the NE.

Studies investigating the role of gp210 have yielded conflicting results, thus the function of gp210 remains elusive (Antonin et al., 2005; Cohen et al., 2003; Drummond and Wilson, 2002; Stavru et al., 2006b). RNAi experiments in both HeLa cells and *C. elegans* embryos suggest that gp210 is essential for cell viability (Cohen et al., 2003) and that depletion results in aberrant NPCs (Cohen et al., 2003; Stavru et al., 2006b). These observations are, however, difficult to reconcile with the comparatively late recruitment of gp210 to the chromatin periphery (Bodoor et al., 1999; Chaudhary and Courvalin, 1993) and the report finding no observable defect in NE formation upon immunodepletion of gp210 from *Xenopus* extracts (Antonin et al., 2005).

1.6.3 The Role of Ran in NE and NPC biogenesis

As a blueprint has emerged for the mechanism of how Ran contributes to nucleocytoplasmic transport (see section 1.4.2) so has the idea that Ran provides a spatial and temporal cue for nuclear assembly (reviewed in Burke and Ellenberg, 2002; Hetzer et al., 2002; 2005). Central to the role of Ran in both of these processes is the production of Ran-GTP at locations near the chromatin by the action of the chromatin associated Ran-GEF, RCC1 (Bilbao- Cortés et al., 2002; Hinkle et al., 2002; Kalab et al., 2002).

The role of Ran in NE assembly in both yeast and metazoan cells has been well established (Askjaer et al., 2002; Bamba et al., 2002; Demeter et al., 1995; Hetzer et al., 2000; Matynia et al., 1996; Ryan et al., 2003; Walther et al., 2003; Zhang and Clarke, 2000; 2001). For example, in *Xenopus* extracts, depletion of either Ran or Ran-GEF blocks NE assembly from progressing past the vesicle docking stage (Hetzer et al., 2000). Zhang and Clarke (2000, 2001) implicated Ran as having a direct role in NE fusion through their elegant studies with Ran-coupled Sepharose beads. Remarkably, in the absence of chromatin, these beads were sufficient to assemble NEs that contained NPCs and were transport competent.

It is not clear, however, precisely how mechanistically Ran contributes to this process. Nonetheless, important clues are offered by observations hinting that kaps are also involved. Walther and colleagues (2003) showed that Ran-GTP is required to release Importinβ/Kap-β1 from Nup107, Nup153, and Nup358, target them to chromatin where they promote association of multiple distinct nup subcomplexes, and, finally, in the terminal steps of NE assembly, trigger NPC insertion into membranes (D'Angelo et al., 2006 and see 1.6.4).

1.6.4 NPC assembly in intact membranes

Through a considerably less studied process, NPC number has been shown to double in S-phase (Maul et al., 1971; 1972) indicating that, in this stage of the cell cycle, machinery must be in place that would allow for NPC assembly in a continuous double membrane. This is also the case for yeast which undergo a 'closed' mitosis, where the NE does not break down. Presumably, in both cases this would involve fusion of the INM and ONM to create a channel in which NPC components could be assembled. Until very recently, significant issues regarding these concepts had not been addressed. For example, the apparatus governing INM and ONM fusion remains to be identified (Burke and Ellenberg, 2002). Moreover, it was not clear whether NPC assembly occurs from the nucleoplasmic and/or cytoplasmic side(s) of the NE (Burke and Ellenberg, 2002) and if NPCs form *de novo* or from pre-existing NPCs (Bodoor er al., 1999; Hetzer et al., 2005; Rabut et al., 2004). Observations made by D'Angelo and colleagues (2006) using an elegant NPC insertion assay in *Xenopus* egg extracts, however, have begun to shed some light on the mechanisms governing NPC formation within an intact NE. In these experiments, nuclei were assembled by incubating sperm chromatin and cytosol. Existing NPCs were labelled with fluorescently labelled wheat germ agglutinin (WGA) which binds to nups that have been post-translationally modified by glycosylation (Davis and Blobel, 1987; Finlay and Forbes, 1991; Hanover et al., 1987; Holt et al., 1986; 1987; Park et al., 1987; Schindler et al., 1987; Radu et al., 1993; 1994). Following nuclear growth and expansion, the newly formed NPCs were labelled again, this time with WGA that was labelled with a different fluor. The new NPCs were found to be formed *de novo*, rather than from pre-exisiting pores.

The authors also demonstrated that NPC insertion required Ran-GTP in both cytoplasmic and nucleoplasmic compartments. Investigation into the mechanism of this Ran-GTP dependence resulted in additional evidence that Ran-GTP mediates release of the Nup107-160 complex from Importin-β (Walther et al., 2003), on both the nuclear and cytoplasmic face of the NE, strongly suggesting that NPC assembly is initiated from both faces of an intact NE.

1.7 Thesis Focus

This thesis encompasses a variety of experiments designed to explore the functional role of the conserved Nup53-complex in the processes of post-mitotic NE and

NPC assembly. In uncovering the tight association of Nup53 with the NE and the nuclear lamina, that it is involved in the assembly of an interacting group of nups, and dissecting these interactions, we provide evidence for a model in which the Nup53-Nup155 is critical for the normal progression of NE and NPC assembly.

Chapter II: *Experimental procedures*

2.1 *Xenopus* Nup53 antibody production

The ORF of *Xenopus laevis* Nup53 (xNup53) was inserted into the EcoR1 site of pGEX-4T-1 (Amersham Biosciences Inc., Baie D'Urfe, Quebec). This plasmid was a gift from E.K. Shibuya (Department of Cell Biology, University of Alberta, Canada). An *E. coli* BL21 strain containing pGEX-xNup53 was grown to an OD_{600}=0.8 and induced with 1mM IPTG for 4 h at 30°C. GST-xNup53 was purified on glutathione Sepharose 4B beads (Amersham Biosciences Inc., Baie D'Urfe, Quebec) using the manufacturers instructions, in 50 mM Tris HCl pH 7.4, 150 mM NaCl, 1 mM $MgCl_2$, 0.1% Tween 20, 1 mM DTT and Complete Protease inhibitor cocktail (Roche Diagnostics, Laval, Quebec). xNup53 was released from the column by incubation with 0.6 units of thrombin (Sigma-Aldrich, Oakville, Ontario, Canada) per 10 µl of beads for 4 h at room temperature. Purified recombinant *Xenopus* Nup53 was used to elicit antibodies in rabbits.

2.2 Nup93 and Nup53 plasmid construction

The human Nup93 ORF (accession no. D42085) was amplified with the Expand High Fidelity PCR system from a plasmid containing NUP93 cDNA (clone name ha01471, gene name KIAA0095, Kazusa DNA Research Institute, Japan). The NUP93 PCR product was directionally inserted into the BamHI (5') and KpnI (3') sites in pGEX-6P-1 (Amersham Biosciences Inc., Baie D'Urfe, Quebec).

The human Nup53 ORF (accession no. AF514993) encoding the full length protein (Nup53-1-326) was amplified by PCR as indicated above (Roche Diagnostics, Laval, Quebec) using a Human Fetal Kidney cDNA library (BD Biosciences Clontech, San Jose, CA) as template. The PCR product was inserted into the EcoRI site of pGEX-

6P-1. The Nup53 cDNA encoding the full length protein was also directionally inserted into the EcoRI(5') and KpnI(3') sites of pEGFP-C1 (BD Biosciences Clontech, San Jose, CA). All of the following plasmids contain inserts of PCR products amplified with the Expand High Fidelity PCR system (Roche) using the Human Fetal Kidney cDNA library as template and oligonucleotide primers with EcoRI restriction sites. cDNA encoding the following regions of Nup53 were inserted into the EcoRI site of pGEX-6P-1: Nup53-1-300 , Nup53-1-203, Nup53-1-143, Nup53-1-83, Nup53-167-326, Nup53-84-326, Nup53-204-326, and Nup53-167-300. Identical PCR products to these described were also inserted into the EcoRI site of pEGFP-C1. The GST fusions were used for recombinant Nup53 isolation and subsequent pulldown and *in vitro* binding studies (2.6, 2.7). The GFP fusions were used for localization studies. The DNA sequences of the constructed plasmids were confirmed by DNA sequencing.

2.3 Purification of rat liver nuclei and nuclear envelopes

Rat Liver nuclei and nuclear envelopes (NEs) were prepared as previously described (Blobel and Potter, 1966; Dwyer and Blobel, 1976) with modifications (Wozniak et al., 1989). Twelve Sprague-Dawley rats were euthanized by decapitation and their livers removed. The harvested livers were washed in 0.25 M STEAKM (0.25 M sucrose, 50 mM triethanolamine, 25 mM KCl, 5 mM $MgCl_2$, 0.5 mM PMSF (phenylmethyl sulfonyl fluoride), 1 mM DTT (dithiothreitol)) prior to being sliced into small pieces with a razor blade. The liver was placed in 2X (v/w of liver) of 0.25 M STEAKM and homogenized with a chilled potter for 20 strokes. Homogenized livers were subsequently filtered through cheesecloth prior to centrifugation for 10 min at 4°C at 800 *g*. The remaining pellets were transferred into a potter where they were again homogenized for 5 strokes. 2X (v/v) of 2.3 M STEAKM (2.3 M sucrose, 50 mM triethanolamine, 25 mM KCl, 5 mM $MgCl_2$, 0.5 mM PMSF, 1 mM DTT) was added. The liver homogenate was then underlaid with 5 ml of 2.5 M STEAKM and centrifuged for 75 min at 4°C and 140,000 *g*. The resulting supernatant was quickly aspirated and the purified nuclei were resuspended in 0.25 M STEAKM by hand homogenization. Pellets representing 500 A_{260} units of nuclei (1 A_{260} unit represents the amount of material derived from 1 A_{260} unit of nuclei; ~3 x 10^6 nuclei) were stored at -80°C covered in 0.25 M STEAKM.

The isolation of purified nuclear envelopes was performed as follows. While vortexing using medium speed, 5 ml of NE Buffer A (0.1 mM $MgCl_2$, 0.5 mM PMSF, 1 mM DTT) was added dropwise to a 500 A_{260} unit pellet of nuclei. Addition of 20 ml of NE Buffer B (20 mM TEA pH 8.5, 10% sucrose, 0.1 mM $MgCl_2$, 0.5 mM PMSF, 1 mM DTT) followed. The suspended nuclei were then treated with 25 µl each of DNase (2 mg/ml) and RNase (10mg/ml) for 15 min at 22°C. Following this incubation, the digested nuclei were underlaid with 5 ml of NE Buffer C (20 mM TEA pH 7.5, 30% sucrose, 0.1 mM $MgCl_2$, 0.5 mM PMSF, 1 mM DTT) and centrifuged at 19,000 *g* for 20 min at 4°C. The supernatant, representing the nucleoplasm fraction, was collected and analyzed. The resulting pellet was resuspended in NE Buffer D (20 mM TEA pH 7.5, 10% sucrose, 0.1 mM $MgCl_2$, 0.5 mM PMSF, 1 mM DTT). An additional nuclease digestion was performed in NE Buffer D (20 mM TEA pH7.5, 10% sucrose, 0.1 mM $MgCl_2$ 0.5 mM PMSF, 1 mM DTT) and centrifuged as described above. The purified NE pellet was subsequently resuspended in 1 ml of NE Buffer D and stored in 200 µl aliquots at -80°C.

2.4 Extraction of purified nuclear envelopes

Purified NEs were extracted as described (Radu et al., 1993) with 1 M NaCl, 2 M NaCl, 2 M urea, or 7 M urea in buffer containing 20 mM TEA pH 7.5, 0.1 mM $MgCl_2$, 1 mM DTT, and Complete Protease inhibitor cocktail (Roche Diagnostics, Laval, Quebec) for 15 min at 4°C at a concentration of 100 A_{260} units/ml. The extracted proteins in the supernatant were separated from the pellet by centrifugation at 20,000 *g* for 30 min at 4°C and precipitated with a final concentration of 10% trichloroacetic acid. Alternatively, NEs were extracted with 1% Triton X-100 in buffer containing 20 mM TEA pH 7.5, 0.1 mM $MgCl_2$, 1 mM DTT, and Complete Protease inhibitor cocktail to solubilize the nuclear membrane. Triton X-100 extracted NEs were then recovered in the pellet fraction following centrifugation at 4,000 *g* for 10 min at 4°C. The extracted NE pellets were then re-extracted with 0.1 M, 0.25 M, 0.5 M, or 1 M NaCl in the same buffer as above but lacking Triton X-100 at a concentration of 100 A_{260} units/ml. Supernatant and pellet fractions were produced by centrifugation at 20,000 *g* for 30 min at 4°C and proteins analyzed by SDS-PAGE and Western blotting.

2.5 Purification of nup and nuclear lamina enriched fractions

Nucleoporin- and nuclear lamina-enriched fractions were prepared from purified rat liver NEs as previously described (Cronshaw et al., 2002). 100 A_{260} units of NE were resuspended in 1 ml final volume of NE Buffer D. This mixture was subsequently diluted to 66 A_{260} units/ml using NE buffer D supplemented with 0.3 mg/ml Heparin (0.2 mg/ml final concentration), underlaid with 500 µl of NE Buffer C, and centrifuged at 5500 rpm in a Beckman JS13.1 rotor for 15 min at 4°C. The resulting pellet was resuspended in 1 ml of NE Buffer D (100 A_{260} units/ml) and then diluted to 66 A_{260} units/ml with NE buffer D containing 3% Triton X-100 and 0.075% SDS (2% and 0.050% final concentrations, respectively). This extract was then centrifuged as indicated above. For the final Empigen BB (Calbiochem-Novabiochem, San Diego, CA) extraction, the pellet was again resuspended to 100 A_{260} units/ml in NE Buffer D and diluted to 66 A_{260} units/ml in NE Buffer D containing 0.9% Empigen BB (0.6% final concentration). Following a 5 min incubation on ice, the Empigen BB extract was centrifuged at 10,000 rpm for 15 min at 4°C. The pellet comprised of nuclear lamin proteins was resuspended in SDS-PAGE sample buffer at a final concentration of 0.1 A_{260} U/µl. The supernatant containing solubilized nups was precipitated using a final concentration of 10% TCA and the precipitated proteins were also dissolved in SDS-PAGE sample buffer at the same concentration as above. Empigen BB supernatant and pellet fractions were separated by SDS-PAGE and analyzed by Western blot using antibodies indicated in Fig. 3-2 and the respective legend.

2.6 Protein purification for pulldown and *in vitro* binding studies

For the *in vitro* binding experiment in Fig. 3-3, *E. coli* BL21 strains containing pGEX-4T1-Nup53 or pGEX-6P1-Nup93 were grown to an OD_{600}=0.8 and induced with 1mM IPTG for 4 h at 30°C. GST-Nup53 and GST-Nup93 were purified on glutathione Sepharose 4B beads (Amersham Biosciences Inc., Baie D'Urfe, Quebec) using the manufacturers instructions, in 50 mM Tris HCl pH 7.4, 150 mM NaCl, 1 mM $MgCl_2$, 0.1% Tween 20, 1 mM DTT and Complete Protease inhibitor cocktail (Roche

Diagnostics, Laval, Quebec). GST-Nup53 remained on the GT column and Nup93 was released from the beads by cleavage using the Pre-Scission Protease.

For the GST-pulldown experiments in Fig. 3-3 and 3-7, purification of GST-Nup53 and GST-Nup93 were performed precisely as already described above but eliminating the Nup93 cleavage from the GT column. Those described in Fig. 4-1 and 4-3 were also performed as described with the exception that an *E. coli* BL21CODON strain was used for expression of pGEX-6P1-Nup53.

2.7 GST-pulldown assays

GST-pulldown assays were performed as described (Hawryluk-Gara et al., 2005; submitted; Mansfeld et al., 2006). 100 A_{260} units of purified rat liver NEs were extracted with a combination of 1% Triton X-100 and 400 mM NaCl in 20 mM Tris pH 7.5, 1 mM DTT, 0.1% Tween 20 and Complete Protease inhibitor cocktail at 4°C for 5 min. Extracted proteins were collected in the supernatant fraction following centrifugation at 20,000 *g* for 30 min at 4°C. The supernatant was diluted 3.75-fold to a final concentration of 0.3% Triton X-100 and 106 mM NaCl. The diluted rat liver NE fraction (66 A_{260} units/ml) was incubated with 10 µl of glutathione Sepharose 4B beads (Amersham), pre-loaded with ~6 µg of GST, GST-Nup93, or GST-Nup53, for 2 h at 4°C. Following extensive washing of the beads with 20 mM Tris pH 7.5, 106 mM NaCl, 0.3% Triton X-100, 0.1% Tween 20, 1 mM DTT, and Complete Protease inhibitor cocktail, proteins were eluted from the beads with SDS-PAGE sample buffer and separated by SDS-PAGE. Gels were then silver stained (see 2.9) or transferred to nitrocellulose for Western blotting.

2.8 Direct *in vitro* binding experiments

For the *in vitro* binding assays, ~5 μg of purified, recombinant Nup93 was incubated for 2 h at 4°C with 10 μl of glutathione Sepharose 4B beads pre-loaded with ~10 μg of GST or GST-Nup53. After washing, proteins were eluted from the beads with SDS-PAGE sample buffer then separated by SDS-PAGE. Nup93 was detected with either Coomassie Blue or Western blotting.

2.9 Protein staining procedures

Proteins that were resuspended in SDS-PAGE sample buffer were separated by SDS-PAGE and detected using either Coomassie or silver staining. Bio-Safe Coomassie (Biorad) was used as instructed by the manufacturer. For silver staining, proteins in the gels were first fixed in 40% methanol and 10% acetic acid for 20 min at room temperature. The gels were then incubated for an additional 10 min at room temperature in 40% methanol, and then deionized H_20. Sensitization for 1 min at room temperature using 5% sodium thiosulfate (Sigma) followed. After 2 separate H_20 washes, the gel was stained using a pre-chilled 0.5% silver nitrate (Sigma) solution for 20 min at 4°C. The gels were subsequently washed twice with H_20 and silver stained proteins were detected using a solution containing 2% sodium carbonate (Sigma) and 0.04% formaldehyde (Sigma). The detection reaction was terminated using a 40% methanol and 5% acetic acid solution.

2.10 Mass spectrometry identification

Proteins detected by silver staining in the GST-Nup53 pulldown experiment were excised from the SDS-polyacrylamide gel and subjected to in-gel trypsin digestion followed by LC/MS on a CapLC HPLC (Waters, USA) coupled with a Q-ToF-2 mass spectrometer (Micromass, UK). Subsequent protein identification was performed by searching the non-redundant NCBI database using Mascot Daemon (Matrix Science, UK).

2.11 Sucrose gradient sedimentation

Sucrose gradient sedimentation was performed as described (Fontoura et al., 1999). Extracted NEs were recovered by centrifugation at 4,000 *g* for 15 min at 4°C and resuspended (1000 A_{260} units/ml) in 1% Triton X-100, 0.025% SDS, and 0.1 mg/ml heparin in 20 mM TEA pH 7.5, 0.1 mM $MgCl_2$, and Complete Protease inhibitor cocktail. Following centrifugation at 15,000 *g* for 10 min at 4°C, the supernatant was subsequently loaded onto a 10-40% (wt/vol) sucrose gradient containing 20 mM TEA pH 7.5, 0.1 mM $MgCl_2$, and Complete Protease inhibitor cocktail. Gradients were then centrifuged in a Beckman SW 41 rotor at 40,000 rpm for 17 h at 4°C. Fractions (750 µl) were collected and precipitated with a final concentration of 10% trichloroacetic acid. Proteins were separated by SDS-PAGE and analyzed by Western blotting.

2.12 Transfections and isolation of stable lines

HeLa S3 cells were maintained in DMEM (Invitrogen, Berkeley, CA) supplemented with 10% fetal bovine serum, 1% penicillin/streptomycin, and 1% L-glutamine at 37°C and 5% CO_2. Cells were seeded out 24 h prior to transfection so that they were 30% confluent on the day of transfection. Cells in a 100 mm culture dish were transfected with 0.5 μg of pEGFP-Nup53 using FuGene (Roche Diagnostics, Laval, Quebec) as instructed by the manufacturer. For isolation of stable lines in Fig. 3-1, HeLa cells transfected with pEGFP-Nup53 were seeded into medium containing 800 μg/ml G418 (Sigma-Aldrich, Oakville, Ontario) 48 h following transfection. After three weeks in selection medium, resulting G418 resistant colonies were isolated and screened both by Western blotting of whole cell extracts using mouse monoclonal GFP antibodies (BD Biosciences Pharmingen, San Diego, CA) and by fluorescence microscopy to detect synthesis of the GFP-Nup53 fusion protein. For Fig. 4-4, HeLa cells grown in 6 well culture dishes with coverslips were transfected with 2 μg of GFP-Nup53 plasmids using *Trans*IT-HeLaMONSTER Transfection kit as per manufacturer protocol (Mirus Bio Corporation, Madison, WI).

2.13 Isolation of HeLa cell extracts

In order to isolate total HeLa cell extracts, cells were detached from the culture wells by incubating with 0.05% Trypsin-EDTA (Invitrogen, Burlington, Ontario) for 5 min at 37°C. Cells were washed with PBS and counted with a hemocytometer. Cells were then pelleted, solubilized in SDS-PAGE sample buffer at a concentration of 10^5 cells/10 μl of sample buffer, and sonicated for 15 seconds before incubation at 80°C for 20 min. Proteins from 10 μl of each sample were separated by SDS-PAGE and transferred to nitrocellulose for subsequent Western blotting.

2.14 Immunofluorescence

HeLa cells grown on coverslips were washed twice with PBS and then fixed in 3.7% formaldehyde in PBS for 20 min at room temperature. Cells were then permeabilized with 0.2% Triton X-100 in PBS for 5 min at room temperature and subsequently blocked in 2% skim milk powder in PBS-T (PBS containing 0.1% Tween 20) for 2 h. For detection of Nup93, Nup205, and Mad1, and in the localization studies presented in Fig. 4-4, cells were pre-extracted with 0.2% Triton X-100 in PBS prior to fixation with formaldehyde. Primary antibody incubations were carried out for 1 h at room temperature using rabbit antibodies directed against Nup53 (above), Nup93 (above) emerin (kindly provided by B. Burke), Nup107 (kindly provided by V. Doye), lamin B (Chaudhary and Courvalin, 1993), lamin A/C (Chaudhary and Courvalin, 1993), and guinea pig antibodies directed against Nup155 and Nup 205 (kindly provided by V. Cordes). Nup358, Nup214, Nup153, and p62 were detected with mAb414. For detection of Nup53, antibodies were first affinity purified as described (Harlow and Lane, 1988) with modifications (Marelli et al., 1998). Following incubation with primary antibodies, coverslips were washed three times with PBS-T over a period of 45 min. Antibody binding was detected with donkey anti-mouse antibodies conjugated to Cy3 or FITC, donkey anti-rabbit antibodies conjugated to Cy3, or donkey anti-guinea pig antibodies conjugated to Cy3 (Jackson ImmunoResearch Laboratories, Westgrove, PA). Nuclear DNA was visualized with the DNA-specific Hoechst No. 33342 Dye (Sigma-Aldrich, Oakville, Ontario). Digitonin permeabilization experiments were performed as described (Joseph et al., 2002). Briefly, cells on coverslips were incubated with 0.005% high purity digitonin (Calbiochem-Novabiochem, San Diego, CA) in transport buffer (110 mM

KOAc, 20 mM HEPES pH 7.3, 2 mM $Mg(OAc)_2$, 0.5 mM EGTA, 0.2 mM DTT, and 1 μg/ml each of leupeptin, pepstatin, and aprotinin) for 5 min at room temperature prior to fixation with 3.7% formaldehyde. All subsequent steps were performed as described for other immunofluorescence experiments with the exception that transport buffer was used instead of PBS-T. For visualization of immunofluorescent images, coverslips were mounted in Vectashield mounting medium (Vector Laboratories, Burlington, Ontario). All microscopic images were obtained on a Zeiss Axiovert 100M coupled with a Zeiss LSM510 laser scanning system. Images were obtained with a 63X plan-apochromat objective.

2.15 siRNAs for depletion of nups

All siRNAs (Qiagen-Xeragon) listed below were designed as described in Elbashir et al., 2001 and targeted the human versions of the nups. Concentrations at which the individual siRNAs were used are also indicated. Nup53 (5'-AACCUGCAA GUACUCCUAGGA-3', 480nM), Nup107 (5'-GAAAGUGUAUUCGCAGUUA-3', 8.5 nM), NDC1 (5′-UCAGUGCCACCAUUAGUUA-3′, 35 nM), gp210 (5′-GAACCUCCA UUCACUACAA-3′, 35 nM), Nup93 in Fig 3-7 (5'-GACGCCCUUGACUUUACUC-3', 480 nM), Nup93 in Fig. 4-1(5′-GCGCUAAUUUACUACUGCA-3′, 4.2 nM). HeLa cells were incubated with indicated concentrations of siRNA using Oligofectamine (Invitrogen, Burlington, Ontario) for either 48 or 72 h as noted in the respective figure legends. As controls, cells were exposed to either Oligofectamine alone or one of two ineffective siRNAs. For Fig. 3-3 and 3-7, this was referred to as non-sense siRNA consisting of a scrambled sequence of the Nup53 siRNA. For Fig. 4-1, a control siRNA with the following sequence was used (5′-CUGUGCAAGCCGUUGUGUA-3′).

2.16 RT-PCR

The RNeasy RNA-preparation kit (Qiagen, Mississauga, Ontario) was used to isolate total RNAs from HeLa cells and the reverse transcription reactions were carried out using the OneStep RT-PCR kit (Qiagen, Mississauga, Ontario). Template RNA (0.5 μg) and gene-specific primers (0.6 μM) for both Nup53 and Nup155 were used in a final reaction volume of 50 μl. RT-PCR products were analyzed by agarose gel electrophoresis and ethidium bromide staining.

2.17 Western blotting

For the analysis of rat liver NE fractions, proteins were resuspended in SDS-PAGE sample buffer and 1 A_{260} unit per lane analyzed by SDS-PAGE. Post-transfer Nitrocellulose membranes were incubated in 5% skim milk powder in PBS containing 0.1% Tween 20 for 1 h to block non-specific binding. Antibodies were incubated with the membranes for 1 h at room temperature using rabbit polyclonal antibodies directed against Nup53, gp210, Nup205 (kindly provided by D. Forbes), Nup93 (BD Biosciences Pharmingen, San Diego, CA), lamin B (Chaudhary and Courvalin, 1993), lamin A/C (Chaudhary and Courvalin, 1993), Nup107 (kindly provided by V. Doye) and mouse monoclonal antibodies directed against Nup153 (kindly provided by M. Lohka) and α-tubulin (Sigma-Aldrich, Oakville, Ontario). Nup358, Nup214, Nup153, and p62 were detected with mAb414 (BAbCo, Berkeley, CA). Rat antibodies were used to detect

Mad1 (kindly provided by T. Yen) and Guinea pig antibodies used to detect Nup155 (kindly provided by V. Cordes). Primary antibodies were detected with donkey anti-rabbit, sheep anti-mouse (Amersham Biosciences Inc., Baie D'Urfe, Quebec), goat anti-guinea pig, and goat anti-rat (Sigma-Aldrich, Oakville, Ontario) HRP-conjugated secondary antibodies and the ECL system (Amersham Biosciences Inc., Baie D'Urfe, Quebec).

2.18 Cell cycle analysis in Nup53 depleted HeLa cells

Several different experiments to determine cell cycle effects of Nup53 depletion were performed on HeLa cells that were transfected with either non-sense or Nup53 siRNAs. For FACS analysis, cells were detached from the culture wells by incubating with 0.05% Trypsin-EDTA for 5 min at 37°C. The cells were subsequently fixed in 20°C 70% ethanol and incubated overnight at 4°C. The fixed cell pellets were washed with PBS and then incubated with 0.1% Triton X-100, 0.2 mg/ml propidium iodide, and 0.2 mg/ml DNase-free RNase A in PBS for 1 h at room temperature. FACS data was collected on a FACS Scan (Becton Dickinson, San Jose, CA) and analyzed using CellQuest software.

The viability of control and Nup53 depleted cells was assayed using the trypan blue dye incorporation assay. Cells were trypsinized off of the culture dishes, pelleted, and washed with PBS. The washed cell pellets were resuspended in PBS and 2 volumes of trypan blue dye was added to the resuspended cells. Following a 5 min incubation, the number of cells that remained colorless, indicating they were alive, was compared to the number of dead cells that took up the dye and appeared blue. The number of live cells was expressed as a percentage of the total cells representing cell viability.

The proportion of cells in S-phase in asynchronous non-sense and Nup53 siRNA treated populations was determined using the bromo deoxyuridine (BrdU) incorporation assay. HeLa cells were treated with 40 µM BrDu at 37°C and 5% CO_2 for 1 hour. Following this incubation, the cells were fixed with 2% paraformaldehyde in PBS and permeabilized in 0.5% Triton X-100. Cellular DNA was then denatured by a treatment of 4N HCl for 15 min at room temperature. Following extensive washing, cells that had incorporated BrDu were detected using a monoclonal antibody directed against BrDu (Sigma). The coverlips were processed for confocal microscopy as described in 2.14 and the number of BrDu cells quantitated as a percentage of the total cell population.

The mitotic indexes of asynchronous control and Nup53 depleted HeLa cell populations were obtained by DAPI staining, and visualization of the cells in M-phase by fluorescence microscopy. Similarly, the ability of the cells to arrest in the presence of microtubule destabilizing drugs was assessed by treatment with nocodazole at a concentration of 100 ng/ml for 8 h. Quantitation of M-phase arrested cells was performed as described above for mitotic index determination.

2.19 *Xenopus* egg extract preparation

Cytosol from *Xenopus eggs* was prepared as described (Hartl et al., 1994) with the following changes: After the first low speed centrifugation, the crude low speed extract was centrifuged twice at 225,000 *g* for 40 min at 4°C to obtain the cytosol as a clear supernatant. Floated membranes were prepared as described (Wilson and Newport,

1988) and the two lowest density membrane fractions were combined. Sperm heads were prepared from *Xenopus* testis (Gurdon, 1976).

For NE assembly reactions, 10 µl of cytosol was incubated with 0.5 µl of sperm heads (3000 sperm heads /µl) for 10 min at 20°C to allow for chromatin decondensation. The reaction was then continued by the addition of 0.5 µl of floated membranes, 0.8 µl of energy mix (50 mM ATP, 500 mM creatine phosphate, 10 mg/ml creatine kinase) and 0.2 µl of oyster glycogen (20 mg/ml USB Amersham) and incubation at 20°C for 2 h. For membrane staining, 0.2 µl of 0.1 mg/ml DilC$_{18}$ in DMSO was added for 5 min prior to fixation with 2% paraformaldehyde and 0.5% glutaraldehyde in 80 mM Pipes pH 6.8, 1 mM $MgCl_2$, 150 mM sucrose, and 0.5 µg/ml DAPI. Samples to be processed for immunofluorescence were fixed in freshly prepared 3.7% paraformaldehyde before centrifugation through a cushion of 30% sucrose in PBS onto poly-L-Lysine coated coverslips. Both the membrane staining and immunofluorescence samples were mounted for fluorescence microscopy using Prolong Gold antifade reagent (Molecular Probes). Images were acquired using a wide field optical sectioning deconvolution microscope (Delta Vision; Applied Precission, Issquah, WA). Most images were acquired with 100 x 1.4 Plan-apochromat objective. Three-dimensional images were acquired and deconvolved. Single optical sections or maximum intensity projections were subsequently used.

2.20 Depletion of Nup53 from *Xenopus* oocytes

Saturating amounts of non immune rabbit IgG or rabbit *Xenopus* Nup53 antibody sera were crosslinked to Protein A-Sepharose (Pharamacia) in the presence of 10 mM dimethylpimelimidate (Sigma) to produce resins for mock or Nup53 depletion from *Xenopus egg* extracts. High speed cytosol was incubated with the antibody column for two rounds of 30 min each, at 4°C. Cytosol was used directly for NE assembly reactions or frozen with 3% (w/v) glycerol.

2.21 Transmission Electron Microscopy

In vitro nuclear assembly was performed as described above, scaled up to 60 μl and processed for TEM as described (Macaulay and Forbes, 2006). The assembly reactions containing reconstituted nuclei or intermediates were placed on ice for 15 min to depolymerize the microtubules. The nuclei were fixed by the addition of 0.4 ml of ice cold fixation buffer (25 mM Hepes, 25 mM Pipes, pH 7.2, 1 mM EGTA, 50 mM KCI, 2 mM magnesium acetate, and 5% sucrose) containing 1% glutaraldehyde (Sigma), and incubation on ice for 1 h. The fixed nuclei were pelleted for 5 seconds and the supernatant was carefully aspirated. 0.2 ml of ice cold fixation buffer containing 10 mg/ml tannic acid and 2.5% glutaraldehyde was added to the nuclear pellet. This was incubated on ice for 2 h, and microfuged for 5 seconds to pellet any resuspended nuclei. The nuclear pellet was then washed with 0.4 ml ice cold 0.1 M sodium eacodylate pH 7.2 and postfixed with 1% OsO_4 on ice for 1 h. The nuclear pellet was washed four times with 0.4 ml ice cold H_2O and stained with 0.5% uranyl acetate for 16 h at 4°C. Samples were dehydrated in ethanol, embedded in resin, sectioned, and stained with uranyl acetate and lead citrate.

2.22 Analysis of Nup53 phosphorylation

To determine if human Nup53, like its yeast counterpart Nup53p, was phosphorylated during M-phase, HeLa cells were treated with nocodazole at a concentration of 1 μg/ml for 16 h. The detached arrested cells were collected, centrifuged, and washed in PBS before resuspension in SDS-PAGE sample buffer. In order to investigate if the decreased mobility of Nup53 observed in cells treated with nocodazole was due to phosphorylation, a phosphatase assay was performed. HeLa cells growing in a 35 mm culture dish were treated with nocodazole as indicated above. The arrested cells were collected and centrifuged at 1500 *g* for 5 min at 4°C. 150 μl of ice cold lysis buffer (50 mM Tris HCl pH 8.4, 5 mM $MgCl_2$, 1 mM DTT and Complete protease inhibitor cocktail) was added to the pelleted arrested cells and they were lysed by sonication on ice. The cell lysate was centrifuged at 14,000 rpm for 20 min at 4°C, and the supernatant was carefully collected and transferred to a fresh tube. 15 units of Calf intestinal phosphatase (CIP) (Roche) was added directly to this cytosolic fraction and incubated at 30°C for 30 min. Following this incubation, 200 μl of SDS-PAGE sample buffer was added. Samples were separated by SDS-PAGE, transferred to nitrocellulose, and analyzed by Western blot with Nup53 antibodies.

Cell fractionation by differential centrifugation (Chaudhary et al., 1993) was implemented to examine fractionation properties of unphosphorylated and phosphorylated Nup53. Asynchronous and nocodazole arrested HeLa cells growing in two 100 mm culture dishes each were collected and centrifuged at 1500 *g* for 10 min at 4°C. They were then resuspended in 5 ml of ice cold PBS containing 20 μM cytochalasin B and further incubated on ice for an additional 20 min. Each of the cell samples were split into two equal volumes and centrifuged at 1500 *g* for 10 min at 4°C then resuspended in either 5 ml of hypotonic buffer (10 mM Tris pH 7.5, 10 mM NaCl, 1.5 mM $MgCl_2$, 20 μM cytochalasin B, Complete protease inhibitor cocktail) or hypotonic buffer containing a mixture of phosphatase inhibitors (2.5 mM sodium pyrophosphate, 0.1 mM sodium orthovanadate, 2 mM sodium fluoride, 5 μM aluminum ammonium sulfate). Nocodazole arrested or asynchronous HeLa cells in either hypotonic buffer or hypotonic buffer containing phosphatase inhibitors were then incubated on ice for 15 min. The cells were homogenized for 15 strokes using a dounce homogenizer at 4°C and the cell homogenate was then layered on a 3 ml cushion of hypotonic buffer containing 30% sucrose and centrifuged at 2000 *g* for 10 min at 4°C. The supernatant was carefully collected and centrifuged at 140,000 *g* for 30 min at 4°C. The pellet of this high speed centrifugation, containing total membranes was resuspended in SDS-PAGE sample buffer. Proteins were precipitated from the supernatant by addition of 10% final concentration of trichloroacetic acid and incubation on ice for 2 h. The precipitated cytosolic proteins were collected by centrifugation and resuspended in SDS-PAGE sample buffer.

For *in vivo* labelling of the ER using the ER-Tracker dye (Molecular Probes), nocodazole arrested HeLa cells stably expressing GFP-Nup53 were washed in PBS, DMEM, and then resuspended in DMEM containing ER-Tracker at a final concentration of 100 nM. The cells were incubated at 37°C for 30 min before visualization of the live cells by confocal miscroscopy. The extent of phosphorylation of GFP-Nup53 was assessed by SDS-PAGE and Western blot with antibodies directed against GFP.

2.23 *In vitro* binding experiments with ss- and dsDNA cellulose

Nup53$^{1-326}$, Nup53$^{167-252}$, Nup53$^{1-143}$, Nup53$^{204-326}$, and Nup93 were expressed and purified as in Section 2.6 and cleaved from the GT column using PreScission Protease in buffer containing 50 mM Tris pH 7.5, 150 mM NaCl, 0.01% Tergitol (Type NP-40) (Sigma), 10% Glyerol, and 10 μg/ml BSA. This buffer was also used for equilibration of the DNA cellulose resins and subsequent washing steps. The above purified recombinant proteins were inbuated with 20 μg of ssDNA cellulose at a final concentration of 0.1 μg/μl for 30 min at room temperature. Following washing steps, the bound proteins were eluted from the resin by boiling in SDS-PAGE sample buffer and analyzed using SDS-PAGE and Coomassie blue staining.

Using pGEX-6P1-Nup53 as a template, site-directed mutagensis was performed using the QuikChange Site-Directed Mutagensis Kit (Stratagene) with primers designed from QuickChange Primer Design software at http://labtools.stratagene.com. The following codons, either singly or in combination as indicated were mutated: serine 187 to glutamine, lysine 223 to glutamine, tryptophan 175 to alanine, phenylalanine 179 to alanine, tryptophan 210 to alanine, and phenylalanine 179 and tryptophan 210 to alanines. The GST fusions of these point mutations were expressed and purified as decribed above and used for *in vitro* binding experiments, identical to those described above, using either ss- or dsDNA cellulose.

Chapter III: *Vertebrate Nup53 interacts with the nuclear lamina and is required for the assembly of a Nup93-containing complex*[*]

---

[*] This work was reproduced from Hawryluk-Gara, L. A., E. K. Shibuya, and R. W. Wozniak. (2005). **Vertebrate Nup53 interacts with the nuclear lamina and is required for the assembly of a Nup93-containing complex**. *Molecular Biology of the Cell* 16: 2382-2394 by copyright permission of Garland Publishing, Incorporated.

3.1 Overview

The nuclear pore complex (NPC) is an evolutionarily conserved structure that mediates exchange of macromolecules across the nuclear envelope (NE). It is comprised of ~30 proteins termed nucleoporins that are each present in multiple copies. We have investigated the function of the human nucleoporin Nup53, the ortholog of *Saccharomyces cerevisiae* Nup53p. Both cell fractionation and *in vitro* binding data suggest that Nup53 is tightly associated with the NE membrane and the lamina where it interacts with lamin B. We have also shown that Nup53 is capable of physically interacting with a group nucleoporins including Nup93, Nup155, and Nup205. Consistent with this observation, depletion of Nup53 using small interfering RNAs causes a decrease in the cellular levels of these nucleoporins as well as the spindle checkpoint protein Mad1, likely due to destabilization of Nup53-containing complexes. The cellular depletion of this group of nucleoporins, induced by depleting either Nup53 or Nup93, severely alters nuclear morphology producing phenotypes similar to that previously observed in cells depleted of lamin A and Mad1. On basis of these data, we propose a model in which Nup53 is positioned near the pore membrane and the lamina where it anchors a NPC subcomplex containing Nup93, Nup155, and Nup205.

3.2 Results

3.2.1 Characterization of a vertebrate counterpart to the yeast nucleoporin Nup53p

Amino acid sequence analysis had previously identified potential vertebrate orthologs of the *Saccharomyces cerevisiae* nucleoporin Nup53p (see Fig. 1 in Marelli et al., 1998). These multiple open reading frames (ORFs) encode proteins that contain conserved regions including phenylalanine-glycine (FG) repeat motifs, several potential phosphorylation sites, and a putative COOH-terminal amphipathic helix (Marelli et al., 2001).

An unspecified vertebrate ORF with similarity to yeast Nup53p has previously been tagged with GFP and, following expression of the fused gene in human HeLa cells, the chimeric protein (termed Nup35-GFP) was localized to the NE in a punctate pattern characteristic of NPC localization (Cronshaw et al., 2002). We have elicited polyclonal antibodies in rabbits directed against a recombinant form of the putative *Xenopus* Nup53 to use as a tool to examine the localization and function of the endogenous form of the vertebrate orthologs. Following affinity purification, these antibodies were used to examine the localization of the putative human Nup53 in HeLa cells using immunofluorescence microscopy. The antibody decorated the surface of the NE in a punctate pattern coincident with the position of NPCs, as judged by co-localization with nups recognized by the monoclonal antibody mAb414 (Fig. 3-1A). A similar pattern was detected with a GFP-tagged chimera of the human ORF (Fig. 3-1B). In addition, Western blotting analysis was used to evaluate the subcellular fractionation properties of the putative vertebrate Nup53. The results of these experiments demonstrated that the endogenous protein was enriched in fractions of purified rat liver nuclei and NEs (Fig. 3-1C) further supporting its classification as a nup. We propose to designate this protein as Nup53 (in contrast to the previously

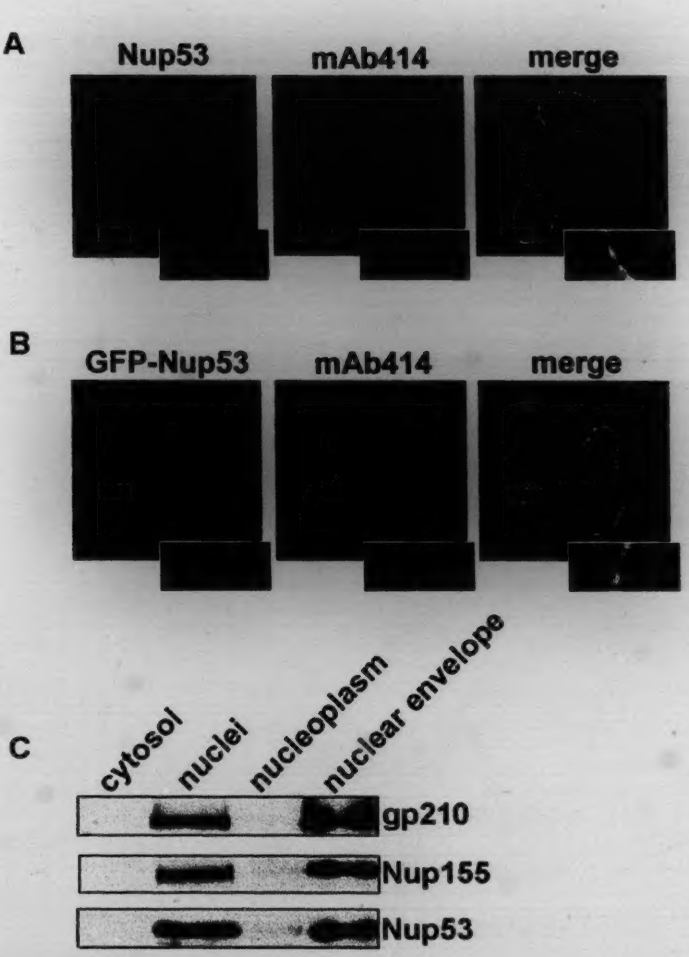

Figure 3-1. Localization of endogenous Nup53 to the NPC.

(A) HeLa cells were processed for immunofluorescence microscopy and probed with affinity-purified rabbit antibodies directed against a putative vertebrate counterpart of Nup53 and a mouse monoclonal antibody (mAb414) that binds a subset of FG-nups. Binding was detected with Cy3-labeled and FITC-labeled secondary antibodies, respectively. Images of both fluorophores were acquired using a confocal microscope. Merged images are shown on the right. Magnifications of portions of the NE are indicated with a white box. (B) HeLa cells were transfected with a plasmid encoding GFP-Nup53 and a stable cell line was isolated. Cells were fixed and probed with mAb414 as in (A) but detected with Cy3-labeled secondary antibodies. The cellular distribution of GFP-Nup53 (green), the mAb414 react nups (red), and a merged image are shown. Bar, 10 µm. (C) Proteins derived from indicated rat liver subcellular fractions (1 A_{260} unit/lane) were separated by SDS-PAGE and probed with Nup53 specific antibodies, as well as antibodies directed against the NPC proteins gp210 and Nup155. Nup53 was detected in fractions enriched in nuclei and nuclear envelopes.

proposed Nup35). This nomenclature more clearly depicts the relationships between nups of different species and is consistent with that which has been used to name vertebrate nups first identified in yeast (Belgareh et al., 2001).

3.2.2 Nup53 is tightly associated with the nuclear membrane and lamina

In yeast, Nup53p is part of a defined subcomplex of nups (Marelli et al., 1998; Fahrenkrog et al., 2000; Lusk et al., 2002) and Nup53p has been suggested to interact directly with the NE membrane (Marelli et al., 2001). We have examined the association of vertebrate Nup53 with NEs using differential extraction procedures and Western blotting. For these experiments, isolated rat liver NEs were extracted with salts, detergents, or urea, and the extracted proteins were separated from the membrane and/or insoluble lamina by centrifugation. We have previously used urea extraction procedures to selectively extract nups from the NE membrane and the nuclear lamina (Radu et al., 1993). Extraction of NEs with 2M urea quantitatively releases Nup93, Nup153, and Nup155 from a membrane fraction containing the integral protein gp210 (Fig. 3-2A). In contrast, the majority of Nup53 remains in a pelletable fraction with the lamins (as exemplified by lamin B). The extraction of Nup53 also parallels that of lamins at higher concentrations of urea, where the majority of Nup53 and lamin B was extracted from the NE with 7 M urea (Fig. 3-2A). Similarly, we observed that, while the treatment of NEs with 2 M NaCl partially extracted Nup93, Nup153, and Nup155, Nup53 remained exclusively in the pellet fraction with the lamins.

The most likely explanation for these results is that Nup53 interacts more tightly with either the membrane and/or the lamina than the other nups examined. In an effort to

Figure 3-2. Nup53 interacts tightly with the nuclear envelope membrane and lamina.

(A) Purified rat liver NEs (50 A_{260} units) were extracted with 1 M NaCl, 2 M NaCl, 2 M urea or 7 M urea and then centrifuged to produce a supernatant fraction (S) and a membrane pellet (P) fraction. The equivalent of 1 A_{260} unit of NEs and S and P fractions of extractions were separated by SDS-PAGE and proteins were analyzed by Western blotting using specific antibodies. (B) Alternatively, NE membranes were extracted with Triton X-100 and an insoluble NPC and lamina-containing fraction was recovered by centrifugation. This extracted NE (eNE) fraction was then treated with increasing concentrations of NaCl to release nups from the lamina. Following centrifugation to produce supernatant and pellet fractions, proteins were analyzed by Western blotting as in (A). (C) A previously described extraction protocol of NEs (Matunis et al., 1996; Cronshaw et al., 2002) that concludes with empigen BB induced release of NPCs from the lamina was also used to evaluate the association of Nup53 with the lamina. Following extraction with empigen BB and centrifugation, proteins in a nup-enriched (S) fraction and a lamin-enriched (P) fraction were analysis by Western blotting using the antibodies specific to the indicated proteins.

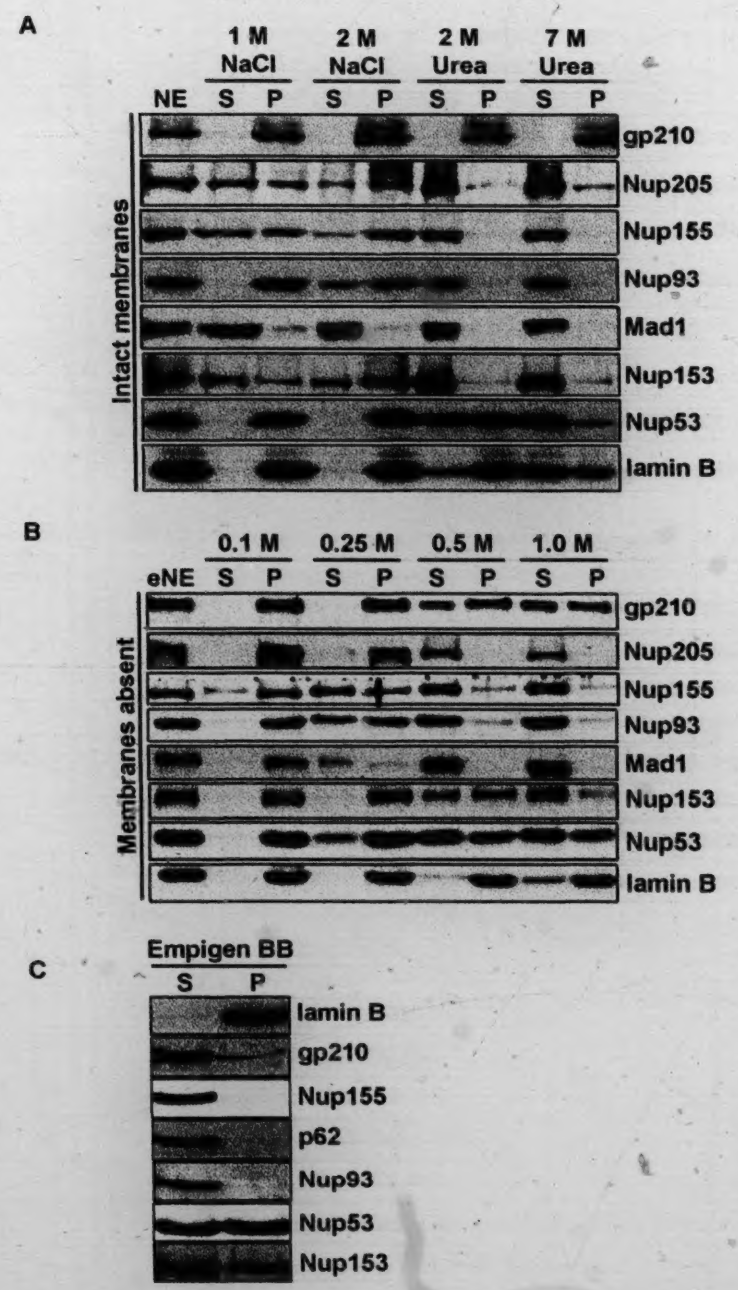
A
1 M NaCl
2 M NaCl
2 M Urea
7 M Urea
NE
S
P
Intact membranes
gp210
Nup205
Nup155
Nup93
Mad1
Nup153
Nup53
lamin B
B
0.1 M
0.25 M
0.5 M
1.0 M
eNE
Membranes absent
gp210
Nup205
Nup155
Nup93
Mad1
Nup153
Nup53
lamin B
C
Empigen BB
S
P
lamin B
gp210
Nup155
p62
Nup93
Nup53
Nup153

Figure 3-2. Nup53 interacts tightly with the nuclear envelope membrane and lamina.

differentiate between these possibilities, we first extracted NEs with the nonionic detergent Triton X-100. This treatment releases most NE membrane proteins with the exception of those that are tightly associated with the pelletable fraction containing NPCs attached to the lamina (Schirmer et al., 2003). To compare the extractability of various nups from the lamina, the pellet fraction was then extracted with increasing concentrations of NaCl. As shown in Fig. 3-2B, Nup93 and Nup155 are efficiently extracted from the lamina by 0.5 M NaCl, whereas Nup53, as well as Nup153, were more resistant to extraction with ~50% of each being extracted at similar concentrations of NaCl. These observations are consistent with previously proposed interactions between Nup153 and the lamina (Smythe et al., 2000).

A differential extraction of Nup53 and Nup153 from the nuclear lamina was also observed when NEs were sequentially extracted with a Triton X-100/SDS cocktail followed by the zwitterionic detergent Empigen BB. Matunis and coworkers have previously shown that this procedure releases the nups into a soluble supernatant fraction and produces a pellet fraction consisting largely of lamins (Matunis et al., 1996; Cronshaw et al., 2002). However, Western blotting of these fractions showed that approximately 50% of Nup53 and Nup153 remained associated with the lamina fraction following Empigen BB extraction (Fig. 3-2C). These represented a significantly higher level of retention with the lamina than observed with gp210, p62, and Nup155 (Fig. 3-2C) and is higher than previously reported for most nups (Fontoura et al., 1999; Cronshaw et al., 2002). These results further support the idea that Nup53, like Nup153, is physically linked to the nuclear lamina.

3.2.3 Nup53 interacts with Nup93, Nup155, and Nup205

We further investigated the physical interactions between Nup53 and neighboring proteins in the NE by attempting to reconstitute these interactions *in vitro*. For these experiments, rat liver NEs were treated with a combination of 1% Triton X-100 and 400 mM NaCl to solubilize the nups and a significant fraction of the lamins. Following dilution, the extract was incubated with a purified, recombinant GST-Nup53 fusion protein immobilized on glutathione Sepharose beads. NE proteins that bound GST-Nup53 were detected using SDS-PAGE and silver staining. Two species of approximately 90 and 200 kD were identified (Fig. 3-3A). Mass spectrometry analysis of peptide fragments derived from these polypeptides revealed that the 200 kD and 90 kD proteins were Nup205 and Nup93, respectively, two nups that had previously been shown to interact with each other (Grandi et al., 1997). These results were confirmed by Western blotting using Nup205 and Nup93 antibodies, which recognized the corresponding bands (Fig. 3-3A). In an effort to identify any other Nup53-interacting partners, we also probed the eluted fraction with a variety of other antibodies. Interestingly, Western blotting using antibodies specific to Nup155 and lamin B, detected both proteins in the GST-Nup53 bound fraction (Fig. 3-3A). In contrast, we failed to detect a variety of other nups, including those nups recognized by mAb414 (Fig. 3-3A). Moreover, lamins A and C were generally not detected in bound fractions (Fig. 3-3A).

In an effort to begin to map the interactions between Nup53 and the nups detected in the GST pulldown assay, we tested whether purified recombinant GST-Nup53 could bind directly to recombinant Nup93. When purified Nup93 was incubated with GST-Nup53 immobilized on glutathione Sepharose beads, it was largely retained in the bound

Figure 3-3. Identification of Nup53 interacting partners using *in vitro* binding assays.
(A) Purified rat liver NEs were extracted with 400 mM NaCl and 1% Triton X-100. Following centrifugation to remove insoluble material, the supernatant fraction, containing nups and lamins, was diluted 3.75 fold (NE extract, 1 A_{260} unit loaded on gel) and 25 A_{260} units were incubated with purified recombinant GST-Nup53 or GST alone immobilized on glutathione Sepharose 4B beads. Following binding and washing steps, the bead-bound proteins were eluted and 10% of the total bound fraction was separated by SDS-PAGE. The proteins were then detected with silver staining (SS). Protein species that specifically bound Nup53 are indicated with an arrow. Samples were also analyzed by Western blotting (WB) using polyclonal antibodies directed against the indicated proteins or mAb414 to detect Nup358, Nup214, Nup153, and p62. (B) Purified recombinant Nup93 was incubated with GST-Nup53 or GST alone immobilized on glutathione Sepharose 4B beads. Following washing, beads were eluted with sample buffer. Proteins were separated by SDS-PAGE and analyzed by Coomassie Blue staining (CB) or Western blotting (WB) using antibodies directed against Nup93. The positions of mass markers in kilodaltons are indicated.

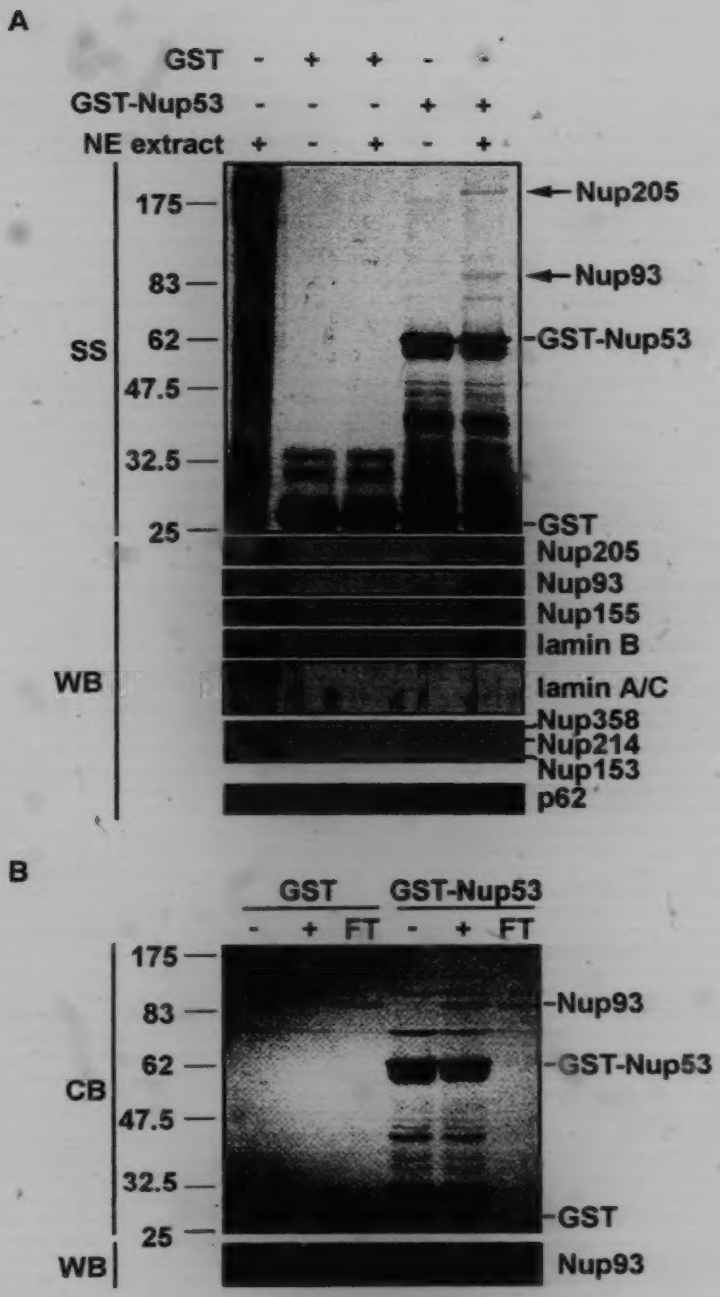
A
GST - + + - -
GST-Nup53 - - - + +
NE extract + - + - +
SS
175
83
62
47.5
32.5
25
Nup205
Nup93
GST-Nup53
GST
WB
Nup205
Nup93
Nup155
lamin B
lamin A/C
Nup358
Nup214
Nup153
p62
B
GST
GST-Nup53
- + FT - + FT
CB
175
83
62
47.5
32.5
25
Nup93
GST-Nup53
GST
WB
Nup93

Figure 3-3. Identification of Nup53 interacting partners using *in vitro* binding assays.

fraction as detected by Coomassie blue staining and Western blotting with anti-Nup93 antibodies (Fig. 3-3B). In contrast, no binding of Nup93 was detected to GST alone. This result suggests a direct interaction between Nup53 and Nup93.

3.2.4 Depletion of Nup53 inhibits the assembly of interacting nups and the spindle checkpoint protein Mad1 into the NPC

In an effort to investigate cellular functions of Nup53, small interfering RNAs (siRNAs) specific for Nup53 mRNA were transfected into HeLa cells to deplete cellular levels of Nup53. Following transfection, we monitored changes in both the level of mRNA and protein using RT-PCR and Western blotting, respectively. HeLa cells were transfected either with transfection reagent alone, non-sense siRNAs, or with human Nup53-specific siRNA duplexes. Levels of Nup53 mRNA were significantly reduced 48 hours following transfection while the level of mRNA encoding another nup, Nup155, was not affected, demonstrating the specificity of this approach (Fig. 3-4A). The reduced level of Nup53 mRNA was accompanied by a depletion of Nup53 as detected by Western blotting (Fig. 3-4A). Consistent with these observations, immunofluorescence analysis revealed that levels of Nup53 at the NE were greatly reduced in 50-70% of the Nup53 siRNA treated cells, while cells treated with non-sense siRNAs showed no change in the punctate nuclear rim staining (Fig. 3-4B).

The siRNA-mediated depletion of Nup53 was accompanied by distinct changes in cell growth. As shown in Figure 3-5A, cell cultures treated with Nup53-specific siRNAs doubled at a rate approximately half that observed in cultures treated with non-sense siRNAs. The decreased growth rate observed was not due to changes in cell viability

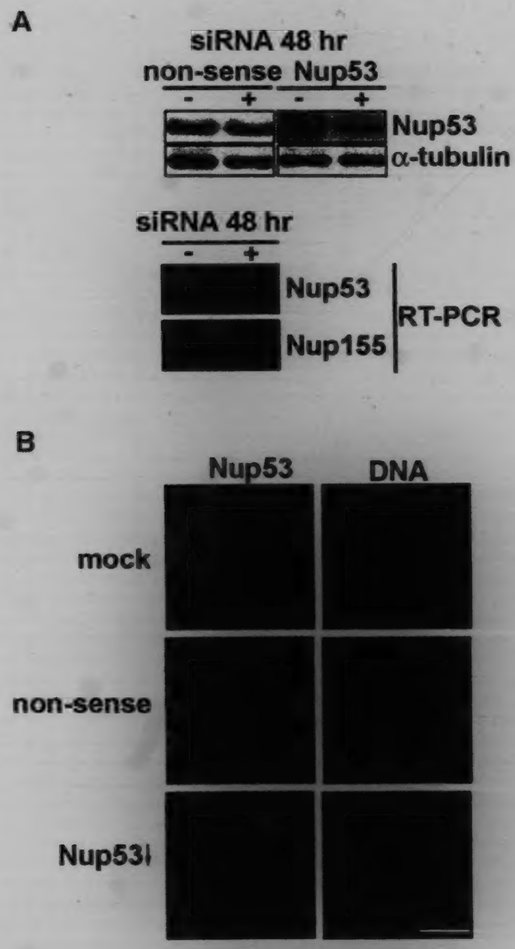

Figure 3-4. ***In vivo*** **depletion of Nup53 using small interfering RNAs.**

(A) HeLa cells were incubated for 48 h in the presence of either transfection reagent alone (-) or siRNA (+) corresponding to non-sense siRNAs (scrambled sequence) or Nup53 siRNAs. Samples were then collected and the cellular levels of Nup53 and α-tubulin (for comparison of total protein loaded in each fraction) were analyzed by Western blotting of total cell extracts. Total RNA was isolated from cells that were either treated with non-sense siRNAs (-) or Nup53 siRNAs (+) for 48 h. The mRNA levels of Nup53 and Nup155 were analyzed by RT-PCR. (B) HeLa cells growing on coverslips were incubated for 48 h with transfection reagent alone (mock), non-sense siRNAs (non-sense) or Nup53 (Nup53) siRNAs and processed for immunofluorescence. Cells were probed with anti-Nup53 antibodies and binding detected with Cy3-labeled secondary antibodies. Nuclear DNA was detected by staining with the DNA-binding dye Hoechst. Bar, 10 μm.

(Fig. 3-5C). Moreover, several assays suggested that the Nup53-depleted cells exhibited a general growth inhibition as they were not delayed in progression through a specific phase of the cell cycle. FACS analysis of both Nup53-depleted and non-depleted cells revealed similar profiles (Fig. 3-5B). In addition, the number of cells in S-phase (as detected using bromodeoxyuridine labeling) and M-phase (as detected by Hoechst staining) were similar, ~40% and ~4%, respectively, in depleted and non-depleted cultures (Fig. 3-5C).

We next examined the effects of removing Nup53 on the assembly and stability of other nups in the NPC. At 48 hours following Nup53 siRNA transfection, depleted cells were analyzed by immunofluorescence using antibodies directed against several nups including Nup93, Nup107, and the mAb414 reactive nups (p62, Nup214, Nup153, and Nup358). Levels of Nup107 and the mAb414 reactive nups were not affected by depletion of Nup53; however, we observed a striking decrease in the NE levels of Nup93 (Fig. 3-6A). The loss of NE bound Nup93 was accompanied by a corresponding decrease in cellular levels of Nup93 as determined by Western blot analysis of whole cells extracts (Fig. 3-6B). Similarly, we observed that other Nup53 interacting proteins (see above), including Nup155 and Nup205, were also present in reduced amounts in Nup53-depleted cells (Fig. 3-6A and 6B). The Nup53 depletion data are consistent with the idea that Nup53, Nup93, Nup205 and Nup155 interact with one another and that Nup53 is required for the assembly and/or stability of these nups within the NPC. As a complement to these studies, we also examined the effects of depleting Nup93 on levels of other members of this interacting group. As shown in Fig. 3-7, treatment of HeLa cells with

Figure 3-5. HeLa cells depleted of Nup53 exhibit a growth delay.

(A) Equal numbers of HeLa cells were transfected with either non-sense or Nup53-specific siRNA duplexes and incubated for the indicated times. At each time point, cells were collected, their viability was assessed using trypan blue and the number of viable cells was plotted versus time. Note, both non-sense and Nup53-specific siRNA treated cells showed a similar viability (>90%). The results shown are representative of three separate trials. (B) As in A, HeLa cells were transfected with either non-sense or Nup53-specific siRNA duplexes and incubated for the indicated times. Cells were then collected and processed for FACS analysis. The positions of the 2C and 4C peaks are indicated. (C) HeLa cells that were treated with non-sense or Nup53 siRNAs were treated for 48 hrs and analyzed as followed. Cell viability was assessed by trypan blue dye incorporation. The amount of cells in S-phase in treated populations was determined by BrDu incorporation. DAPI staining was used to stain the cells to allow for quantification of the percentage of the cell population in M-phase in asynchronous cultures. Finally, the ability of the treated cells to arrest in the presence of microtubule destabilizing drugs was assayed by nocodazole treatment, DAPI staining, and quantification of the percentage of M-phase cells in the population. The results shown are representative of three separate trials.

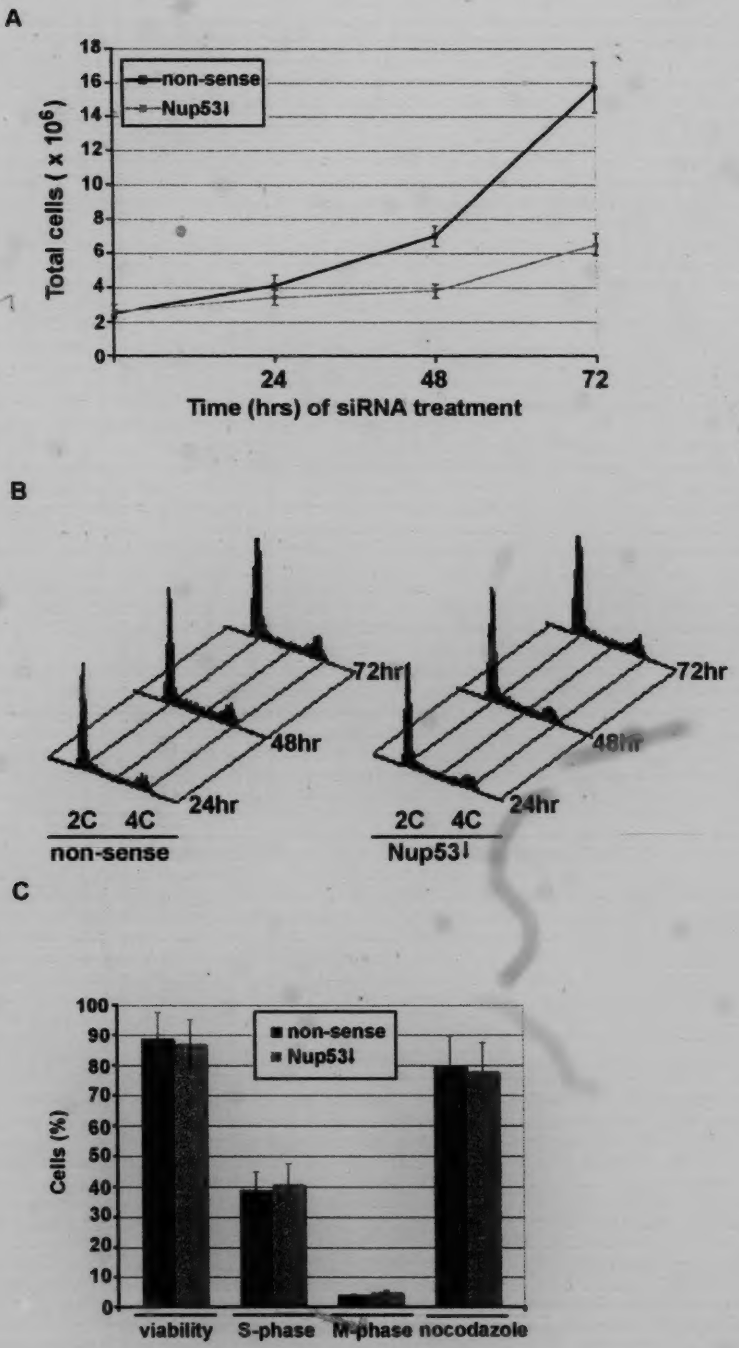

Figure 3-5. HeLa cells depleted of Nup53 exhibit a growth delay

Nup93-specific siRNAs reduced cellular levels of Nup93 and, as previously shown, the mAb414-reactive nups (Fig. 3-7A and 7B; Krull et al., 2004). Similarly, depleting Nup93 reduced cellular levels of Nup53, Nup155, and Nup205, but did not affect levels of Nup107, gp210, Mad1 or lamin B (Fig. 3-7). We have also performed *in vitro* binding experiments with GST-Nup93 and NE extracts similar to those described above using GST-Nup53 (Fig. 3-3). As shown in Fig. 3-7C, GST-Nup93 is capable of binding Nup53, Nup155, and Nup205, but not Nup107.

In yeast, physical and genetic interactions have also been detected between Nup53p and the spindle checkpoint protein Mad1p (Iouk et al., 2002). Similarly, Mad1 is bound to the vertebrate NPC during interphase (Campbell et al., 2001). We investigated the possible functional link between human Nup53 and Mad1 by examining the effects of siRNA induced Nup53 depletion on the localization and cellular levels of Mad1. As shown in Figure 3-6A, depletion of Nup53 was accompanied by decreased, but detectable, levels of Mad1 at the NPC as seen by immunofluorescence microscopy. Moreover, Western blot analysis showed that cellular levels of Mad1 were also decreased (Fig. 3-6B). In contrast, depletion of Nup93 had no effect on Mad1 levels (see Fig. 3-7A and 7B). Despite the reduced levels of Mad1 in the Nup53 depleted cells, we did not detect a clear defect in the spindle assembly checkpoint as judged by monitoring their ability to arrest in mitosis following treatment with microtubule destabilizing drugs (Fig. 3-5C). These results suggest sufficient Mad1 remains in the depleted cells to maintain an active checkpoint response.

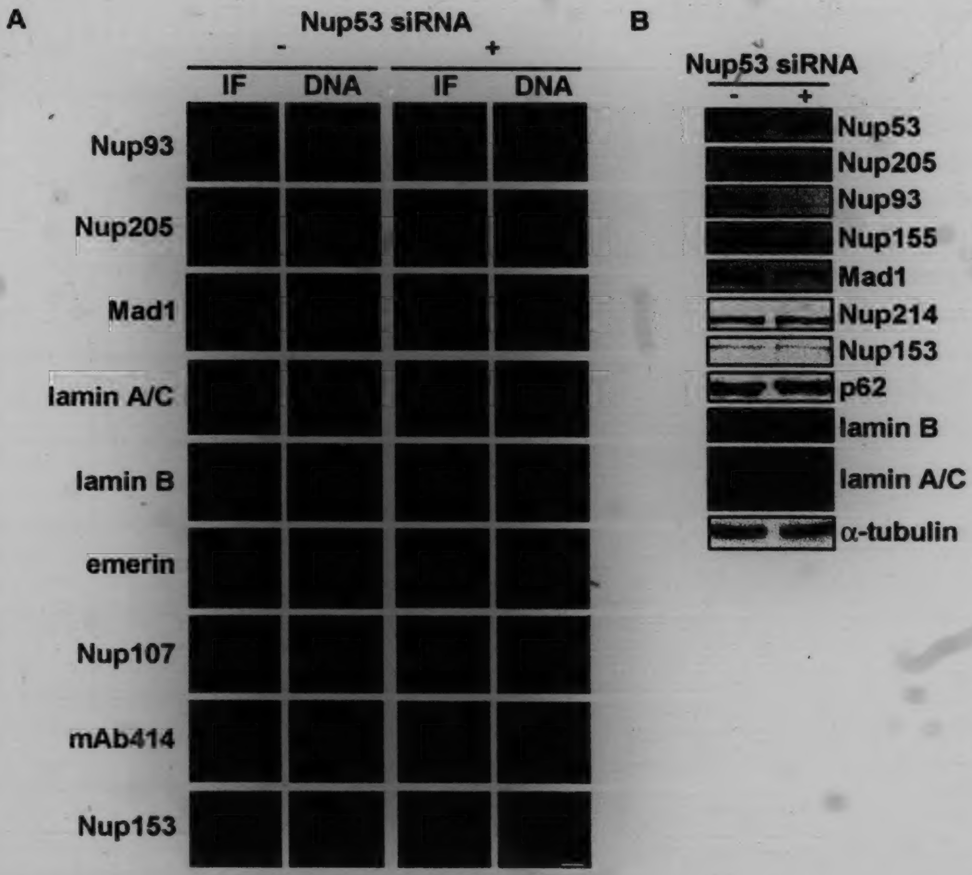
A
Nup53 siRNA
-
+
IF
DNA
IF
DNA
Nup93
Nup205
Mad1
lamin A/C
lamin B
emerin
Nup107
mAb414
Nup153
B
Nup53 siRNA
-
+
Nup53
Nup205
Nup93
Nup155
Mad1
Nup214
Nup153
p62
lamin B
lamin A/C
α-tubulin

Figure 3-6. *In vivo* depletion of Nup53 leads to co-depletion of a subset of interacting nups and the mitotic checkpoint protein Mad1.

(A) 48 hrs following the transfection of HeLa cells with either non-sense (-) or Nup53 (+) siRNAs, cells were processed for indirect immunofluorescence (IF). Samples were probed with antibodies directed against the indicated proteins and binding detected with Cy3-labeled secondary antibodies. Mab414 binding was detected with FITC-labeled secondary antibodies. Nuclear DNA was detected by staining with the DNA-binding dye Hoechst (DNA). Bar, 10 μm. (B) Cells were transfected as described in (A) and total cell extracts were isolated and proteins separated by SDS-PAGE. Western blot analysis was performed using antibodies directed against the indicated proteins. Note, mAb414 was used to visualize the levels of p62, Nup153, and Nup214. Antibodies directed against α-tubulin were used for comparing total protein loads in each fraction.

3.2.5 Depletion of Nup53 or Nup93 leads to aberrant nuclear morphology

Strikingly, cells that were depleted of Nup53 or Nup93 exhibited an aberrant nuclear morphology that was not observed in mock-treated or non-sense siRNA transfected cells (see Fig. 3-4B, 3-6A, and 3-7B). Nuclei of the depleted cells uniformly lost their round or oval shape, and often appeared elongated, lobular, or kidney-shaped. Their shape directly reflected the shape of the chromatin mass, as the NE membrane appeared to maintain direct contact with its surface (see Fig. 3-6A). To investigate the functional basis for this morphological defect, we looked at the patterns of various nuclear markers in non-sense siRNA transfected and the Nup53 or Nup93 depleted cells. In light of the data presented above suggesting that Nup53 interacts with nuclear lamins (Fig. 3-2B, 3-2C, and 3-3A), we examined lamin B and lamins A/C distribution in HeLa cells that had been treated for 48 hours with Nup53 siRNAs. We observed that the levels of lamin B, lamins A/C, and the inner nuclear membrane protein emerin, appeared to remain unchanged in these cells (see Fig. 3-6A, 3-6B). Similarly, the localization of lamin B was not affected in cells depleted of Nup93.

3.3 Discussion

Both morphological analysis and an accumulating body of biochemical data suggest that the NPC is composed of modular subunits consisting of specific subsets of nups. Several of these subcomplexes have been identified as a consequence of their resistance to extraction conditions that partially disassemble NPCs, while in other cases the functional complexes are inferred based on networks of interactions, both

Figure 3-7. *In vivo* depletion of Nup93 and the identification Nup93 interacting partners using in vitro binding assays.
(A) 48 hrs following the transfection of HeLa cells with either non-sense (-) or Nup93 (+) siRNAs, total cell extracts were isolated and proteins separated by SDS-PAGE. Western blot analysis was performed using antibodies directed against the indicated proteins. Antibodies directed against α-tubulin were used for comparing total protein loads in each fraction. (B) Cells were transfected as described in (A) and processed for indirect immunofluorescence (IF). Samples were probed with antibodies directed against the indicated proteins and binding detected with Cy3-labeled secondary antibodies. Mab414 binding was detected with FITC-labeled secondary antibodies. Nuclear DNA was detected by staining with the DNA-binding dye Hoechst (DNA). Bar, 10 mm. (C) Purified recombinant GST-Nup93 or GST alone were immobilized on glutathione Sepharose 4B and incubated with or without rat liver NEs extracts as described for Nup53 in Figure legend 3A. The bead-bound proteins were eluted, separated by SDS-PAGE, and analyzed by Western blotting using antibodies directed against the indicated nups.

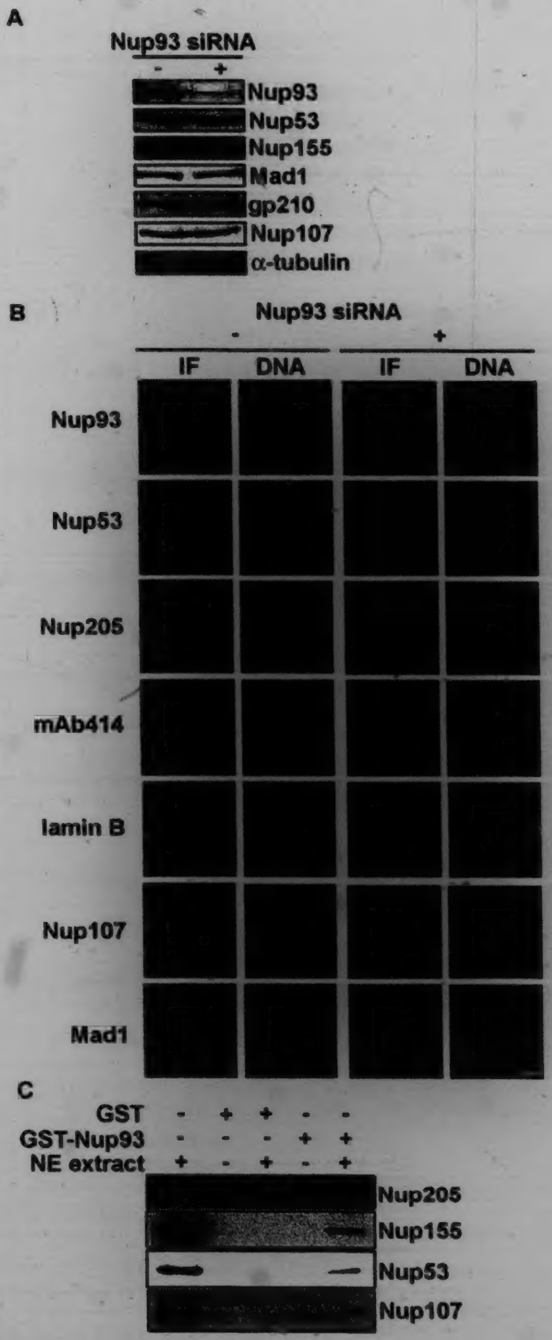
A
Nup93 siRNA
-
+
Nup93
Nup53
Nup155
Mad1
gp210
Nup107
α-tubulin
B
Nup93 siRNA
-
+
IF
DNA
IF
DNA
Nup93
Nup53
Nup205
mAb414
lamin B
Nup107
Mad1
C
GST - + + - -
GST-Nup93 - - - + +
NE extract + - + - +
Nup205
Nup155
Nup53
Nup107

Figure 3-7. ***In vivo*** **depletion of Nup93 and the identification Nup93 interacting partners using** ***in vitro*** **binding assays.**

biochemical and genetic, detected between groups of nups. The conservation of the structural features of the NPC between different species suggests that the compositions of the subcomplexes are also conserved. However, sequence similarity between nups of yeast and vertebrates is variable and several nups present in one species have no clear counterparts in the other (see Cronshaw et al., 2002). Thus, it remains to be determined to what degree individual subcomplexes are functionally conserved.

Genetic and biochemical analyses have established that yeast Nup53p is part of a network of interacting nups that includes Nup170p, Nup59p, Nic96p, Nup157p, and Nup192p (Aitchison et al., 1995b; Marelli et al., 1998; Kosova et al., 1999; Fahrenkrog et al., 2000; Lusk et al., 2002; Makhnevych et al., 2003). A model for how these nups are organized within the NPC is beginning to emerge. Nup53p can bind directly to Nup170p and Nic96p (Lusk et al., 2002; Makhnevych et al., 2003; C.P. Lusk and R.W. Wozniak, unpublished data). However, their interactions are cell cycle regulated. Nup53p binds to Nup170p during interphase, which blocks the ability of Nup53p to bind the karyopherin Kap121p. In contrast, during mitosis Nup53p is no longer detected in association with Nup170p but is instead bound to Nic96p and Kap121p (Makhnevych et al., 2003). How Nup59p, Nup157p, and Nup192p fit into this developing model is less clear. Proposals must consider the fact that Nup59p and Nup157p are likely products of gene duplications that also gave rise to Nup53p and Nup170p, respectively (Aitchison et al., 1995b; Marelli et al., 1998). Thus, while these pairs of related proteins are not functionally identical, it is possible that they are structurally interchangeable within the repetitive subunits of the NPC, creating a mosaic of structurally similar subcomplexes composed of different combinations of these related nups. In contrast to the redundancy observed in yeast, vertebrate Nup53 and Nup155 (the ortholog of Nup170p and Nup157p) represent the only forms of these nups. Together with Nup93 (the ortholog of yeast Nic96p) and Nup205 (the ortholog of yeast Nup192p) they likely form a similar, evolutionarily conserved, structure. We interpret the lack of paralogs in vertebrates to suggest that these Nup53-containing complexes are more homogenous and potentially lack certain functions that have evolved in the yeast counterpart (see Makhnevych et al., 2003). This may include the ability to regulate import controlled by the mammalian counterpart of Kap121p, as vertebrate Nup53 lacks the Kap121p binding domain found in yeast Nup53p.

On the basis of data presented in this paper and by analogy to the yeast NPC, we propose that Nup53 interacts with Nup155 and a previously identified Nup93-Nup205 complex (Grandi et al., 1997). This latter complex may also be physically associated with Nup188 (Miller et al., 2000), the yeast ortholog of which has been functionally linked to Nup53p and Nup170p (Aitchison et al., 1995b; Marelli et al., 1998). We have shown that both GST-Nup53 and GST-Nup93 are capable of binding Nup155 and Nup205, as well as Nup93 and Nup53, respectively. These data and the observed decreases in cellular levels of these nups in response to depletion of either Nup53 or Nup93 suggest they exist as a complex within the NPC. This complex, however, has been refractory to direct isolation, likely due to it being labile under conditions required to disassemble the NPC. For example, extraction conditions that have allowed the identification of complexes containing Nup107-Nup133 or gp210 on sucrose gradients appear to largely produce monomeric Nup53, Nup93, and Nup155 (Fig. 3-8).

This group of nups likely contributes to the symmetrical core structures of the NPC. Recent immunoelectron microscopy data from Krull et al. (2004), suggest that both Nup93 and Nup205 are centrally positioned within the NPC near the pore membrane. Also consistent with this idea, Nup155 is symmetrically distributed on both faces of the NPC (Radu et al., 1994). In addition, we observed that Nup53 is accessible to cytoplasmically presented antibodies in the presence or absence of the NE membrane (Fig. 3-9). The localization of these nups to the NPC core is also consistent with data showing that Nup93 and Nup205 play a role in the permeability of the NPC (Galy et al., 2003), a property that is shared with the yeast counterpart of Nup155 (Shulga et al., 2000).

Data are also consistent with the idea that this complex of nups lies near the circumference of the NPC at the pore membrane. This conclusion is based both on the localization of Nup93 and Nup205 as discussed above (Krull et al., 2004) and on the tight association between Nup53 and the NE membrane. We have shown, using various urea extraction conditions, that the release of Nup53 from the NE membrane appears to largely parallel that of the lamins, requiring significantly higher concentrations of urea for extraction from the membrane than other nups. These results are similar to those previously documented with yeast Nup53p (Marelli et al., 2001). In yeast, the association of Nup53p with the membrane was shown to be dependent on a putative amphipathic helix at its COOH-terminus; a structure that also appears to be present within the last 13 amino acid residues of vertebrate Nup53. Nup53 also appears to interact with the nuclear lamina. We have observed that Nup53 remains tightly

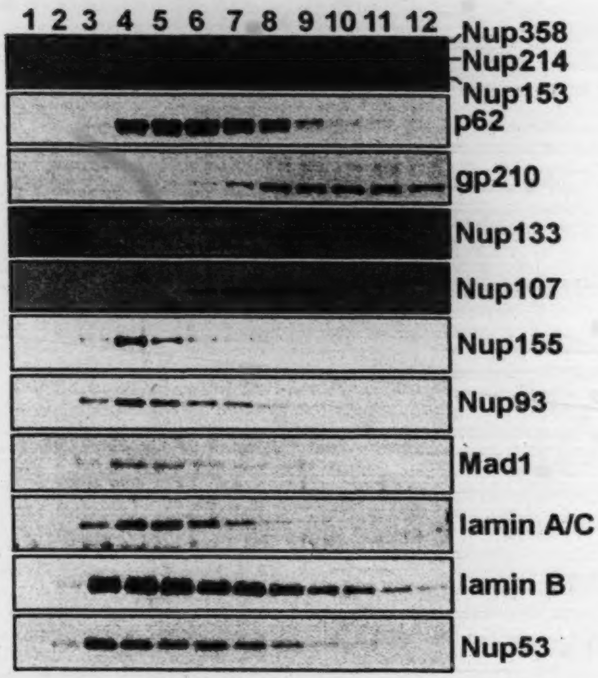
1 2 3 4 5 6 7 8 9 10 11 12
Nup358
Nup214
Nup153
p62
gp210
Nup133
Nup107
Nup155
Nup93
Mad1
lamin A/C
lamin B
Nup53

Figure 3-8. Sucrose gradient analysis of rat liver NE extracts.

Proteins derived from extracts of rat liver NE were separated by centrifugation on a 10-40% linear sucrose gradient. Proteins derived from fractions spanning the gradient (numbered above) were separated by SDS-PAGE and analyzed by Western blotting using antibodies directed against the indicated nups. Note, mAb414 was used to detect p62, Nup153, Nup214, and Nup358.

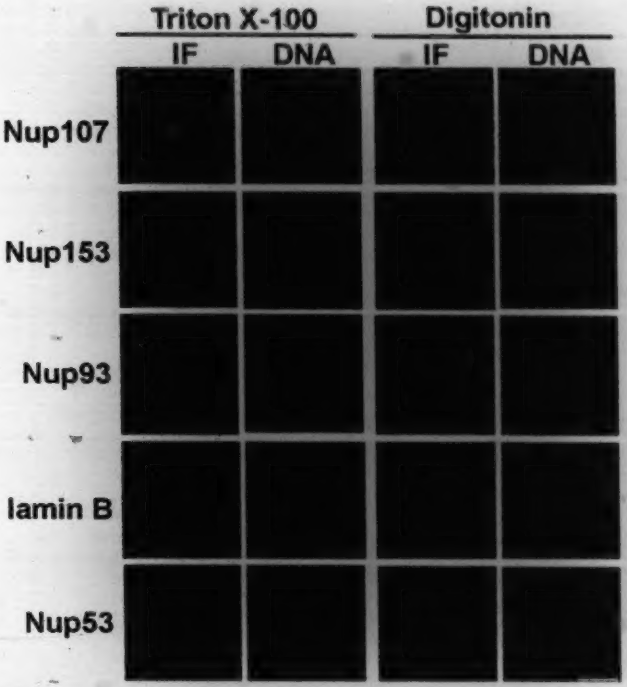

Figure 3-9. Nup53 is accessible to specific antibodies in the presence and absence of the NE membrane.

HeLa cells were treated with either Triton X-100 or digitonin and then fixed with formaldehyde. Cells were then probed with antibodies directed against the indicated proteins and antibody binding was detected using Cy3-labeled secondary antibodies (IF). Nuclear DNA was detected by staining with the DNA-binding dye Hoechst. Bar, 10 μm. Nup53, like Nup107, was detected at the nuclear rim in either digitonin or Triton X-100 permeabilized cells. Nup153, Nup93 and lamin B were not detected in HeLa cells treated with digitonin, but were detected in cells permeabilized with Triton X-100.

associated with the lamina after removal of the NE membrane with detergent (Fig. 3-2B). Moreover, we have detected lamin B bound to recombinant Nup53 using *in vitro* binding assays (Fig. 3-3A) and we have observed that Nup53 and lamin B co-sediment on sucrose gradients (Fig. 3-8). In the aggregate, our data support a model in which Nup53 is positioned at the interface between the pore membrane and the lamina where it could anchor other nups to these structures.

Nup53 is one of two nups that have so far been implicated in linking the NPC to the nuclear lamina. Smythe and colleagues (2000) have suggested that *Xenopus* Nup153 binds to lamin B_3. Nup153 is located on the nuclear side of the NPC (Sukegawa and Blobel, 1993; Cordes et al., 1993) and it has been suggested that it links the core structures to the nuclear basket and the nuclear filamentous protein Tpr (Krull et al., 2004). These data place Nup153 in a separate subcomplex from the core associated Nup53. Considering these data and ours, its would seem possible that different subcomplexes of the NPC may possess distinct lamin binding members, with Nup53 functioning to link the Nup93-containing complex, and perhaps more generally the NPC core, to the nuclear lamina.

At the pore membrane Nup53 is strategically positioned to function in the assembly of nups into a forming NPC. Using RNA interference to deplete endogenous Nup53, we showed that reducing the cellular levels of Nup53 produced a corresponding decrease in Nup93, Nup205, and Nup155 while not affecting other nup complexes (Fig. 3-6). A likely explanation for this phenomenon is that reduced levels of Nup53 inhibit the assembly of these nups into the NPC, leading to unstable, partially assembled complexes that are more rapidly degraded. Similar results have also been documented for other nup complexes, including the depletion of the Nup107-Nup160 complex, where the stability of the complex is decreased by depletion of individual members (Boehmer et al., 2003; Harel et al., 2003; Walther et al., 2003).

A striking consequence of depleting Nup53 is the loss of normal nuclear morphology. Nup53 depleted cells lose their spherical shape, generally adopting an elongated lobular or kidney-shape. This observation was intriguing in light of the interactions between Nup53 and the lamina and the similarity of this morphology to that previously detected in cells lacking lamin A (Sullivan et al., 1999). However, we have not observed any interactions between Nup53 and lamin A/C nor have we detected changes in the levels or the distribution of the lamins or the inner membrane protein emerin (Fig. 3-6). Both of these classes of proteins are evenly distributed along the irregular nuclear periphery of the Nup53-depleted cells, each following the contour of the underlying chromatin mass. Thus, the relationship between the nuclear morphologies of cells lacking Nup53 and the lamin A depleted cells is unclear. Not surprisingly, we also observed a similar phenotype in cells depleted of Nup93 where levels of Nup53 are also reduced. This raises the question of whether the altered nuclear morphology is related directly to the loss of Nup53 function or whether it is a result of the co-depletion of Nup93 or other interacting nups.

Depletion analysis of the *C. elegans* counterparts of the Nup93, Nup205, Nup155 and Nup53, has also been performed in embryos. This study conducted by Galy and co-workers (2003) suggests that distinct morphological phenotypes are associated with the depletion of these nups. While depletion of each causes an embryonic lethal phenotype, depletion of the counterparts of Nup53 or Nup155 appears to block nuclear formation following mitosis. The cause of this block is yet to be determined. In contrast, embryos lacking Nup93 and Nup205 exhibit abnormal peripheral chromatin condensation and what appears to be an altered distribution of NPCs in the NE. We have not detected similar phenotypes in HeLa cells depleted of either Nup53 or Nup93 (Fig. 3-6A, Fig. 3-7B). Moreover, unlike the depleted HeLa cells, the *C. elegans* embryos lacking counterparts of Nup93 or Nup53 do not exhibit any alterations in nuclear shape (Galy et al., 2003).

A disruption of nuclear morphology similar to that detected in cells depleted of Nup53 was also observed in cell lines depleted of Mad1 (Luo et al., 2002). The most well defined function of Mad1 is its role in the spindle assembly checkpoint, a quality control feature of chromosome segregation that monitors spindle attachment to kinetochores during mitosis (reviewed in Lew and Burke, 2003). Intriguingly, Mad1 is localized to the NPC during interphase in both mammalian and yeast cells (Campbell et al., 2001; Iouk et al., 2002). However, it remains to be determined what function the association of Mad1 with the NPC plays in the spindle assembly checkpoint or to what degree Mad1 contributes to the function of the NPC. In yeast, the docking of Mad1p to the NPC has been shown to occur, in part, through its interaction with the Nup53p-containing complex (Iouk et al., 2002). Consistent with this, yeast cells exhibit diminished levels of Mad1p at the NPC in *nup53Δ* cells (Iouk et al., 2002). Our data are consistent with a similar interaction occurring in mammalian cells, where the levels of Mad1 are reduced, but still detectable, at the NE in the Nup53-depleted cells (Fig. 3-6). We conclude from these observations that Mad1 may interact with more than one nup at the NPC. Of note, siRNA induced depletion of Nup93, which reduces NE levels of

Nup53, does not appear to alter cellular levels of Mad1. A potential explanation for these results is that Mad1 interacts with a separate pool of Nup53 distinct from that bound to the Nup93-containing complex.

Previous studies of cell lines specifically depleted of Mad1 using RNA interference have shown that these cells exhibit defects in spindle checkpoint function (Martin-Lluesma et al., 2002). We have performed similar experiments on Nup53-depleted cells to determine whether the reduced NPC association and cellular levels of Mad1 are sufficient to abrogate spindle checkpoint function. However, we failed to detect an obvious chromosome segregation defect that would suggest that this pathway is inhibited. Presumably, sufficient levels of Mad1 remain to conduct its essential role in spindle checkpoint function. What role the NPC association plays in the function of this remaining pool of Mad1 will await the identification of its other NPC binding sites.

During prometaphase Mad1 is recruited to kinetochores (Chen et al., 1998; Campbell et al., 2001). In contrast, we have not detected Nup53 (using either indirect immunofluorescence or GFP fusions) or Nup93 at kinetochores during mitosis, suggesting that any interaction of Mad1 with Nup53 is not maintained at the kinetochores. Of note, members of the Nup107-containing complex and Nup358 (RanBP2), while largely distributed throughout the cytoplasm during mitosis, have also been detected at kinetochores (Belgareh et al., 2001; Joseph et al., 2002; Loïodice et al., 2004). The functional role of the Nup107-Nup160 complex at kinetochores is not established and no specific defects in the function of this structure have been attributed to the depletion of these nups. In contrast, depletion of Nup358 leads to severe defects in kinetochore structure and a reduction in the recruitment of Mad1 and Mad2 to kinetochores (Salina et al., 2003; Joseph et al., 2004). However, the spindle checkpoint remains active in these cells. Thus it appears unlikely that these nups play a critical role in basal levels of spindle checkpoint activity. A more plausible scenario is that the association of nups with kinetochores, as well as interactions of the Mads with the NPC, may function to regulate the fidelity of the spindle checkpoint response.

Chapter IV: *Nup53 interacts with the transmembrane nup NDC1 and is required for nuclear envelope and nuclear pore complex assembly*[*]

---

[*] This chapter includes data from two publications. Fig. 4-1 was published in Jörg Mansfeld, Stephan Güttinger, Lisa A. Hawryluk-Gara, Nelly Pantè, Moritz Mall, Petra Mühlhäusser, Richard W. Wozniak, Iain W. Mattaj, Ulrike Kutay and Wolfram Antonin. (2006). **The conserved transmembrane nucleoporin NDC1 is required for nuclear pore complex assembly in vertebrate cells**. *Molecular Cell* 22: 93-103 with permission from Elsevier. The remainder of the work comprises a submitted manuscript: Lisa A. Hawryluk-Gara, Melpomeni Platani, Rachel Santarella, Richard W. Wozniak, Iäin W. Mattaj. (2007). **Nup53 is Required for Nuclear Envelope and Nuclear Pore Complex Assembly**. *Molecular Biology of the Cell. Submitted.* L.A. Hawryluk-Gara and M. Platani made equal contributions to this work. Contributions made by J. Mansfeld, M. Platani, and R. Santarella are noted in respective figure legends.

4.1 Overview

In this study we uncovered a previously uncharacterized link between the transmembrane protein NDC1 and Nup53, and investigated the role of Nup53 in NPC and NE formation. We identified the regions of Nup53 necessary for its interactions with the neighbouring nucleoporins Nup93, Nup155, Nup205, and the membrane protein NDC1. These experiments established that Nup53 interacts with its binding partners through distinct regions. This information was applied to the analysis of the functions of these regions in mediating the NPC association of Nup53 in HeLa cells and their role in NPC assembly and NE formation using the *Xenopus* nuclear reconstitution assay. Using this latter assay, we showed that Nup53 is required for both NE and NPC assembly. Depletion of Nup53 results in docking of membrane vesicles to chromatin but a block in NE membrane fusion and NPC formation, reminiscent of the defect observed following depletion of Nup155, POM121, or NDC1. Our data further suggest that the interaction between Nup53 and Nup155 is critical for proper NPC and NE assembly.

4.2 Results

4.2.1 A Link between NDC1 and Nup53 Complex

Previous experiments have shown that RNAi-mediated knockdown of components of two nucleoporin subcomplexes, namely the Nup107-160 and the Nup53 complexes, led to failures in NPC assembly (Harel et al., 2003; Krull et al., 2004; Walther et al., 2003; Fig. 3-6 and 3-7). To investigate if NDC1, a conserved transmembrane nup, is linked to one of these two nup subcomplexes, we performed combinatorial RNAi targeting Nup93 and Nup107 in combination with NDC1. Codepletion of Nup93 and NDC1 resulted in nuclei displaying a distorted morphology and reduced mAb414 staining (Fig. 4-1A). Cells treated with combinations of NDC1 and Nup107 siRNAs showed unchanged levels of FG-repeat containing nucleoporins at the NE and normal nuclear shape. One possible interpretation of the synergistic effect is that NDC1 interacts with members of the Nup93-53 complex, but not the Nup107-160 complex.

To address the role of NDC1 in NPC targeting of members of the Nup93-53 subcomplex, we investigated the effect of NDC1 RNAi on localization of subcomplex proteins. Downregulation of NDC1 in HeLa K cells reduced NPC association of Nup53, Nup93, and Nup205 as shown by immunofluorescence (Fig. 4-1B). In contrast, Nup107 targeting was only slightly affected by NDC1 depletion.

Yeast and vertebrate Nup53 interact closely with the pore membrane (Marelli et al., 2001; Fig. 3-2). Using *in vitro* binding assays previously employed to identify interactions between members of the Nup53 complex (Fig. 3-3), we tested whether

Figure 4-1. NDC1 interacts with the Nup53 complex.

(A) Combined depletion of Nup93 and NDC1 by RNAi reveals a functional link between NDC1 and the Nup93 complex. HeLa cells were treated with combinations of control siRNAs, Nup93 siRNAs, or Nup107 siRNAs. After 72 hours, cells were fixed and analyzed by mAb414 and Nup107 antibody staining as indicated in Chapter II. (B) NDC1 depletion by RNAi affects binding of Nup53, Nup93, and Nup205 to the NPC. HeLa K cells were transfected with siRNAs as in (A), subjected to immunofluorescence analysis with mAb414 and antibodies directed against Nup205, Nup93, Nup53, and Nup107, and analyzed by confocal microscopy. (C) *In vitro* binding of NDC1 from detergent extracts of rat liver NEs to immobilized recombinant Nup53. 25 A_{260} units of rat liver NE extracts in buffer containing 0.3% Triton X-100 and 106 mM NaCl were incubated with purified recombinant GST, GST-Nup53$^{1-326}$, GST-Nup53$^{1-300}$, or GST-Nup53$^{204-326}$ immobilized on glutathione Sepharose 4B beads. After binding and washing, the bound proteins were eluted with SDS sample buffer, 10% of the total bound fraction separated by SDS-PAGE, and analyzed by Western blotting using antibodies directed against POM121, gp210, Nup93, and NDC1. Experiments in panels (A) and (B) were performed by J. Mansfeld in the laboratory of U. Kutay at the Swiss Federal Institute of Technology.

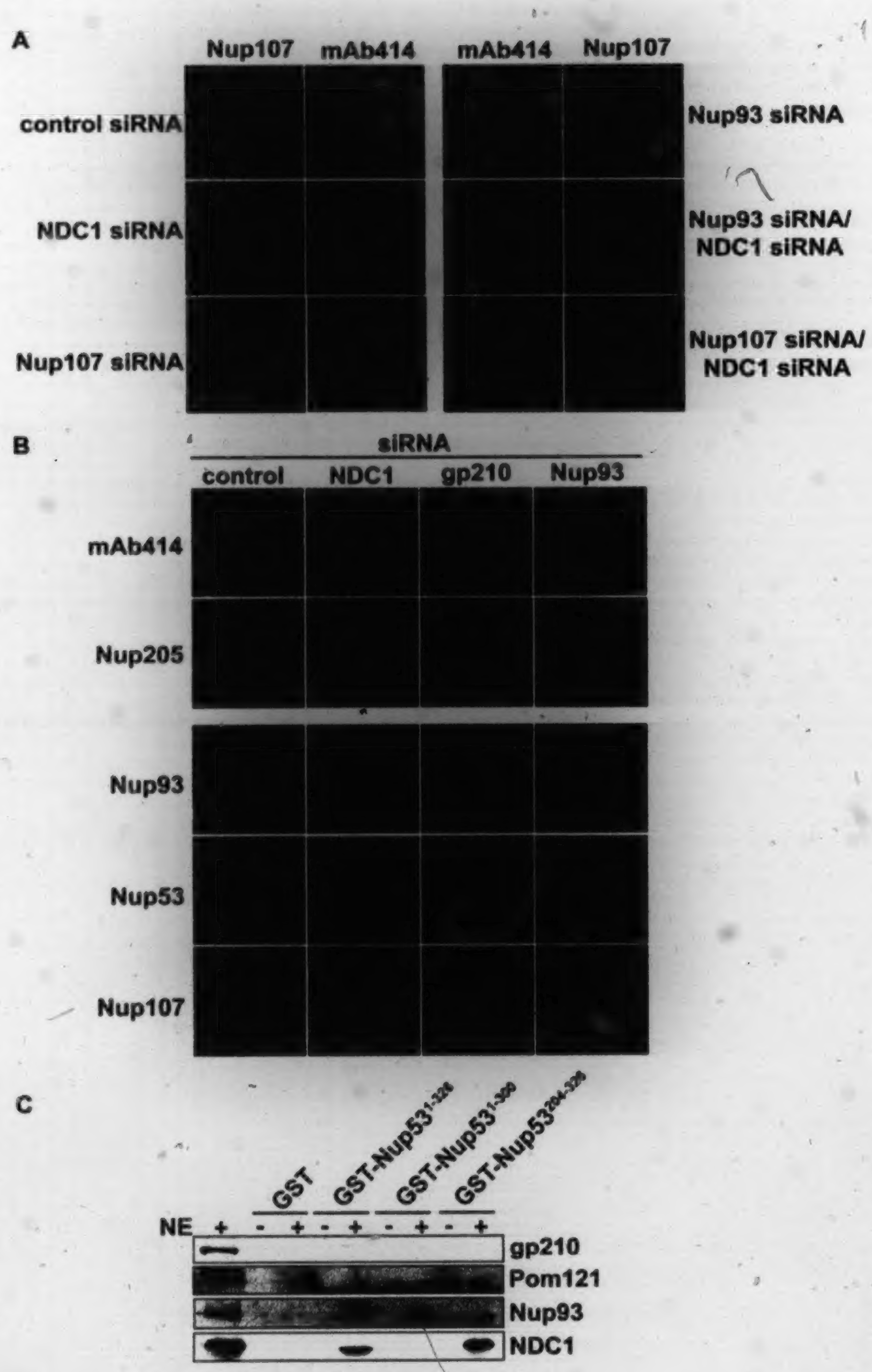
A
Nup107
mAb414
mAb414
Nup107
control siRNA
NDC1 siRNA
Nup107 siRNA
Nup93 siRNA
Nup93 siRNA/ NDC1 siRNA
Nup107 siRNA/ NDC1 siRNA
B
siRNA
control
NDC1
gp210
Nup93
mAb414
Nup205
Nup93
Nup53
Nup107
C
GST
GST-Nup53$^{1-326}$
GST-Nup53$^{1-300}$
GST-Nup53$^{204-326}$
NE
+
- +
- +
- +
- +
gp210
Pom121
Nup93
NDC1

Figure 4-1. NDC1 interacts with the Nup53 complex

NDC1 was capable of binding this complex. Recombinant GST-Nup53 was immobilized on glutathione Sepharose beads and incubated with rat liver NE extracts containing solubilized nucleoporins. Western blot analysis of the bound fractions showed that GST-Nup53 specifically interacted with NDC1, but not gp210 or POM121 (Fig. 4-1C and Fig 3-3). NDC1, however, did not bind to a COOH-terminal truncation of Nup53 that lacks the last twenty six amino acid residues, suggesting that this region is necessary for their association. This observation is consistent with our previous data showing that the tight association of yeast Nup53p with the NE membrane is dependent on this conserved COOH-terminal region (Marelli et al., 2001). In contrast, full-length and COOH-terminally truncated Nup53 bound to Nup93, whereas the COOH-terminal fragment of Nup53 bound NDC1, but not Nup93. These results suggest that the binding of NDC1 to Nup53 does not occur through Nup93. Instead, their interaction is either direct or mediated by an as yet undefined protein. Taken together, our data are consistent with the notion that NDC1 facilitates recruitment of the Nup53 complex to the assembling NPC.

4.2.2 Mapping the interactions between Nup53 and neighbouring nups

Vertebrate Nup53 is tightly associated with the NE membrane and the nuclear lamina where it appears to interact, either directly or indirectly, with several neighbouring Nups including Nup93, Nup155, and the pore membrane protein NDC1 (Fig. 3-3; Fig. 4-1). Here it is strategically positioned to function in mediating the interactions between the pore membrane and the core structures of the NPC and potentially participate in NE

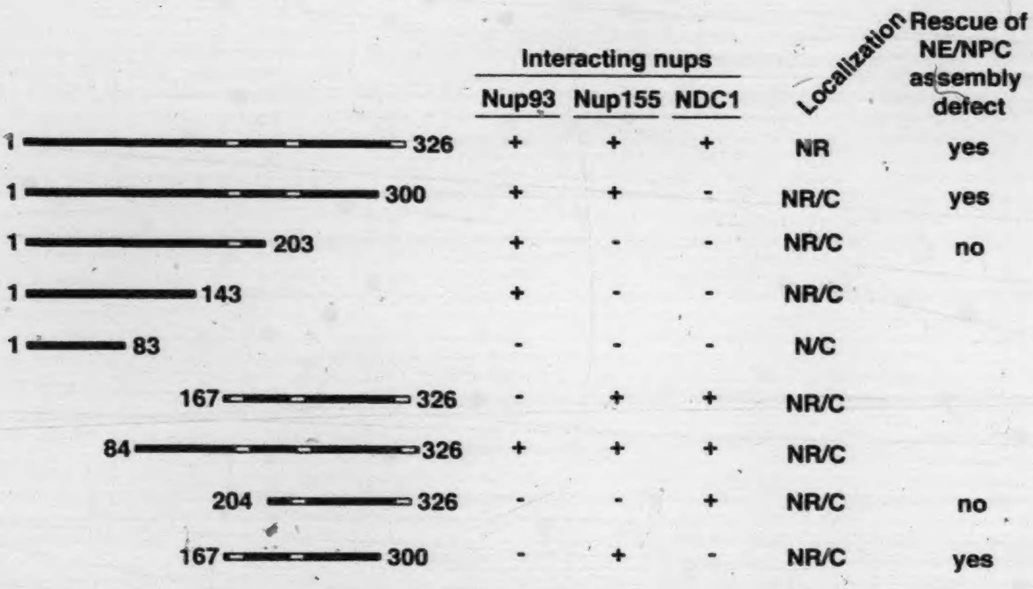

	Interacting nups			Localization	Rescue of NE/NPC assembly defect
	Nup93	Nup155	NDC1		
1–326	+	+	+	NR	yes
1–300	+	+	-	NR/C	yes
1–203	+	-	-	NR/C	no
1–143	+	-	-	NR/C	
1–83	-	-	-	N/C	
167–326	-	+	+	NR/C	
84–326	+	+	+	NR/C	
204–326	-	-	+	NR/C	no
167–300	-	+	-	NR/C	yes

Figure 4-2. Summary of human Nup53 truncation characterization

Compilation of Nup53 truncation interaction, localization, and depletion phenotype rescue data. NH_2- and COOH-terminal human Nup53 truncations were constructed based on regions that are well conserved among orthologs with considerations of predicted secondary structure. Helical stretches from amino acid residues 181-193, 216-226 and 314-326 are represented by light grey bars. Interaction data was obtained either by silver staining, Western blot or both. Interactions detected (+) or not detected (-) between indicated Nups and Nup53 truncations are shown. Localization was scored as either nuclear rim (NR), nuclear (N), or cytoplasmic (C). The ability of the various Nup53 truncations to rescue the Nup53 depletion phenotype was monitored by $DilC_{18}$ NE membrane staining.

Figure 4-3. Nup53 domain interaction analysis using GST-pulldown assays (A-C). Purified recombinant GST, GST-Nup53, or various GST-Nup53 truncations immobilized on glutathione Sepharose 4B beads were incubated with extracts from purified rat liver NEs (+) or buffers alone (-). After binding and washing, bead bound proteins were eluted, separated by SDS-PAGE and detected with either silver staining (SS) or Western blotting (WB) using antibodies against the indicated Nups. Positions of GST-fusions (white asterisks), relevant Nups (black asterisks and name) and mass markers are indicated in kilodaltons.

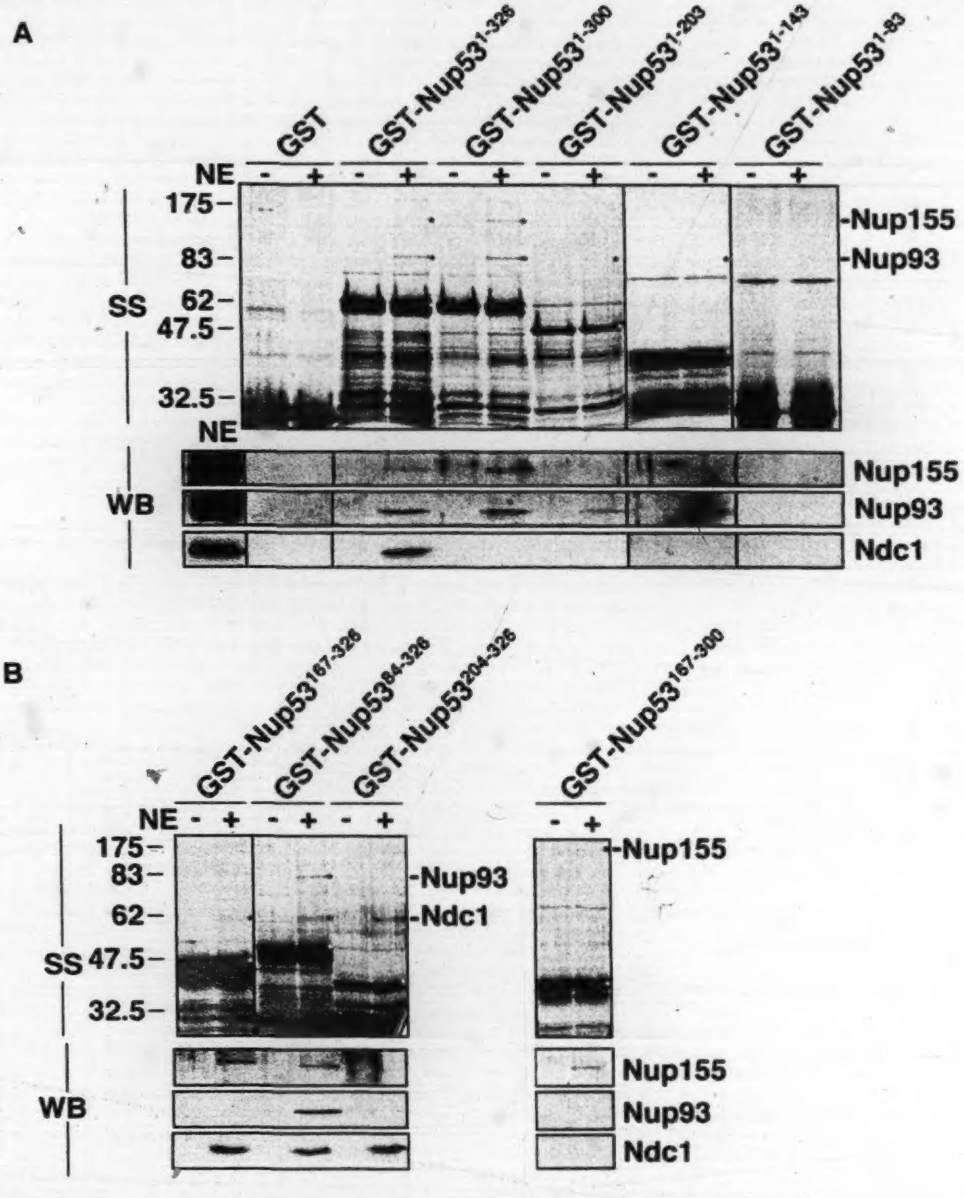
A
GST
GST-Nup53$^{1-326}$
GST-Nup53$^{1-300}$
GST-Nup53$^{1-203}$
GST-Nup53$^{1-143}$
GST-Nup53$^{1-83}$
NE - + - + - + - + - + - +
175-
83-
62-
47.5-
32.5-
SS
NE
WB
-Nup155
-Nup93
Nup155
Nup93
Ndc1
B
GST-Nup53$^{167-326}$
GST-Nup53$^{84-326}$
GST-Nup53$^{204-326}$
GST-Nup53$^{167-300}$
NE - + - + - +
- +
175-
83-
62-
47.5-
32.5-
SS
WB
-Nup155
-Nup93
-Ndc1
Nup155
Nup93
Ndc1

Figure 4-3. Nup53 domain interaction analysis using GST-pulldown assays

and NPC assembly. To more clearly define the function of Nup53 in these processes, we have mapped the regions of Nup53 that mediate its interactions with other nups. For these experiments we have employed an *in vitro* binding assay using recombinant forms of Nup53 and Nups derived from extracts of rat liver NEs. Using this assay we have previously reconstituted interactions between full length recombinant Nup53 and rat liver NE-derived Nup93, Nup155, and NDC1 (Fig. 3-2; Fig. 4-1C; Fig. 4-3A). Similar binding experiments were performed with a series of NH_2- and COOH-terminal deletions of Nup53. These truncated forms of Nup53 were synthesized in *E. coli* as GST fusions and bound to Glutathione-Sepharose. The bead-bound fusions were then incubated with rat liver NE extract containing solubilized Nups and the bound fractions analyzed by SDS-PAGE and Western blotting. As predicted, full length Nup53 (GST-Nup53$^{1\text{-}326}$) bound Nup93, Nup155, and NDC1 while no binding was detected to GST alone. Removal of the last 26 amino acid residues of Nup53 (GST-Nup53$^{1\text{-}300}$), that contains a predicted amphipathic helix, eliminates NDC1 binding (Fig. 4-1C). However, the GST-Nup53$^{1\text{-}300}$ fusion binds Nup93 and Nup155 (Fig. 4-2A). Surprisingly, further truncating the COOH-terminus to amino acid residues 203 and 143 (Nup53$^{1\text{-}203}$ and Nup53$^{1\text{-}143}$, respectively) abolished Nup155 binding, but not the ability of these GST-fusions to interact with Nup93, albeit with reduced efficiency when compared to full-length Nup53. Binding to these latter nups was finally lost when the COOH-terminal truncation extended to residue 83 (Nup53$^{1\text{-}83}$).

Similar experiments were performed with NH_2-terminal Nup53 truncations. As shown in Fig. 4-3B, deletion of the NH_2-terminal 83 residues of Nup53 (Nup53$^{84\text{-}326}$) did not affect its ability to bind Nup93, Nup155, and NDC1. However, further deleting residues 1-203 (Nup53$^{204-326}$) eliminated the binding to all but NDC1. As predicted, removal of residues 1-166 (Nup53$^{167-326}$) resulted in an inability of Nup53 to interact with Nup93, but binding to Nup155 and NDC1 was not altered.

Our data were consistent with a model in which Nup93 binds to a region within amino acid resides 1-143 and NDC1 binds within residues 204-326. In contrast, the region of Nup53 required for binding Nup155 appeared to lie more centrally in Nup53. Consistent with this idea, we detected binding of Nup155 to Nup53$^{167-300}$ (Fig. 4-3C). This fragment, however, failed to bind Nup93 and Ndc1. These data, coupled with the observations that recombinant Nup53 directly interacts with both recombinant Nup93 (Fig. 3-3B) and Nup155 (J.M. Mitchell and R.W. Wozniak, manuscript in preparation), but that Nup155 and Nup93 do not appear to directly interact with each other, supports the conclusion that Nup93 and Nup155 bind to unique sites on Nup53. Cumulatively, our data support a model in which the binding regions for Nup93, Nup155, and NDC1 in Nup53 lie primarily within residues 1-143, 167-300, and 204-326, respectively (see Fig. 3-1).

4.2.3 *In vivo* localization of Nup53 truncations

Truncation mutants of Nup53 similar to those used to define its interactions with binding partners were also used to construct GFP fusion genes for expression in mammalian cells. These experiments were designed to define regions of Nup53 that play a critical role in mediating its NPC association and to correlate important targeting regions with those required for specific Nup interactions. Various GFP-Nup53 chimeric

Figure 4-4. ***In vivo*** **localization of EGFP-Nup53 truncations**

(A/B) Plasmids encoding either full-length Nup53 or the indicated truncations fused to EGFP were transfected into HeLa cells. Cellular distributions of the GFP chimeras (GFP) and nuclear DNA was determined by fluorescence microscopy following 24 hours of transient expression. Nuclear DNA was detected by staining with the DNA binding dye Hoechst. Merged images are also shown (GFP-DNA). The transfected cells growing on coverslips were processed for microscopy either by formaldehyde fixation followed by Triton X-100 permeabilization (F/T) or Triton X-100 permeabilization prior to formaldehyde fixation (T/F). Scale bar,10 μm. (C) GFP-expressing HeLa cells were either fixed with formaldehyde (F) or permeabilized with Triton X-100 (T) before they were collected from the culture dish and lysed by boiling in SDS-PAGE sample buffer. Cell extracts were separated by SDS-PAGE, and analyzed by Western blot with GFP antibodies. A black asterisk denotes a cross reacting band of the GFP antibody. Positions of the GFP-Nup53 fusions are indicated with red asterisks.

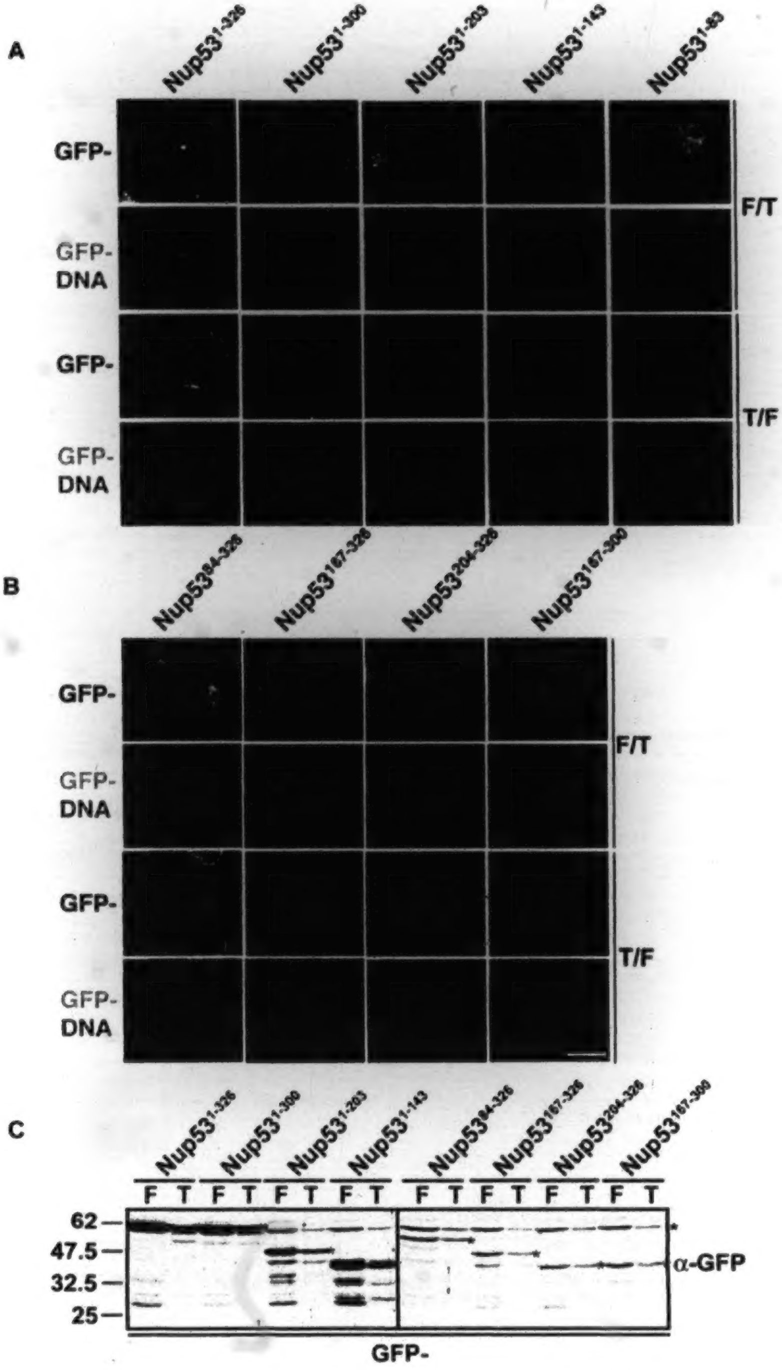
A
$Nup53^{1-326}$
$Nup53^{1-300}$
$Nup53^{1-203}$
$Nup53^{1-143}$
$Nup53^{1-83}$
GFP-
GFP-DNA
GFP-
GFP-DNA
F/T
T/F
B
$Nup53^{84-326}$
$Nup53^{167-326}$
$Nup53^{204-326}$
$Nup53^{167-300}$
GFP-
GFP-DNA
GFP-
GFP-DNA
F/T
T/F
C
$Nup53^{1-326}$
$Nup53^{1-300}$
$Nup53^{1-203}$
$Nup53^{1-143}$
$Nup53^{84-326}$
$Nup53^{167-326}$
$Nup53^{204-326}$
$Nup53^{167-300}$
F T F T F T F T F T F T F T F T
62
47.5
32.5
25
*
α-GFP
GFP-

Figure 4-4. ***In vivo*** **localization of EGFP-Nup53 truncations**

genes were introduced into HeLa cells. The resulting GFP-tagged Nup53 truncations were then examined by confocal microscopy twenty four hours after transfection. Importantly, Western blot analysis of extracts derived from the transfected HeLa cells revealed that each of GFP-Nup53 chimeras exhibited a molecular mass consistent with that predicted from its sequence (Fig. 4-4C). As shown in Fig. 4-4A, full-length GFP-Nup53 (Nup53$^{1-326}$) localized to the nuclear rim in a characteristic pattern exhibited by Nups including endogenous Nup53 (Fig. 3-2B). This pattern was observed in cells exhibiting a range of expression levels within the transfected cultures. Similarly, GFP-Nup53$^{1-300}$, which lacks the COOH-terminal region required for NDC1 binding but contains the Nup93 and Nup155 binding sites, was also visible at the nuclear rim. However, its ability to concentrate at the NE appeared to be compromised as GFP-Nup53$^{1-300}$ was also detected diffusely distributed throughout the cytoplasm and in the nucleoplasm. Further COOH-terminal deletion mutants GFP-Nup53$^{1-203}$, GFP-Nup53$^{1-143}$, and GFP-Nup53$^{1-83}$ failed to visibly associate with the NE and were distributed diffusely throughout the nucleus and cytoplasm. As both GFP-Nup53$^{1-203}$ and GFP-Nup53$^{1-143}$ fusions contain the Nup93 binding region, we tested whether these fusions might partially associate with NPC, but that this binding might be masked by nuclear and cytoplasmic levels of the fusions. Indeed, both GFP-Nup53$^{1-203}$ and GFP-Nup53$^{1-143}$, but not the GFP-Nup53$^{1-83}$, fusions could be detected at the NE following mild extraction with Triton X-100 to release the soluble pool of fusion protein (Fig. 4-4A). As the cellular levels of these fusion proteins were less than GFP-Nup53 (Fig. 4-4C), we conclude that increased cytoplasmic and nucleoplasmic signal was not related to their overproduction but rather their reduced ability to target to or associate with binding sites at the NPC.

The localization patterns of several NH_2-terminal deletion mutants were also examined (Fig. 4-4B). Nup53$^{84-326}$, which contains all of the identified Nup binding regions, was concentrated primarily at the NE, appearing similar to the full-length protein but with a slightly higher cytoplasmic signal. Upon further deletion of the NH_2-terminus to residues 167 or 204, the resulting fusions (GFP-Nup53$^{167-326}$ and GFP-Nup53$^{204-326}$) showed an increase in cytoplasmic signal and, in the case of GFP-Nup53$^{204-326}$, no NE accumulation. Similarly, expression of GFP-Nup53$^{167-300}$ (containing the Nup155 binding region) revealed that this fusion protein is diffusely distributed throughout the nucleus and cytoplasm (Fig. 4-4B). However, as was seen with several of the COOH-terminal truncations, extraction with Triton X-100 revealed that each of these fusions bind to the NE (Fig. 4-4B). Cumulatively these results, together with those obtained using the COOH-terminal deletions, suggest that each of the three Nup binding regions of Nup53 is capable of binding the NPC, presumably through interactions with its cognate binding partner (summarized in Figure 4-2). Together each of the Nup binding regions contribute to optimal NPC binding.

4.2.4 Removal of Nup53 leads to a block in NPC formation and NE membrane fusion

Several observations suggest that human Nup53 and its counterparts are positioned at or near the pore membrane where it interacts with components of the NPC including Nup155 (Marelli et al., 1998; 2001 and Chapter III). This model places Nup53 at a location where it might play a role in NPC assembly. Consistent with this idea, RNAi studies in *C.elegans* have shown that Nup53 is required for nuclear assembly following mitosis (Galy *et al.*, 2003).

To study the function of Nup53 in more detail, we took advantage of the *Xenopus* nuclear reconstitution system. The *Xenopus in vitro* system recapitulates pronuclear assembly and mimics the events of postmitotic NE assembly (Forbes *et al.*, 1983; Lohka and Masui, 1983; Newport, 1987). Mock and Nup53-immunodepleted cytosolic fractions were prepared. Following two rounds of depletion, more than 95% of soluble Nup53 was removed (Fig. 4-5A). Like Nup155 (Franz *et al.*, 2005), Nup53 was also present in the total membrane fraction and could not be easily extracted by salt washes. This suggested that like Nup155, Nup53 might be pelleted with membranes as part of a large but soluble membrane complex. Floating the total membrane fraction through a sucrose step gradient (Wilson and Newport, 1988) and using the lowest density membrane fraction for the assembly reaction allowed for the preparation membranes devoid of Nup53. The immunodepleted cytosol was then mixed with sperm chromatin, floated membrane vesicles and an ATP regeneration system to assemble nuclei *in vitro*. Nuclei were allowed to form for two hours at 20°C. Membranes were immediately stained with the lipophilic dye DilC$_{18}$ prior to fixation. Nuclei assembled using mock-depleted extracts were able to form a smooth and continuous NE membrane with an efficiency of >80% (Fig. 4-5E). These mock-depleted nuclei were competent for nuclear import of fluorescently labelled BSA-NLS (Fig. 4-7A) and chromatin decondensation was observed. Furthermore, mAb414-reactive Nups (Nup62, Nup153, Nup214, and Nup358)

Figure 4-5. Depletion of Nup53 from cytosol blocks formation of a closed NE
(A) Amount of Nup53 in mock-depleted (Mock) and Nup53-depleted (ΔNup53) cytosolic extracts (equal volumes) were compared by SDS-PAGE and western blotting using α-Nup53 antibodies. Varying amounts of untreated cytosol were loaded for comparison. A cross-reacting band indicated with an asterisk serves as a loading control. (B) For add-back experiments, amounts of recombinant proteins corresponding to approximately endogenous levels of *Xenopus* Nup53 (extract) were used. Purified full length Nup53$^{1\text{-}326}$ and truncation fragments (Nup53$^{1\text{-}300}$, Nup53$^{1\text{-}203}$, Nup53$^{204\text{-}326}$, Nup53$^{167\text{-}300}$) were analyzed by SDS-PAGE and Western blotting using α-Nup53 antibodies. Mass markers are indicated in kilodaltons. (C) Equal amounts of mock depleted (Mock) or Nup53 depleted (ΔNup53) cytosolic extracts were analyzed by SDS-PAGE and Western blotting using antibodies directed against Nup155, Nup93 and Nup205. (D) Nuclei assembled *in vitro* in Mock, ΔNup53 extracts, or ΔNup53 extracts after addition of full length Nup53. Membranes are visualised by using the membrane dye DilC$_{18}$ (red). Chromatin was stained with DAPI (blue). Scale bar,10 µm. (E) Quantitation of closed NE formation of experiments performed as in (D). More than 100 randomly chosen chromatin substrates per reaction were counted. Average of three independent experiments are shown. Experiments presented in this Figure were performed by M. Platani in the laboratory of I. Mattaj at the EMBL.

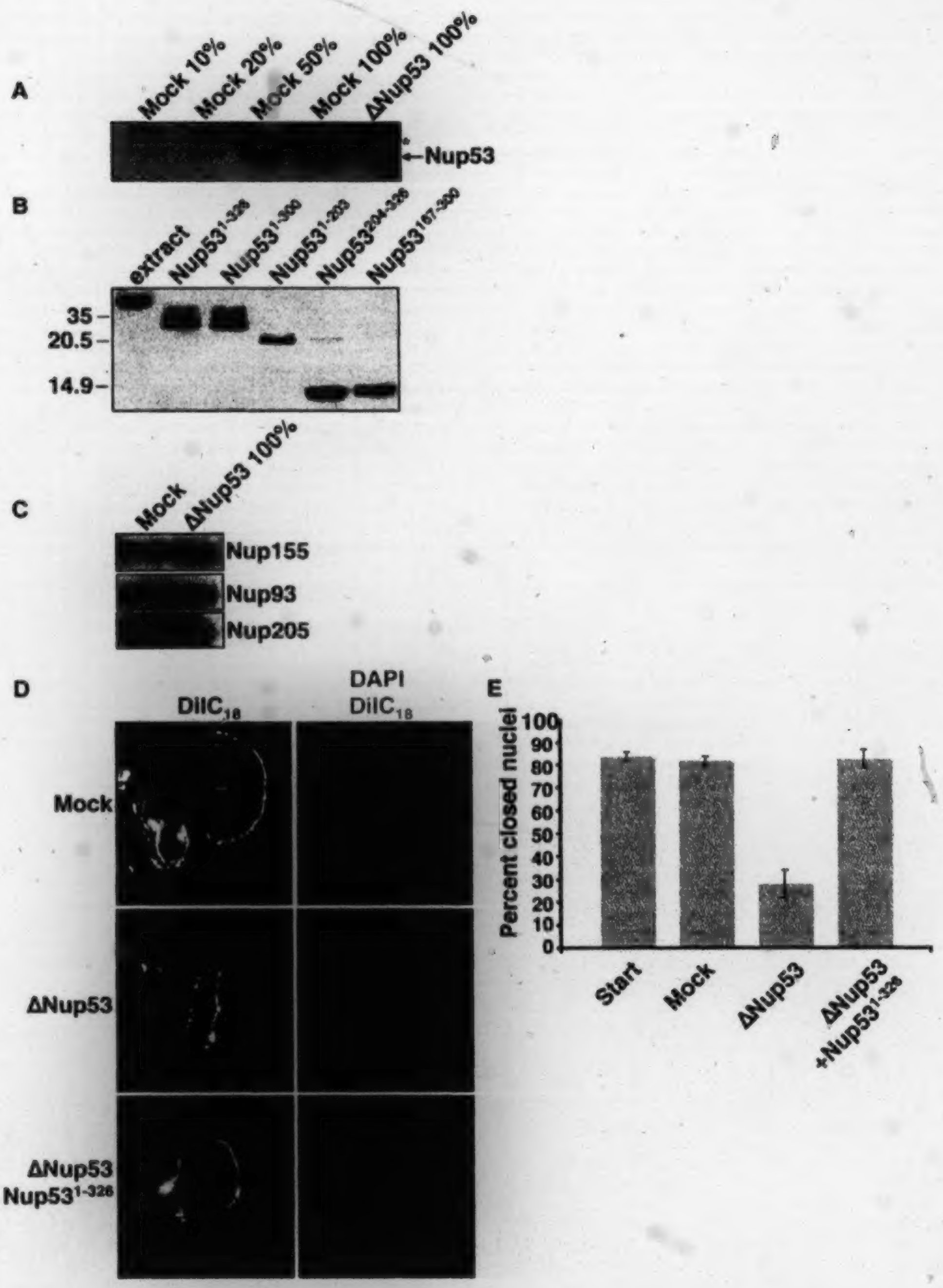

Figure 4-5. Depletion of Nup53 from cytosol blocks formation of a closed NE

were detected on the nuclear rim (Fig. 4-6B, mock). In contrast, when Nup53 was depleted from cytosol, membrane vesicles associated with chromatin but they failed to form a smooth and continuous NE (Fig. 4-5D). At the same time, due to the inability to form a closed NE, the sperm chromatin remained condensed and mAb414 staining was dramatically reduced (Fig. 4-6B, depleted), suggesting a block in NPC formation.

In order to confirm the specificity of the Nup53 depletion phenotype, full-length human Nup53 was purified under native conditions and used to complement the depleted cytosolic extracts. The purified protein was added back to roughly endogenous levels (Fig. 4-4B). When complemented extracts were used in an assembly reaction, nuclei with closed NEs were formed (Fig. 4-5D), mAb414 staining was restored (Fig. 4-6B), and nuclei were competent to import fluorescently labelled BSA-NLS (Fig. 4-7A). The efficiency of both the mock and full-length human Nup53 rescue experiments was quantified. In mock-depleted extracts, > 80% of sperm templates were surrounded by a closed NE. This value was dramatically reduced to ~20% in the Nup53 depleted extracts and was restored to ~80% upon addition of the full-length Nup53 protein (Fig. 4-5E).

The incorporation of recombinant Nup53 into the reformed nuclei was confirmed by immunofluorescence. Due to technical difficulties, we were unable to successfully use the anti-hNup53 antibodies for immunofluorescence analysis of the *in vitro* assembled nuclei. For this reason, the full length GST-Nup53 protein was also used in the add-back reaction to confirm the incorporation of the Nup53 at the NE. Using anti-GST antibodies, we were able to visualize the incorporation of GST-Nup53 in the reformed NE by immunofluorescence (Fig. 4-7B).

Figure 4-6. Depletion of Nup53 from cytosol blocks NPC assembly

(A) Transmission electron microscopy of nuclear assembly reactions of Mock, ΔNup53 extracts, or ΔNup53 extracts after addition of full length Nup53. Black scale bar 2 μm, white scale bar 210 μm. (B) Nuclear assembly reactions of Mock, ΔNup53 extracts, or ΔNup53 extracts after addition of full length Nup53. Reactions were analyzed by immunofluorescence with mAb414 (green). Chromatin was stained with DAPI (blue). Scale bar, 10 μm. Experiments presented in this Figure were performed by M. Platani and R. Santarella in the laboratory of I. Mattaj at the EMBL.

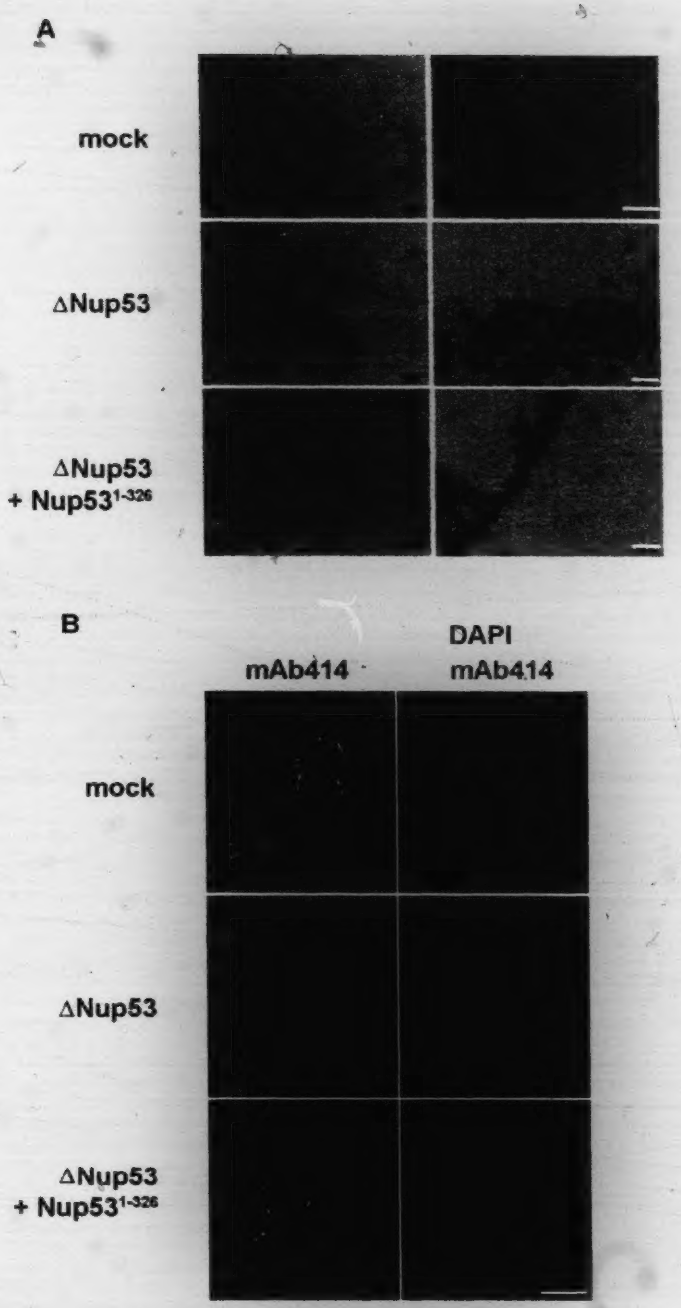
A
mock
ΔNup53
ΔNup53
+ Nup53¹⁻³²⁶
B
mAb414
DAPI
mAb414
mock
ΔNup53
ΔNup53
+ Nup53¹⁻³²⁶

Figure 4-6. Depletion of Nup53 from cytosol blocks NPC assembly

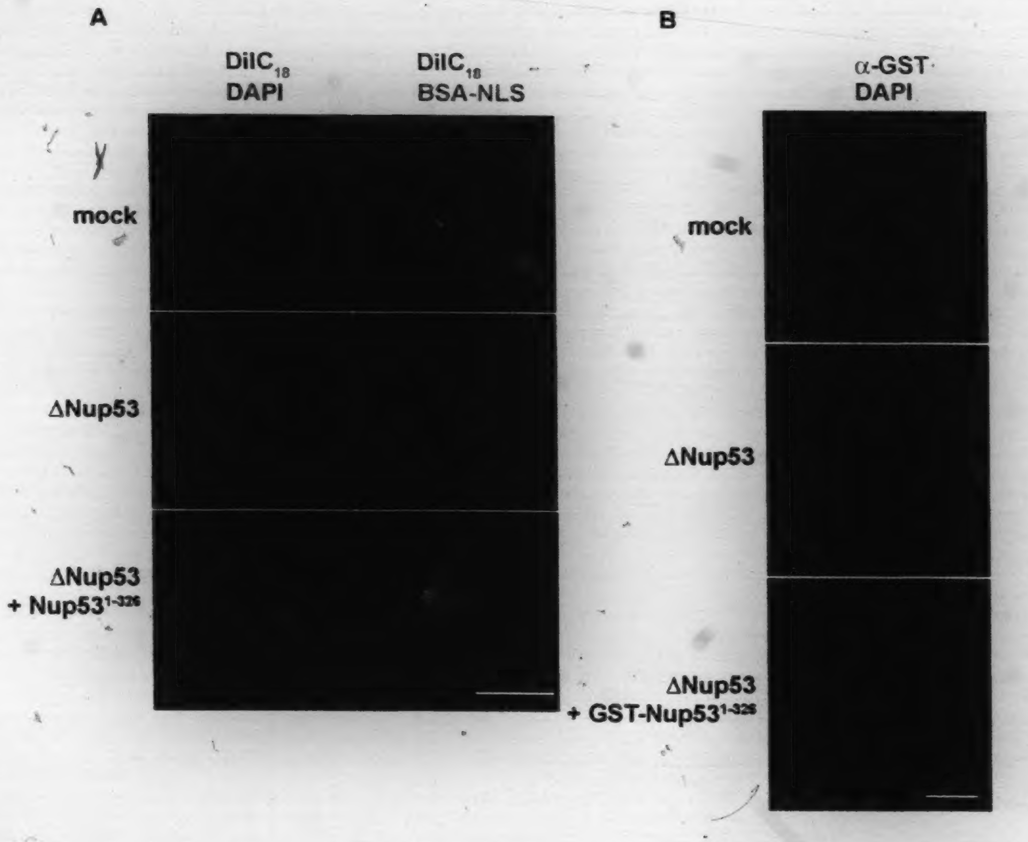
A
DiIC$_{18}$
DAPI
DiIC$_{18}$
BSA-NLS
mock
ΔNup53
ΔNup53
+ Nup53$^{1\text{-}326}$
B
α-GST
DAPI
mock
ΔNup53
ΔNup53
+ GST-Nup53$^{1\text{-}326}$

Figure 4-7. Characterization of *in vitro* assembled nuclei

(A) Nuclei assembled *in vitro* in Mock, ΔNup53 extracts, or ΔNup53 extracts after addition of full length Nup53. Nuclear import reaction was performed using FITC labelled BSA–NLS (green), 20-30 min prior to fixation. Membranes are visualized by using the membrane dye DilC$_{18}$ (red). Chromatin was stained with DAPI (blue). Scale bar,10 μm. (B) Nuclei assembled *in vitro* in Mock, ΔNup53 extracts, or ΔNup53 extracts after addition of GST-Nup53. Localization of the recombinant protein was analyzed by immunofluorescence using α-GST (red). Chromatin was stained with DAPI (blue). Experiments presented in this Figure were performed by M. Platani in the laboratory of I. Mattaj at the EMBL.

We have also analyzed the *in vitro* reconstituted nuclei by transmission electron microscopy (TEM). In mock-depleted extracts, nuclei with a continuous double bilayer perforated by NPCs were observed (Fig. 4-6A). Upon Nup53 depletion, docked vesicles were visualized on the chromatin surface together with short regions of fused membranes but neither complete membrane fusion nor NPCs were detected. Again both membrane fusion and NPC insertion were restored upon addition of recombinant human Nup53 (Fig. 4-6A).

4.2.5 The Nup53-Nup155 interaction is required for nuclear envelope formation

Many of the characteristics of Nup53 depletion phenotype are similar to those previously observed upon removal of Nup155 (Franz *et al.*, 2005). Since Nup53 has been shown to interact with Nup155, as well as Nup93, in both yeast and vertebrate cells (Marelli et al., 1998; Chapter III), it is possible that the observed Nup53 depletion phenotype arises from the disruption of a single function linked to one or more of these interactions. These interactions are likely established or stabilised during reassembly of the NPC, as we observed no codepletion of Nup93, Nup155, or Nup205 upon removal of Nup53 from the *Xenopus* extract (Fig. 4-5C). Moreover, the recruitment of Nup93, Nup205, and Nup155 to sperm chromatin is dependent on Nup53. Depletion of Nup53 from the soluble extracts inhibits the association of these Nups with the assembling NEs and this can be reversed by the addition of recombinant full-length Nup53 (Fig. 4-10).

To study the functions of these Nup interactions in more detail and understand their role in NE and NPC formation, we tested the ability of various truncation mutants of

Figure 4-8. Nup53 fragments that interact with NDC1 or Nup93 alone are not sufficient to restore NE formation

(A) Nuclei assembled *in vitro* in Mock, ΔNup53 extracts, or ΔNup53 extracts after addition of Nup53 $^{1\text{-}300}$, Nup53$^{1\text{-}203}$, and Nup53 $^{204\text{-}326}$. Membranes are visualized by using the membrane dye DiIC$_{18}$ (red). Chromatin was stained with DAPI (blue). Scale bar,10 μm. (B) Quantitation of closed NE formation of experiments performed as in (A) including the truncation fragment Nup53$^{167\text{-}300}$. More than 100 randomly chosen chromatin substrates per reaction were counted. Average of three independent experiments is shown. Experiments presented in this Figure were performed by M. Platani in the laboratory of I. Mattaj at the EMBL.

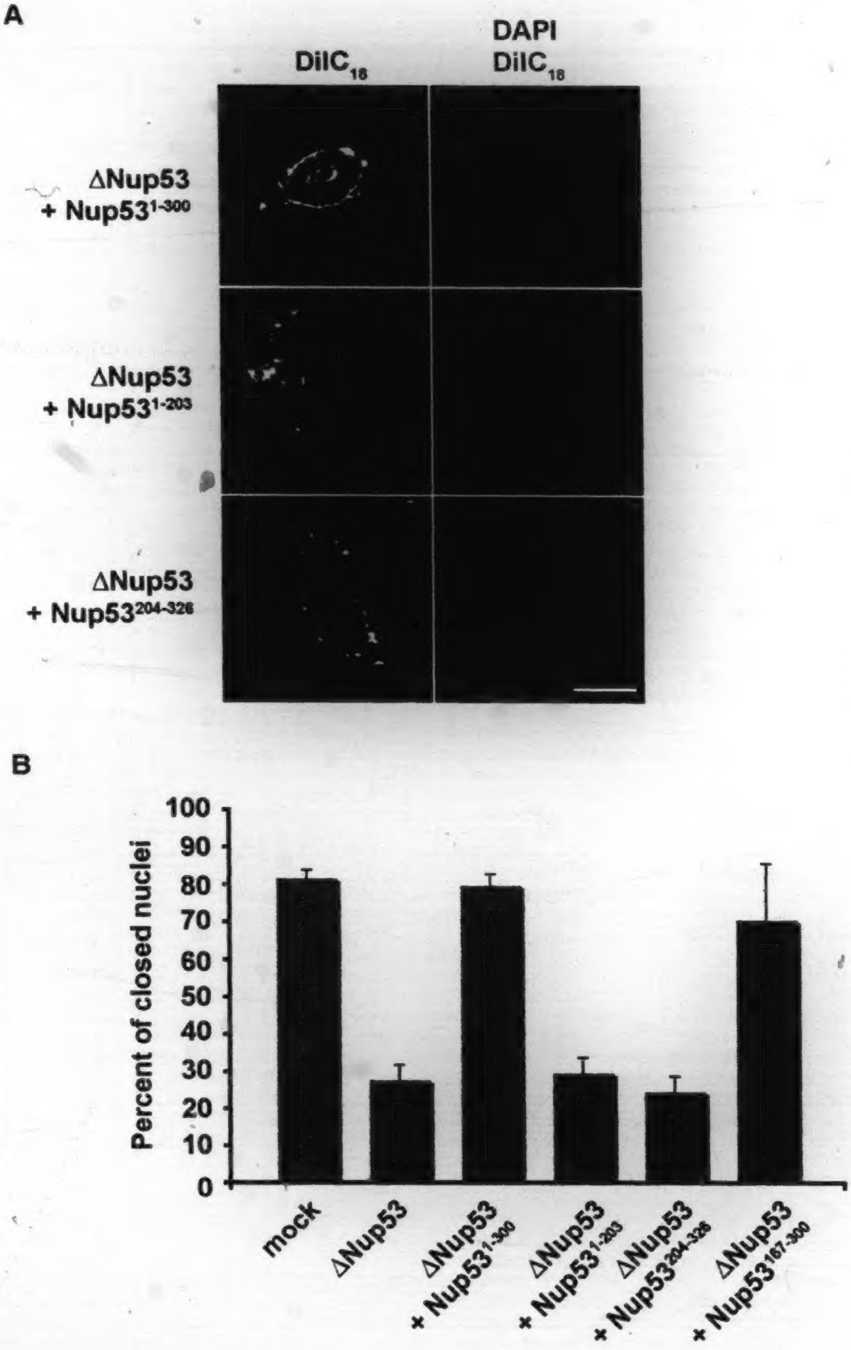

Figure 4-8. Nup53 fragments that interact with NDC1 or Nup93 alone are not sufficient to restore NE formation.

Nup53 to reconstitute NE assembly in the Nup53 depleted *Xenopus* extracts. Truncations were chosen based on the characterization of their Nup binding properties and their targeting to the NPC as defined above. The Nup53$^{1\text{-}300}$, Nup53$^{1\text{-}203}$, Nup53$^{204\text{-}326}$, Nup53$^{167\text{-}300}$ truncations were selected for analysis as each of these fragments was capable of interacting with a specific subset of Nups, thereby allowing us to dissect which interaction domains are necessary for the formation of a closed and functional NE. As human Nup53 is 72% identical to its *Xenopus* counterpart, the human versions were used to supplement the depleted *Xenopus* extracts. Nup53 deletion fragments were purified under native conditions and added to the Nup53-depleted cytosolic extracts. Similar to the addition of full-length Nup53, the purified fragments were added in amounts approximately equal to endogenous levels (Fig. 4-5B). First, we asked whether the Nup53 interaction with NDC1 is required for the formation of a closed NE. When depleted extracts were supplemented with Nup53$^{1\text{-}300}$, the fragment lacking the NDC1 interaction domain, and used in an assembly reaction, nuclei with closed NEs were formed (Fig. 4-8A) at a similar frequency to that seen with full length Nup53 (Fig. 4-5E). On the basis of these results, it appears that the COOH-terminal region of Nup53, previously shown to interact closely with the pore membrane, is not essential for Nup53 recruitment to membranes and NE and NPC assembly (Mansfeld et al., 2005; Marelli et al., 2001; Chapter III). Consistent with this idea, a Nup53 fragment containing the NDC1 interaction domain, Nup53$^{204\text{-}326}$, failed to rescue the NE and NPC assembly activity of the Nup53 depleted extracts (Fig. 4-8A and B), further suggesting that interaction between NDC1 and Nup53 is neither required nor sufficient to rescue NE and NPC formation. Importantly, the Nup53$^{1\text{-}300}$ fragment, which contains both the Nup155 and

Figure 4-9. A Nup53 fragment that interacts with Nup155 is sufficient to restore NE formation

(A) Nuclei assembled *in vitro* in Mock, ΔNup53 extracts, or ΔNup53 extracts after addition of full length Nup53, and fragment Nup53$^{167\text{-}300}$. Maximum intensity projections of 3D stack are shown. Membranes are visualized by using the membrane dye DiIC$_{18}$ (red). Chromatin was stained with DAPI (blue). (B) Nuclei assembled as in (A) were analyzed by immunofluorescence using Nup155 antibodies (red). Chromatin was stained with DAPI (blue). (C) Nuclei assembled as in (A/B) were analyzed by immunofluorescence using Nup93 antibodies (red). Chromatin was stained with DAPI (blue). Scale bar,10 μm. (D) Following add back of the Nup53$^{167\text{-}300}$ fragment, samples were processed for TEM as in 4-6A. Experiments presented in this Figure were performed by M. Platani and R. Santarella in the laboratory of I. Mattaj at the EMBL.

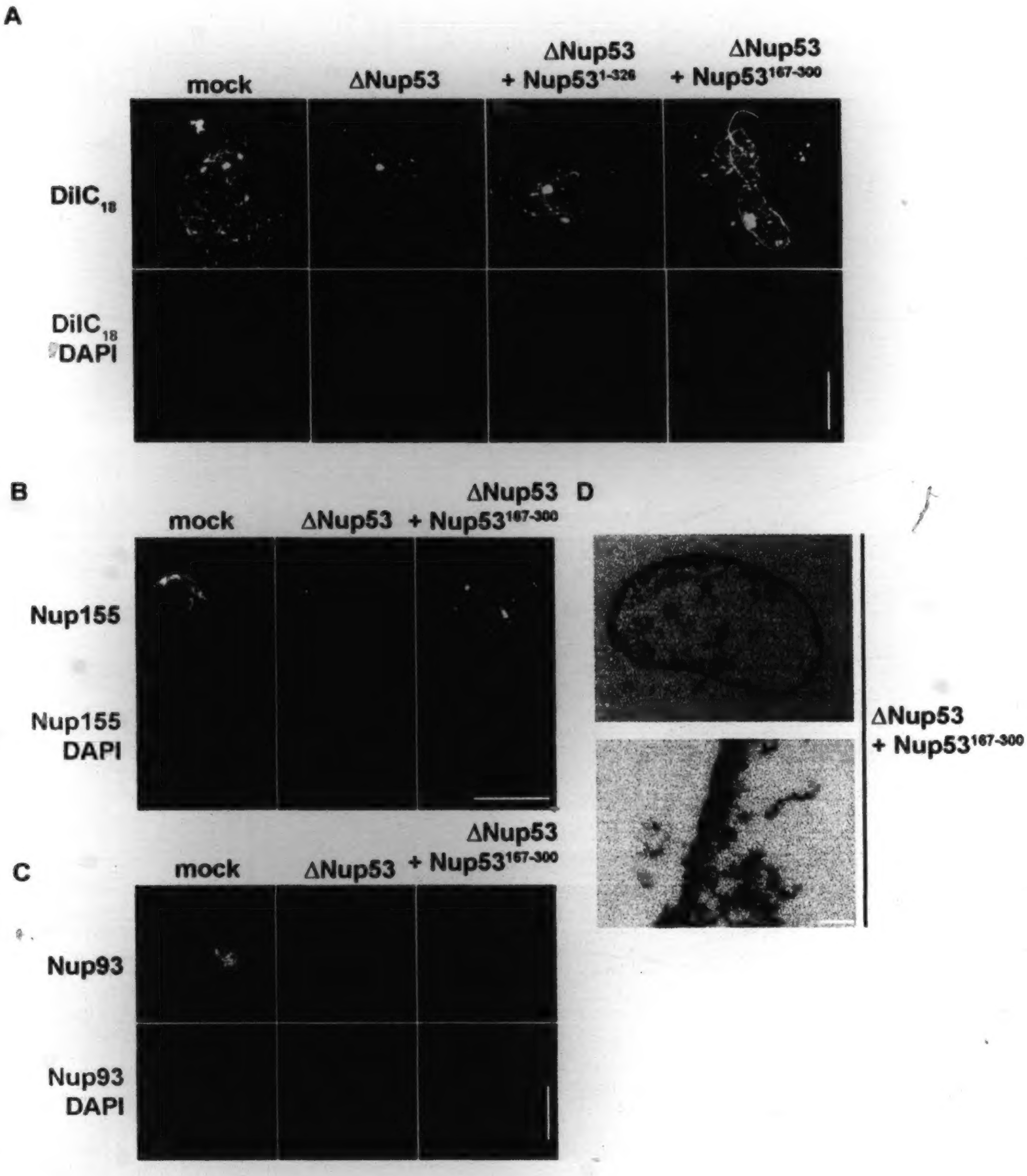
A
mock
ΔNup53
ΔNup53 + Nup53$^{1-326}$
ΔNup53 + Nup53$^{167-300}$
DiIC$_{18}$
DiIC$_{18}$ DAPI
B
mock
ΔNup53
ΔNup53 + Nup53$^{167-300}$
Nup155
Nup155 DAPI
C
mock
ΔNup53
ΔNup53 + Nup53$^{167-300}$
Nup93
Nup93 DAPI
D
ΔNup53 + Nup53$^{167-300}$

Figure 4-9. A Nup53 fragment that interacts with Nup155 is sufficient to restore NE formation

the Nup93 binding regions (Fig. 4-3A), was capable of replacing Nup53 in the NE reconstitution assays. We next tested whether the domain sufficient for interaction with Nup93 could rescue the depletion phenotype. Supplementing Nup53 depleted extracts with Nup53$^{1\text{-}203}$ did not rescue the depletion phenotype. Membranes associated with chromatin but did not fuse to form a closed NE and the percentage of the nuclei that did have a closed NE was similar to that observed with the depleted extracts (Fig. 4-8A and B).

Finally, we examined whether the Nup155 interacting region of Nup53 alone was sufficient to restore proper NE and NPC assembly by supplementing depleted extracts with Nup53$^{167\text{-}300}$. This construct binds Nup155 but neither NDC1 nor Nup93. When Nup53$^{167\text{-}300}$ was added to the depleted extracts, nuclei were formed that had both a closed NE as judged by membrane staining with DilC$_{18}$ (Fig. 4-9A) and NPCs as judged by electron microscopy analysis (Fig. 4-9D). Futhermore, quantitation revealed that 60-80% of sperm templates formed closed NEs (Fig. 4-8B). The Nup53$^{167\text{-}300}$ reconstituted nuclei were also able to recruit Nup155 as judged by immunofluorescence (Fig. 4-9B). In contrast, these nuclei failed to efficiently accumulate Nup93, showing lower levels of NE association than the mock depleted samples (Figure 4-9C). Taken together, these data suggest that the interaction between Nup53 and Nup155 is sufficient to reverse the depletion phenotype and results in the formation of a closed NE.

4.3 Discussion

Using both *in vivo* and *in vitro* approaches we have shown that Nup53 plays an essential role in nuclear pore complex assembly and nuclear envelope formation.

Through our analysis, we have identified the regions of Nup53 that are necessary for its interactions with its neighbours Nup93, Nup155, and the transmembrane nup NDC1 and defined the roles of these regions of Nup53 in mediating its targeting to the nuclear rim *in vivo* and its function in NPC and NE assembly *in vitro*. Each of the nup interacting regions of Nup53 can associate with the NPC *in vivo*. However, all three regions are required for the efficient targeting of Nup53 to the NPC. The involvement of NDC1 in Nup53 localization is consistent with our previous conclusion that the interaction of the Nup53 subcomplex with the membrane is mediated by NDC1 via its association with the COOH-terminal region of Nup53 (Fig. 4-4B; 4-1C). In addition, we have shown that the region of Nup53 required for binding to Nup155 plays a critical role in NPC and NE assembly in the *Xenopus* system, suggesting the formation of a Nup53/Nup155 complex is a key step in this process.

The NPC is a multi-subunit complex composed of several structurally defined components positioned at specific locations within the NPC (Fahrenkrog, 2006; Schwartz, 2005). A major challenge in the field is to develop a model for how individual Nups within the subcomplexes are locally organized and how, in turn, these subcomplexes interact with one another and the pore membrane. This portrait of the NPC is, however, only the initial step in our understanding of the complex and dynamic steps that lead to its assembly. As a step towards addressing this process, we have focused on defining interactions between Nup53 and several of its evolutionarily conserved binding partners, including Nup93 and Nup155. This subcomplex is a component of the NPC core and interactions of two members of this subcomplex, Nup53 and Nup155, with pore membrane proteins (Mansfeld et al., 2006; Fig. 4-3; J. Mitchell and R. Wozniak, manuscript in preparation) suggest it lies adjacent to the membrane.

In this study, we assessed the interactions between members of the Nup53-containing subcomplex utilizing human Nup53 truncations. Minimal binding regions of Nup53 were defined that are required for maintaining interactions with its known partners. Interestingly, as shown in Fig. 4-3, these regions are separable and not entirely interdependent. Nup93 binds an NH_2-terminal segment (amino acids residues 1-143) of Nup53, Nup155 interacts specifically with a more central region (residues 167-300) of Nup53, while NDC1 binds a COOH-terminal segment that contains an amphipathic helix located in the last 26 amino acid residues of Nup53. It is noteworthy that the $Nup53^{1\text{-}300}$ fragment, lacking the NDC1 interaction domain, binds better to Nup155 than full length Nup53. We interpret these data to suggest that while the Nup155 and NDC1 binding sites on Nup53 are distinct, the binding of Nup53 to the two partner Nups is not entirely independent. One possible explanation for the increased binding of the $Nup53^{1\text{-}300}$ fragment to Nup155 is that the COOH-terminal 26 amino acid residues of Nup53 inhibits binding to Nup155. *In vivo* this could function to inhibit their interaction until the COOH-terminal region of Nup53 engages the membrane, binds NDC1, or interacts with an as yet unidentified protein. In our *in vitro* binding assays these factors would be absent (in the case of membrane) or potentially present in substoichiometric amounts (i.e. free NDC1) thus leading to the reduced binding of Nup155 to full length Nup53 as compared to the $Nup53^{1\text{-}300}$ fragment. This model is attractive as it is consistent both with the observation that Nup155 is not removed from Nup53-depleted soluble extracts

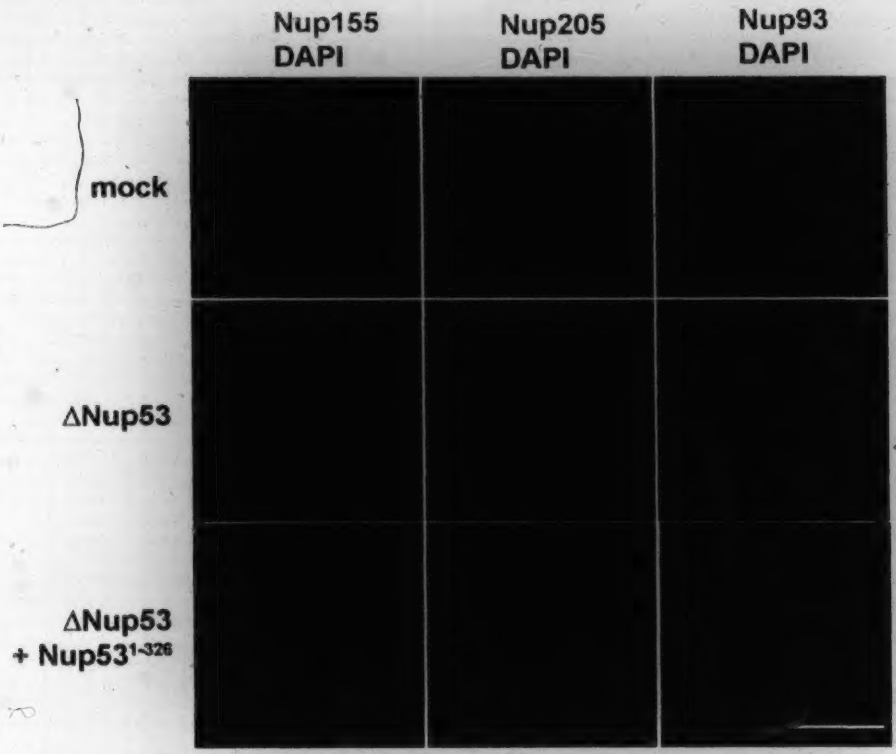
Nup155
DAPI
Nup205
DAPI
Nup93
DAPI
mock
ΔNup53
ΔNup53
+ Nup53$^{1-326}$

Figure 4-10. Analysis of Nup53-interacting nucleoporins

Nuclei assembled as in Fig. 4-5D, 4-6B, 4-7, 4-8A, and 4-9 were analyzed by immunofluorescence using antibodies directed against Nup155 (red; left), Nup205 (green; middle), and Nup93 (green; right). Scale bar, 10 μm. Experiments presented in this Figure were performed by M. Platani in the laboratory of I. Mattaj at the EMBL.

(Fig 4-4C) and with the apparent interdependence of Nup53 and Nup155 for incorporation into the assembling NE and NPC (Franz et al., 2005; Fig. 4-9).

In vivo analysis of the Nup53 truncation mutants showed that each of the interaction domains of Nup53 with its neighbouring nups (Nup93, Nup155, and NDC1) play a role in the efficient incorporation of Nup53 into the NPC. Individually, these separate regions can bind the NPC to some extent, but with reduced efficiency relative to the wild type protein. This would suggest that the cumulative interactions of Nup53 with its neighbours, rather than one specific binding event, is required for the stable association of Nup53 with the NPC. Studying the dynamics of GFP-Nup53 truncation mutants in more detail in live vertebrate cells and using molecular dynamics simulation approaches, as used to study the binding of importin-β to FG repeat nucleoporins (Isgro and Schulten, 2005), could shed more light on the interactions between the individual members of the Nup53 subcomplex.

Our data suggest that Nup53 plays an important role in nuclear envelope assembly. Previously, depletion of the protein from mammalian cultured cells by RNAi (Fig. 3-6) was shown to cause a severe defect in nuclear morphology as well as reduction of accumulation of Nup93, Nup155, and Nup205 at the nuclear rim suggestive of defects in NPC assembly. Moreover, depletion of the *C. elegans* counterpart of Nup53 caused an embryonic lethal phenotype along with a severe block to nuclear formation after mitosis (Galy et al., 2003). As in the *C. elegans* case, upon depletion of Nup53 from *Xenopus* extracts, we observed a strong inhibition of NE formation. Membrane vesicles were bound to the chromatin surface but did not fuse to form a closed NE and no NPC assembly was detected either by immunofluorescence or electron microscopy. Of the nucleoporins thus far tested, depletion of only three has produced a similar defect in NE formation (Finlay et al., 1991; Grandi et al., 1997; Powers et al., 1995; Walther et al., 2001; Walther et al., 2002). Two are the integral pore membrane proteins NDC1 and POM121 (Antonin et al., 2005; Mansfeld et al., 2006) that reside, together with lamin B receptor, in a membrane vesicle population which has a high avidity for the chromatin surface (Antonin et al., 2005; Ulbert et al., 2006). The third is Nup155 (Franz et al., 2005). The depletion of Nup155 from *C. elegans* embryos also prevents NE formation (Franz et al., 2005). Nup155, although recruited late during NE formation, therefore defines an essential step in NPC and NE assembly.

The similarities in phenotype observed upon depletion of POM121, NDC1, Nup53, and Nup155 might suggest that these proteins function on a similar branch of the assembly pathway. In support of this idea, our analysis of the Nup53 truncation mutants revealed that the region that bound Nup155 (Nup53 $^{167\text{-}300}$, Fig. 4-8) was sufficient to restore both NE and NPC formation and Nup155 recruitment in assembly assays depleted of Nup53. These results suggest that complex formation with Nup155 is critical to the function of Nup53 in NE and NPC assembly. Interestingly, the Nup53 $^{1\text{-}300}$ fragment, which, as discussed above, binds Nup155 *in vitro* at a higher efficiency than full length Nup53 but does not interact with NDC1, rescues the depletion phenotype to almost the same extent as full-length Nup53. This implies that while NDC1 interacts with Nup53, and this association is likely to play a role in linking Nup53 to the pore membrane, this specific interaction is not essential for the assembly of the Nup53/Nup155 complex within the NPC. It is possible that functionally redundant mechanisms exist that mediate the association of the Nup53/Nup155 complex with the pore membrane including, for example, the presence of additional interactions interfaces between this complex and NDC1 or other membrane proteins. Recent observations suggest the latter may exist as we have detected a direct interaction between Nup155 and POM121 (J. Mitchell and R. Wozniak, manuscript in preparation).

This work is the first extensive *in vitro* and *in vivo* analysis of nucleoporin truncation fragments. It clearly highlights the importance of defining specific protein interaction domains within a known nucleoporin subcomplex, and has allowed the analysis of key interactions in the process of NE and NPC assembly (Fig. 4-2). Moreover, we provide further evidence for the proposed checkpoint that links NE and NPC assembly in *Xenopus* egg extracts (Antonin *et al.*, 2005) by demonstrating that the soluble nucleoporin Nup53 must be present and able to interact with Nup155 in order for NE membrane and NPC assembly to occur. Our data suggest that Nup53, although recruited to chromatin later than the Nup107-160 complex or POM121 (Franz et al., 2005) plays a key role in the events that bring together the chromatin-associated Nup107-160 complex, vesicle bound transmembrane nucleoporins and soluble Nup155.

Chapter V: *Perspectives*

5.1 Synopsis

S. cerevisiae Nup53p was initially identified as a member of a complex of nups including Nup170p and Nup157p, and as a specific binding site for Kap121p at the NPC (Marelli et al., 1998). Kap121p plays a role in the assembly of Nup53p into the NPC (Lusk et al., 2001), and Nup53p inhibits Kap121p-mediated transport during mitosis (Makhnevych et al., 2003). The metazoan ortholog of Nup53p was identified by sequence homology to its yeast counterpart (Chapter III) and in a proteomic analysis of a rat liver-derived NPC fraction (Cronshaw et al., 2002). The work described in this thesis establishes functional insight into the role of vertebrate Nup53 in NE and NPC formation. In this chapter, this work will be discussed from a more global perspective and it will be integrated into an overview of exciting developments in our understanding of NPC function. Moreover, by drawing parallels between what we currently understand about the roles of the yeast and metazoan orthologs of Nup53, the evolution of the function of Nup53 will be discussed. This final discussion will also include a degree of speculation on certain aspects of Nup53 function based on preliminary data that are presented in Chapter VII.

5.2 Alternative NPC functions

The past decade has seen an evolution in our understanding of NPC biology. A growing body of work has indicated that we are but scratching the surface of what is clearly a complex biological function of the NPC. A central theme is one of the NPC as a strategically positioned host to a repertoire of proteins with well characterized roles in processes distinct from nuclear transport. As a case in point, the SAC proteins Mad1 and

Mad2 reside predominately at pores in both yeast and higher eukaryotes during interphase. Upon checkpoint activation, these proteins redistribute to the kinetochore (Campbell et al., 2001; Iouk et al., 2002; Scott et al., 2005). In this regard, it has been proposed that in yeast the NPC sequesters these proteins until they are required to perform critical roles at the kinetochore (Scott et al., 2005). But the NPC does not appear to be a passive participant in this process. Instead, it is believed that the specific NPC proteins involved in the pore tethering of Mad1p may be involved in the regulation of their release (Scott et al., 2005). Once released from the NPC, the targeting of Mad1p to the kinetochore has been shown to be mediated by the exportin, Xpo1p (R.J. Scott and R.W. Wozniak, manuscript in preparation). These data are consistent with the idea that specific nups and transport factors could function as key modulators of the SAC response.

Another intriguing example of alternative NPC function is the association of the members of the sumoylation pathway with NPCs. Both vertebrate SENP2 and yeast Ulp1p are SUMO isopeptitases that interact with specific NPC components (Makhnevych et al., 2007; Panse et al., 2003; Zhang et al., 2002). Targeting of these proteins to the septin ring in yeast has been shown to involve the β-kap, Kap121p (Makhnevych et al., 2007). In addition, several findings support the notion that the SUMO machinery is also required for nuclear transport. SUMOylation has been shown to trigger hnRNP release from mRNA during export (Vassileva and Matunis, 2004) and Nup358, a component of the cytoplasmic fibrils with a well documented role in transport, has intrinsic E3 ligase activity (Bernad et al., 2004; Forler et al., 2004; Pichler et al., 2002). Taken together, the data described above highlight that nups play critical roles in other processes apart from transport. Moreover, karyopherins not only faciliate the transport of substrates between the nucleoplasm and the cytoplasm but they are capable of targeting NPC resident proteins with roles in the SAC and the SUMO pathway to cellular destinations where they execute their function.

5.3 Crystal structure of the NPC

Obtaining high resolution molecular details of nups and individual subcomplexes is pivitol to our understanding of how they are arranged and assembled into functional NPCs. Therefore, there is a growing demand for a structural inventory of the NPC building blocks. A low resolution portrait of NPCs from several different organisms has already been provided to a certain extent by electron cryomicroscopy and tomography studies (Beck et al., 2004; Jarnik and Aebi, 1991; Stoffler et al., 1999; 2003; Yang et al., 1998). Fragments derived from approximately one third of the nups have been studied in atomic detail owing to their solved crystal structures: Nsp1p, Nup1p, Nup116p, and Nup159p in yeast (Bayliss et al., 2000; Liu and Stewart, 2005; Robinson et al., 2005; Weirich et al., 2004) and Nup214/CAN, Nup98, Nup133, and Nup53 in metazoans (Berke et al., 2004; Fribourg et al., 2001; Handa et al., 2006; Hodel et al., 2002). Computational approaches of Devos and colleagues (2004, 2006) have extended this analysis to all nups in a structure prediction-based categorization of domains (see section 1.3.1 and Fig. 1-2). The three-dimensional models based on this analysis underscore the overall simplicity of the composition and modularity of NPCs and hint at the evolutionary origins of NPCs. Their proposed "protocoatomer hypothesis" predicts that nups such as Nup170p/Nup155 and the Nup84p/Nup107-160 complex and components of the vesicle coating machinery evolved from a common ancestor and they perform shared functions in the bending and stabilization of curved membranes. Indeed, *bona fide* vesicle coat components Seh1p and Sec13p are members of the yeast Nup84p complex. The implication of this hypothesis is, firstly, that it provides insight into the evolution of the NPC. Secondly it offers an explanation as to how the specific NPC constituents contribute to the maintenance of the membrane curvature which results in the pores in which they reside. Undoubtedly, this represents a critical aspect of NPC and NE formation. In this regard, it would be interesting to determine if members of the Nup84p complex are present in the transcisternal pores of the intranuclear membranes resulting from Nup53p overexpression in yeast (Marelli et al., 2001). These pores were found to contain Nup53p, Ndc1p, and Pom152p and determining whether Nup84 complex components are also present by immunoelectron microscopy analysis could offer insight on the ability of these nups to contribute to pore membrane curvature *in vivo*.

Surely the coming years will see additional solved nup structures and whether the deduced tertiary structure of the NPC in its entirety will reveal a similar organization as the predicted model awaits this comprehensive structural information. Regardless, these studies have provided the groundwork for all future NPC structural analysis.

5.4 Organization of Nup53 within the NE

Nup53 is symmetrically localized on both faces of the NPC (Rout et al., 2000; Fig. 3-9) and displays a comparatively high degree of association with the NE membrane (Marelli et al., 1998 and Fig. 3-2) and nuclear lamina (Fig. 3-2). The interaction analysis of Nup53 presented in Chapter III and IV has uncovered multiple binding partners, in

ONM
Nup192
Nic96
Nup53/Nup59
Ndc1
Pom152
Nup170/Nup157
PM
Pom34
Nup205
Nup93
Nup53
NDC1
Nup155
POM121
gp210
INM
Yeast
Vertebrates

Figure 5-1. Model of conserved yeast and vertebrate Nup53 complexes.

Schematic of the organization of the Nup53 complex in both yeast and vertebrates (blue spheres). Transmembrane nups are depicted as red spheres.

several domains of the NE. At the core of the NPC, Nup53 is a member of a conserved complex of nups comprised of Nup93, Nup155, and Nup205. Interactions between Nup53 and the nuclear lamina protein lamin B have also been detected which may explain, in part, the tight NE membrane association of this nup. This can further be explained by the interaction between Nup53 and the pore membrane nup NDC1 (Mansfeld et al., 2006 and Fig. 4-1). Furthermore, it has been proposed that yeast Nup53p can interact directly with the NE membrane itself, and this interaction is likely to be mediated by the COOH-terminal amphipathic helix, which is also present in metazoan Nup53 (Marelli et al., 1998; 2001; Chapter III). Indeed, removal of this region results in an inability of Nup53 to interact with NDC1 (Fig. 4-1C; 4-3).

It is unlikely that Nup53 interacts with all of its binding partners in one defined complex. We have proposed in Chapter III that there may be distinct pools of Nup53 within the NPC (see Discussion and Fig. 3-8). The possibility remains, however, that these interactions could also be regulated within the context of the cell cycle, as observed for the yeast counterpart of this complex of nups (Makhnevych et al., 2003). Moreover, these interactions may be temporally regulated during NE formation. This is highlighted by our data in Chapter IV, clearly demonstrating that the Nup53-Nup155 interaction appears to be critical for NE formation, whereas interactions between Nup53 and other members of the subcomplex are dispensible. This suggests that interactions between Nup53, Nup155, and NDC1 may form earlier within the context of NPC formation than the interaction between Nup53 and Nup93/Nup205, and lamin B.

5.5 The phosphorylation of Nup53

Nup53 is a member of a group of nups that have been shown to be phosphorylated during the cell cycle both *in vitro* and *in vivo* (Favreau et al., 1996; Glavy et al., 2007; Lusk et al., 2007; Marelli et al., 1998; Fig. 7-1). The functional significance of these modifications are ill defined but proposals to date have centered around the reversible disruption of nup-nup interactions ultimately contributing to NPC disassembly (Bodoor et al., 1999; Favreau et al., 2996; Macaulay and Forbes, 1995). Unlike other nups that are phosphorylated in all stages of the cell cycle, or specifically in both S- and M-phase, Nup53, in both yeast and metazoan cells, appears to be phosphorylated solely in mitosis (Favreau et al, 1996; Lusk et al., 2007; Marelli et al., 1998; and see Appendix Fig. 7-1). It has been hypothesized that Nup53p phosphorylation in yeast would trigger the rearrangements of the NPC shown to result in Kap121p-mediated transport inhibition during M-phase (Makhnevych et al., 2003). Additional data further suggests that Nup53p phosphorylation may also play a role in the spindle assembly checkpoint (SAC) response (Iouk et al., 2002; Lusk et al., 2007; Scott et al., 2005).

Both *Xenopus* and human Nup53 are phosphorylated in mitosis (Stukenberg et al., 1997 and Fig. 7-1). Currently, phosphorylation has been implicated neither in rearrangement of interactions within the metazoan Nup53 complex, nor in the SAC. Therefore, the function of this modification is less understood than for yeast Nup53p. The initial characterization of human Nup53 (Chapter III) involved a preliminary analysis of its phosphorylation. This work is currently not published but is presented in Fig. 7-1. Based on these data, it is possible that Nup53 phosphorylation may potentially be involved in the regulation of Nup53 membrane binding. This is supported by the finding that endogenous, dephosphorylated Nup53 fractionates with membranes in mitotic Hela cells (Fig. 7-1C). Furthermore, GFP-Nup53, which is phosphorylated significantly less efficiently than endogenous Nup53, partially associates with the mitotic ER (Fig. 7-1E). An important prediction of this working model would be that this modification would occur in the COOH-terminal amphipathic helix, which is believed to be critical for membrane interaction. This does not appear to be the case for the sites recognized by one the kinases shown to be responsible for yeast Nup53p phosphorylation (Lusk et al., 2007). However, more than one kinase contributes to this modification in yeast, and the kinases involved in the metazoan Nup53 phosphorylation have not yet been determined.

As an added layer of complexity, it is plausible that the Nup53-Nup155 interaction, which is critical for NE and NPC assembly (Fig. 4-9), may be regulated by phosphorylation. This is based primarily on the observation in yeast that Nup53p is phosphorylated in M-phase, during which time no interaction between Nup53p and Nup170p is detected (Makhnevych et al., 2003). The regulation of Nup53 membrane binding and/or the Nup53-Nup155 interaction by Nup53 phosphorylation could represent a critical, regulated step in the process of NE formation. Experiments designed at differentiating these possibilities would include the mapping of the phosphorylation sites of Nup53, followed by point mutagenesis studies. The extent of Nup155 binding to the various Nup53 mutants could be examined using *in vitro* binding assays. Moreover, similar add back experiments to those described in 4.2.5 would assess the ability of the phosphorylation mutants to rescue the NPC and NE assembly defect observed in extracts depleted of Nup53.

5.6 The conserved RNA recognition motif (RRM) of Nup53

Computational analysis of nup secondary structure has predicted that Nup53 contains an evolutionarily conserved RNA recognition motif (RRM) (Devos et al., 2006). The crystal structure of this domain has recently been solved for *M. musculus* Nup53 (Handa et al., 2006). In this manuscript, the authors proposed that the Nup53 RRM, rather than acting as a nucleic acid binding domain, might be a homodimerization domain or contribute to protein-protein interactions. However, experiments aimed at characterizing the function of the human Nup53 RRM have clearly revealed that the Nup53 RRM is not sufficient for interactions with neighbouring nups (Fig. 7-2). Moreover, the possibility remains that it may be responsible for homodimerization as this has not been directly tested *in vitro*. However, if indeed homodimerization were critical for NPC or NE assembly, one might expect that add back of this domain to the Nup53-depleted *Xenopus* extracts would rescue the phenotype, but it did not (Fig. 7-3) or, alternatively, that a dominant negative effect would arise when it was added in excess to assembly reactions. This was also not the case (Fig. 7-3).

Our analysis has uncovered a novel nucleic acid binding property of Nup53 (Fig. 7-2). It is capable of binding *in vitro* to both single- and double-stranded DNA cross-linked to cellulose. Nup53 is also capable of binding robustly to ribosomal RNA in gel-shift assays performed by collaborators (M. Oeffinger and M. Rout, personal communication). These data suggest that the RRM of Nup53 may be playing a role in RNA metabolism, such as mRNA export or in processing of mRNP particles as they traverse the NPC during nuclear mRNA export. To address this question, localization of mRNA could be examined using *in situ* hybridization in cells either depleted of Nup53 using RNAi or over-expressing versions of Nup53 that contain point mutations in the RRM.

In agreement with our previously reported tight association of Nup53 with the NE (Fig. 3-2), Nup53, together with Nup155, were also found in purified membrane fraction of *Xenopus* oocytes (M. Platani, personal communication). Taken together with the ability of Nup53 to bind to nucleic acid, it would be an attractive possibility that Nup53 could be involved in membrane vesicle docking to chromatin. However, NE membrane vesicles remain capable to bind to chromatin in Nup53 depleted conditions (Fig. 4-5). Regardless, this possibility cannot be completely disregarded given recent reports that there are several other proteins involved in this docking event, that would possibly be sufficient to mediate binding in the absence of Nup53 (Ulbert et al., 2006; see section 1.6.1). Nup53 mediated NE membrance vesicle docking to chromatin could be analyzed by reconstituting membrane vesicles that are lacking those INM proteins that have been previously implicated in DNA binding and examining the ability of these Nup53 NE membrane vesicles to bind to DNA *in vitro* (Ulbert et al., 2006).

5.7 Nup53 and the NE/NPC assembly checkpoint

The observation that depletion of the vertebrate Nup107-160 complex resulted in a closed NE lacking detectable NPCs demonstrated that NE and NPC assembly are separable (Walther et al., 2003; Harel et al., 2003). This finding rekindled interest in developing models of NE formation in metazoan cells and laid the foundation for all future types of analyses. The Nup107-160 complex, together with POM121, were

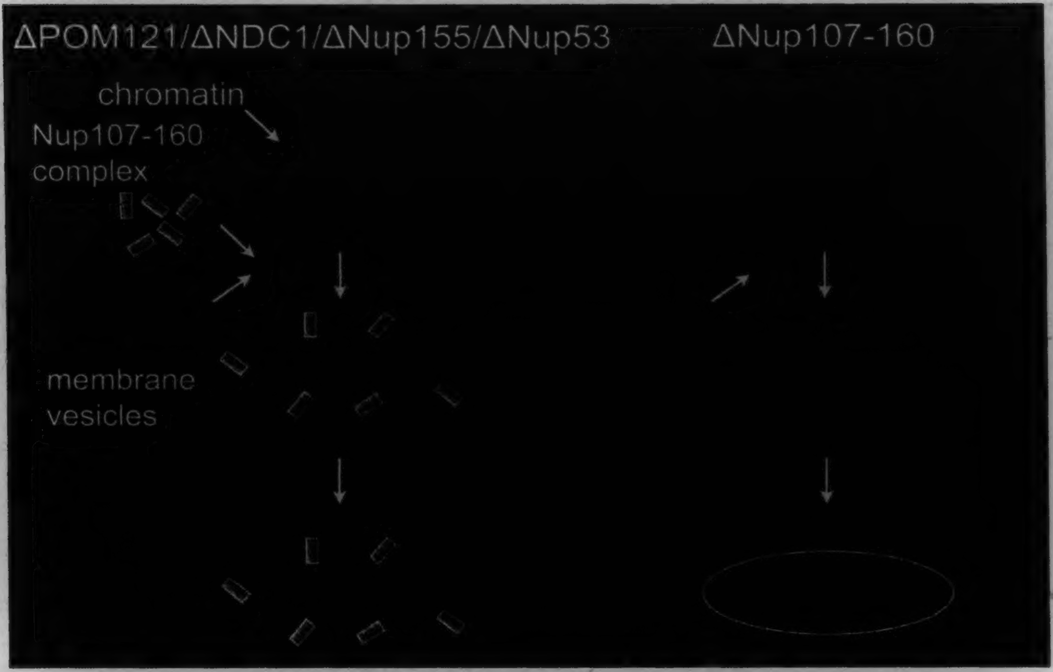
ΔPOM121/ΔNDC1/ΔNup155/ΔNup53
ΔNup107-160
chromatin
Nup107-160 complex
membrane vesicles

Figure 5-2. Model representing the critical players linking NE and NPC assembly.

Schematic representation comparing the phenotypes observed upon depletion of various nups using the *Xenopus* nuclear reconstitution assay. When either POM121, NDC1, Nup155, or Nup53 are depleted, the Nup107-160 complex and NE membrane vesicles are still capable of binding to the chromatin surface but no further NPC or NE assembly was observed. When the 107-160 complex was depleted, NE membrane vesicles bind to the chromatin surface and fuse to form a closed and continuous NE that lacks NPCs. Adapted from Antonin et al., 2005; Franz et al., 2005, Harel et al., 2003; Hawryluk-Gara et al., 2007 (submitted) and Chapter IV; Mansfeld et al.; 2006; Walther at al., 2003.

proposed to participate in a checkpoint that prevented NE vesicle fusion until chromatin recruitment of POM121 was detected (Antonin et al., 2005). Detection of POM121 was proposed to be mediated through a physical interaction between the Nup107-160 complex and POM121, though this was not shown. In line with this notion, data from our laboratory has provided compelling evidence for a physical interaction between POM121 and members of the Nup107-160 complex, (J.M. Mitchell and R.W. Wozniak, manuscript in preparation). Nup155, a member of the Nup53 complex, and NDC1, which interacts with Nup53, have also been implicated in this checkpoint (Franz et al., 2005; Mansfeld et al., 2006; Chapter III, IV). Notably, Nup155 and Nup53 are the only known soluble nups whose depletion gives rise to a phenotype that is similar to depletion of either POM121 or NDC1 (Finlay and Forbes, 1990, 1991; Franz et al., 2005; Grandi et al., 1997; Mansfeld et al., 2006; Powers et al., 1995; Walther et al., 2001; 2002, Chapter IV). In this context, the similarity of the depletion phenotypes of these nups suggests that they function within a complex that plays a critical role in the proposed NE/NPC assembly checkpoint. Indeed we have observed interactions between POM121, NDC1, Nup53 and Nup155. Nup53 and Nup155 are recruited to chromatin significantly later than Nup107 or POM121, concomitantly with NE membrane fusion, defining an essential late step in the NE and NPC formation process (Franz et al., 2005).

The work presented in Chapter IV of this thesis represents an important example of an extensive functional interaction analysis within complex of nups. We uncovered that only the interaction between Nup53 and Nup155 is critical for assembly, whereas the Nup53-Nup93 and Nup53-NDC1 interactions were dispensible. Of those nups that are required for NE and NPC assembly, it remains to be defined what domains of these proteins are essential for these processes and what binding partners they interact with. Undoubtedly, this type of investigation into the complex interaction network between individual nups and subcomplexes during NE/NPC assembly is critical in broadening our understanding of this fundamental cellular process.

It is tempting to speculate that Nup53 and Nup155 together comprise a binding platform that participates in an important regulatory step in NE formation. This is supported by key observations. Nup53 and Nup155 interact directly, and with NDC1 and POM121, respectively (Fig. 4-1, 4-3; J.M. Mitchell and R.W. Wozniak, manuscript in preparation). POM121 also interacts with the Nup107-160 complex (see above). Through this web of interactions, Nup53 and Nup155 may function to bring the soluble nups in spatial proximity of the transmembrane nups where higher order interactions would form resulting in an assembled NPC. How the formation of these higher order interactions would trigger membrane fusion is presently not clear, and represents an important question to address in the future. An exciting possibility is that Nup155, Nup107, Nup133, and Nup160, which are structurally similar to membrane vesicle coating complexes, actually contribute to the induction and stabilization of membrane curvature (see 1.3.1.3 and 5.3).

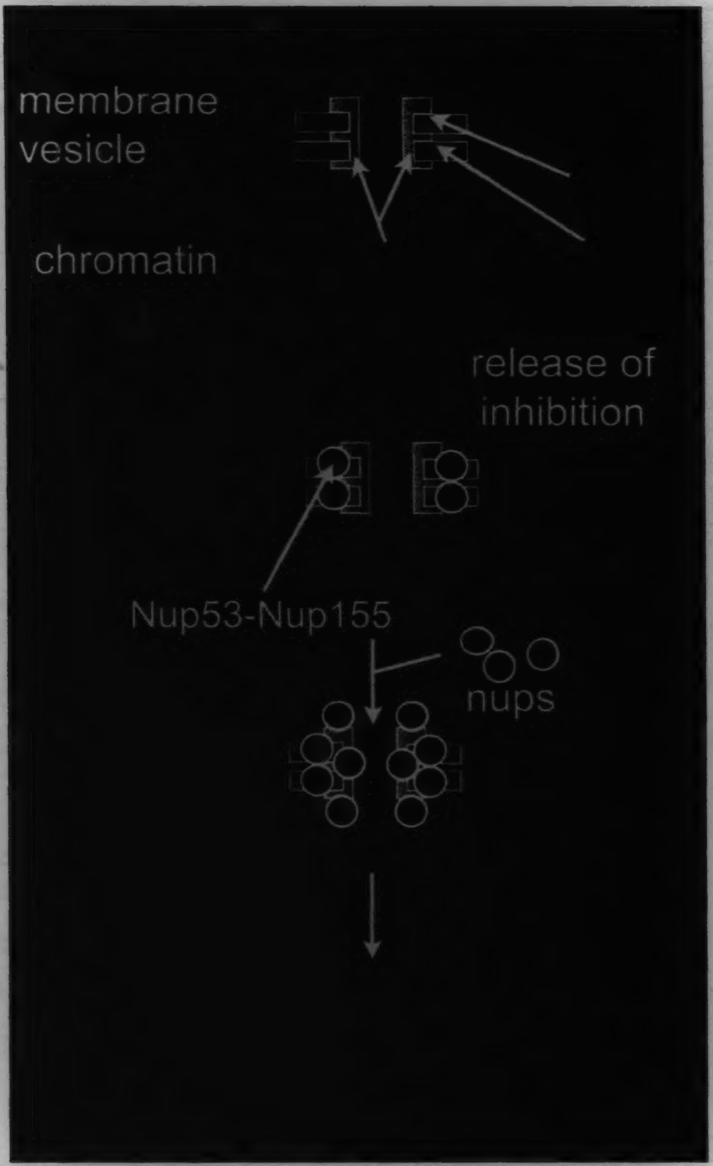
membrane
vesicle
chromatin
release of
inhibition
Nup53-Nup155
nups

Figure 5-3. Model for the Nup53-Nup155 interaction function in NE and NPC assembly.

In this model, the chromatin associated Nup107-160 complex, through an unknown signalling event, inhibits subsequent NE membrane vesicle (grey circles) fusion and NPC assembly. This inhibition is released by an uncharacterized mechanism when POM121, NDC1, Nup53, and Nup155 are present. Adapted from Antonin et al., 2005; Franz et al., 2005, Harel et al., 2003; Hawryluk-Gara et al., 2007 (submitted) and Chapter IV; Mansfeld et al., 2006, Walther at al., 2003.

Chapter VI: *References*

Aitchison, J.D. and Rout, M.P. (2002) A tense time for the nuclear envelope. Cell, 108, 301-304.

Aitchison, J.D., Rout, M.P., Marelli, M., Blobel, G. and Wozniak, R.W. (1995) Two novel related yeast nucleoporins Nup170p and Nup157p: complementation with the vertebrate homologue Nup155p and functional interactions with the yeast nuclear pore-membrane protein Pom152p. J Cell Biol, 131, 1133-1148.

Akey, C.W. and Radermacher, M. (1993) Architecture of the Xenopus nuclear pore complex revealed by three-dimensional cryo-electron microscopy. J Cell Biol, 122, 1-19.

Alber, F., Dokudovskaya, S., Veenhoff, L.M., Zhang, W., Kipper, J., Devos, D., Suprapto, A., Karni-Schmidt, O., Williams, R., Chait, B.T., Sali, A. and Rout, M.P. (2007) The molecular architecture of the nuclear pore complex. Nature, 450, 695-701.

Anderson, D.J. and Hetzer, M.W. (2007) Nuclear envelope formation by chromatin-mediated reorganization of the endoplasmic reticulum. Nat Cell Biol, 9, 1160-1166.

Antonin, W., Franz, C., Haselmann, U., Antony, C. and Mattaj, I.W. (2005) The integral membrane nucleoporin pom121 functionally links nuclear pore complex assembly and nuclear envelope formation. Mol Cell, 17, 83-92.

Antonin, W. and Mattaj, I.W. (2005) Nuclear pore complexes: round the bend? Nat Cell Biol, 7, 10-12.

Bastos, R., Ribas de Pouplana, L., Enarson, M., Bodoor, K. and Burke, B. (1997) Nup84, a novel nucleoporin that is associated with CAN/Nup214 on the cytoplasmic face of the nuclear pore complex. J Cell Biol, 137, 989-1000.

Baur, T., Ramadan, K., Schlundt, A., Kartenbeck, J. and Meyer, H.H. (2007) NSF- and SNARE-mediated membrane fusion is required for nuclear envelope formation and completion of nuclear pore complex assembly in Xenopus laevis egg extracts. J Cell Sci, 120, 2895-2903.

Bayliss, R., Kent, H.M., Corbett, A.H. and Stewart, M. (2000) Crystallization and initial X-ray diffraction characterization of complexes of FxFG nucleoporin repeats with nuclear transport factors. J Struct Biol, 131, 240-247.

Bayliss, R., Littlewood, T. and Stewart, M. (2000) Structural basis for the interaction between FxFG nucleoporin repeats and importin-beta in nuclear trafficking. Cell, 102, 99-108.

Bayliss, R., Littlewood, T., Strawn, L.A., Wente, S.R. and Stewart, M. (2002) GLFG and FxFG nucleoporins bind to overlapping sites on importin-beta. J Biol Chem, 277, 50597-50606.

Bayliss, R., Ribbeck, K., Akin, D., Kent, H.M., Feldherr, C.M., Gorlich, D. and Stewart, M. (1999) Interaction between NTF2 and xFxFG-containing nucleoporins is required to mediate nuclear import of RanGDP. J Mol Biol, 293, 579-593.

Beaudouin, J., Gerlich, D., Daigle, N., Eils, R. and Ellenberg, J. (2002) Nuclear envelope breakdown proceeds by microtubule-induced tearing of the lamina. Cell, 108, 83-96.

Beck, M., Forster, F., Ecke, M., Plitzko, J.M., Melchior, F., Gerisch, G., Baumeister, W. and Medalia, O. (2004) Nuclear pore complex structure and dynamics revealed by cryoelectron tomography. Science, 306, 1387-1390.

Belgareh, N., Rabut, G., Bai, S.W., van Overbeek, M., Beaudouin, J., Daigle, N., Zatsepina, O.V., Pasteau, F., Labas, V., Fromont-Racine, M., Ellenberg, J. and Doye, V. (2001) An evolutionarily conserved NPC subcomplex, which redistributes in part to kinetochores in mammalian cells. J Cell Biol, 154, 1147-1160.

Ben-Efraim, I. and Gerace, L. (2001) Gradient of increasing affinity of importin beta for nucleoporins along the pathway of nuclear import. J Cell Biol, 152, 411-417.

Benavente, R., Dabauvalle, M.C., Scheer, U. and Chaly, N. (1989) Functional role of newly formed pore complexes in postmitotic nuclear reorganization. Chromosoma, 98, 233-241.

Berke, I.C., Boehmer, T., Blobel, G. and Schwartz, T.U. (2004) Structural and functional analysis of Nup133 domains reveals modular building blocks of the nuclear pore complex. J Cell Biol, 167, 591-597.

Bernad, R., van der Velde, H., Fornerod, M. and Pickersgill, H. (2004) Nup358/RanBP2 attaches to the nuclear pore complex via association with Nup88 and Nup214/CAN and plays a supporting role in CRM1-mediated nuclear protein export. Mol Cell Biol, 24, 2373-2384.

Bickel, T. and Bruinsma, R. (2002) The nuclear pore complex mystery and anomalous diffusion in reversible gels. Biophys J, 83, 3079-3087.

Bilbao-Cortes, D., Hetzer, M., Langst, G., Becker, P.B. and Mattaj, I.W. (2002) Ran binds to chromatin by two distinct mechanisms. Curr Biol, 12, 1151-1156.

Bischoff, F.R. and Ponstingl, H. (1991) Catalysis of guanine nucleotide exchange on Ran by the mitotic regulator RCC1. Nature, 354, 80-82.

Blobel, G. and Potter, V.R. (1966) Nuclei from rat liver: isolation method that combines purity with high yield. Science, 154, 1662-1665.

Bodoor, K., Shaikh, S., Enarson, P., Chowdhury, S., Salina, D., Raharjo, W.H. and Burke, B. (1999) Function and assembly of nuclear pore complex proteins. Biochem Cell Biol, 77, 321-329.

Bodoor, K., Shaikh, S., Salina, D., Raharjo, W.H., Bastos, R., Lohka, M. and Burke, B. (1999) Sequential recruitment of NPC proteins to the nuclear periphery at the end of mitosis. J Cell Sci, 112 (Pt 13), 2253-2264.

Boehm, M. and Bonifacino, J.S. (2001) Adaptins: the final recount. Mol Biol Cell, 12, 2907-2920.

Boehmer, T., Enninga, J., Dales, S., Blobel, G. and Zhong, H. (2003) Depletion of a single nucleoporin, Nup107, prevents the assembly of a subset of nucleoporins into the nuclear pore complex. Proc Natl Acad Sci U S A, 100, 981-985.

Boehmer, T. and Schwartz, T.U. (2007) Purification, crystallization and preliminary X-ray analysis of a Nup107-Nup133 heterodimeric nucleoporin complex. Acta Crystallogr Sect F Struct Biol Cryst Commun, 63, 816-818.

Boman, A.L., Delannoy, M.R. and Wilson, K.L. (1992) GTP hydrolysis is required for vesicle fusion during nuclear envelope assembly in vitro. J Cell Biol, 116, 281-294.

Bonifacino, J.S. and Lippincott-Schwartz, J. (2003) Coat proteins: shaping membrane transport. Nat Rev Mol Cell Biol, 4, 409-414.

Bridger, J.M., Foeger, N., Kill, I.R. and Herrmann, H. (2007) The nuclear lamina. Both a structural framework and a platform for genome organization. Febs J, 274, 1354-1361.

Buendia, B. and Courvalin, J.C. (1997) Domain-specific disassembly and reassembly of nuclear membranes during mitosis. Exp Cell Res, 230, 133-144.

Burke, B. (2001) The nuclear envelope: filling in gaps. Nat Cell Biol, 3, E273-274.

Burke, B. and Ellenberg, J. (2002) Remodelling the walls of the nucleus. Nat Rev Mol Cell Biol, 3, 487-497.

Busson, S., Dujardin, D., Moreau, A., Dompierre, J. and De Mey, J.R. (1998) Dynein and dynactin are localized to astral microtubules and at cortical sites in mitotic epithelial cells. Curr Biol, 8, 541-544.

Campbell, M.S., Chan, G.K. and Yen, T.J. (2001) Mitotic checkpoint proteins HsMAD1 and HsMAD2 are associated with nuclear pore complexes in interphase. J Cell Sci, 114, 953-963.

Chaudhary, N. and Courvalin, J.C. (1993) Stepwise reassembly of the nuclear envelope at the end of mitosis. J Cell Biol, 122, 295-306.

Chen, R.H., Brady, D.M., Smith, D., Murray, A.W. and Hardwick, K.G. (1999) The spindle checkpoint of budding yeast depends on a tight complex between the Mad1 and Mad2 proteins. Mol Biol Cell, 10, 2607-2618.

Chial, H.J., Rout, M.P., Giddings, T.H. and Winey, M. (1998) Saccharomyces cerevisiae Ndc1p is a shared component of nuclear pore complexes and spindle pole bodies. J Cell Biol, 143, 1789-1800.

Chook, Y.M. and Blobel, G. (1999) Structure of the nuclear transport complex karyopherin-beta2-Ran x GppNHp. Nature, 399, 230-237.

Cingolani, G., Petosa, C., Weis, K. and Muller, C.W. (1999) Structure of importin-beta bound to the IBB domain of importin-alpha. Nature, 399, 221-229.

Clarke, P.R. and Zhang, C. (2001) Ran GTPase: a master regulator of nuclear structure and function during the eukaryotic cell division cycle? Trends Cell Biol, 11, 366-371.

Clarke, P.R. and Zhang, C. (2004) Spatial and temporal control of nuclear envelope assembly by Ran GTPase. Symp Soc Exp Biol, 193-204.

Cohen, M., Feinstein, N., Wilson, K.L. and Gruenbaum, Y. (2003) Nuclear pore protein gp210 is essential for viability in HeLa cells and Caenorhabditis elegans. Mol Biol Cell, 14, 4230-4237.

Collas, P. (1999) Sequential PKC- and Cdc2-mediated phosphorylation events elicit zebrafish nuclear envelope disassembly. J Cell Sci, 112 (Pt 6), 977-987.

Collas, P. and Courvalin, J.C. (2000) Sorting nuclear membrane proteins at mitosis. Trends Cell Biol, 10, 5-8.

Conti, E., Muller, C.W. and Stewart, M. (2006) Karyopherin flexibility in nucleocytoplasmic transport. Curr Opin Struct Biol, 16, 237-244.

Cotter, L., Allen, T.D., Kiseleva, E. and Goldberg, M.W. (2007) Nuclear membrane disassembly and rupture. J Mol Biol, 369, 683-695.

Courvalin, J.C., Segil, N., Blobel, G. and Worman, H.J. (1992) The lamin B receptor of the inner nuclear membrane undergoes mitosis-specific phosphorylation and is a substrate for p34cdc2-type protein kinase. J Biol Chem, 267, 19035-19038.

Cronshaw, J.M., Krutchinsky, A.N., Zhang, W., Chait, B.T. and Matunis, M.J. (2002) Proteomic analysis of the mammalian nuclear pore complex. J Cell Biol, 158, 915-927.

D'Angelo, M.A., Anderson, D.J., Richard, E. and Hetzer, M.W. (2006) Nuclear pores form de novo from both sides of the nuclear envelope. Science, 312, 440-443.

Daigle, N., Beaudouin, J., Hartnell, L., Imreh, G., Hallberg, E., Lippincott-Schwartz, J. and Ellenberg, J. (2001) Nuclear pore complexes form immobile networks and have a very low turnover in live mammalian cells. J Cell Biol, 154, 71-84.

Dasso, M. (2001) Running on Ran: nuclear transport and the mitotic spindle. Cell, 104, 321-324.

Davis, L.I. and Blobel, G. (1987) Nuclear pore complex contains a family of glycoproteins that includes p62: glycosylation through a previously unidentified cellular pathway. Proc Natl Acad Sci U S A, 84, 7552-7556.

Dechat, T., Vlcek, S. and Foisner, R. (2000) Review: lamina-associated polypeptide 2 isoforms and related proteins in cell cycle-dependent nuclear structure dynamics. J Struct Biol, 129, 335-345.

Demeter, J., Morphew, M. and Sazer, S. (1995) A mutation in the RCC1-related protein pim1 results in nuclear envelope fragmentation in fission yeast. Proc Natl Acad Sci U S A, 92, 1436-1440.

Denning, D.P., Patel, S.S., Uversky, V., Fink, A.L. and Rexach, M. (2003) Disorder in the nuclear pore complex: the FG repeat regions of nucleoporins are natively unfolded. Proc Natl Acad Sci U S A, 100, 2450-2455.

Denning, D.P., Uversky, V., Patel, S.S., Fink, A.L. and Rexach, M. (2002) The Saccharomyces cerevisiae nucleoporin Nup2p is a natively unfolded protein. J Biol Chem, 277, 33447-33455.

Devos, D., Dokudovskaya, S., Alber, F., Williams, R., Chait, B.T., Sali, A. and Rout, M.P. (2004) Components of coated vesicles and nuclear pore complexes share a common molecular architecture. PLoS Biol, 2, e380.

Devos, D., Dokudovskaya, S., Williams, R., Alber, F., Eswar, N., Chait, B.T., Rout, M.P. and Sali, A. (2006) Simple fold composition and modular architecture of the nuclear pore complex. Proc Natl Acad Sci U S A, 103, 2172-2177.

Drummond, S.P. and Wilson, K.L. (2002) Interference with the cytoplasmic tail of gp210 disrupts "close apposition" of nuclear membranes and blocks nuclear pore dilation. J Cell Biol, 158, 53-62.

Dwyer, N. and Blobel, G. (1976) A modified procedure for the isolation of a pore complex-lamina fraction from rat liver nuclei. J Cell Biol, 70, 581-591.

Elbashir, S.M., Harborth, J., Lendeckel, W., Yalcin, A., Weber, K. and Tuschl, T. (2001) Duplexes of 21-nucleotide RNAs mediate RNA interference in cultured mammalian cells. Nature, 411, 494-498.

Ellenberg, J., Siggia, E.D., Moreira, J.E., Smith, C.L., Presley, J.F., Worman, H.J. and Lippincott-Schwartz, J. (1997) Nuclear membrane dynamics and reassembly in living cells: targeting of an inner nuclear membrane protein in interphase and mitosis. J Cell Biol, 138, 1193-1206.

Ellis, J.A., Craxton, M., Yates, J.R. and Kendrick-Jones, J. (1998) Aberrant intracellular targeting and cell cycle-dependent phosphorylation of emerin contribute to the Emery-Dreifuss muscular dystrophy phenotype. J Cell Sci, 111 (Pt 6), 781-792.

Englmeier, L., Olivo, J.C. and Mattaj, I.W. (1999) Receptor-mediated substrate translocation through the nuclear pore complex without nucleotide triphosphate hydrolysis. Curr Biol, 9, 30-41.

Fabre, E. and Hurt, E. (1997) Yeast genetics to dissect the nuclear pore complex and nucleocytoplasmic trafficking. Annu Rev Genet, 31, 277-313.

Fabre, E., Schlaich, N.L. and Hurt, E.C. (1995) Nucleocytoplasmic trafficking: what role for repeated motifs in nucleoporins? Cold Spring Harb Symp Quant Biol, 60, 677-685.

Fahrenkrog, B. (2006) The nuclear pore complex, nuclear transport, and apoptosis. Can J Physiol Pharmacol, 84, 279-286.

Favreau, C., Worman, H.J., Wozniak, R.W., Frappier, T. and Courvalin, J.C. (1996) Cell cycle-dependent phosphorylation of nucleoporins and nuclear pore membrane protein Gp210. Biochemistry, 35, 8035-8044.

Finlay, D.R. and Forbes, D.J. (1990) Reconstitution of biochemically altered nuclear pores: transport can be eliminated and restored. Cell, 60, 17-29.

Finlay, D.R., Meier, E., Bradley, P., Horecka, J. and Forbes, D.J. (1991) A complex of nuclear pore proteins required for pore function. J Cell Biol, 114, 169-183.

Foisner, R. (2001) Inner nuclear membrane proteins and the nuclear lamina. J Cell Sci, 114, 3791-3792.

Foisner, R. and Gerace, L. (1993) Integral membrane proteins of the nuclear envelope interact with lamins and chromosomes, and binding is modulated by mitotic phosphorylation. Cell, 73, 1267-1279.

Fontoura, B.M., Blobel, G. and Matunis, M.J. (1999) A conserved biogenesis pathway for nucleoporins: proteolytic processing of a 186-kilodalton precursor generates Nup98 and the novel nucleoporin, Nup96. J Cell Biol, 144, 1097-1112.

Forbes, D.J., Kirschner, M.W. and Newport, J.W. (1983) Spontaneous formation of nucleus-like structures around bacteriophage DNA microinjected into Xenopus eggs. Cell, 34, 13-23.

Forler, D., Rabut, G., Ciccarelli, F.D., Herold, A., Kocher, T., Niggeweg, R., Bork, P., Ellenberg, J. and Izaurralde, E. (2004) RanBP2/Nup358 provides a major binding site for NXF1-p15 dimers at the nuclear pore complex and functions in nuclear mRNA export. Mol Cell Biol, 24, 1155-1167.

Fornerod, M., van Deursen, J., van Baal, S., Reynolds, A., Davis, D., Murti, K.G., Fransen, J. and Grosveld, G. (1997) The human homologue of yeast CRM1 is in a dynamic subcomplex with CAN/Nup214 and a novel nuclear pore component Nup88. Embo J, 16, 807-816.

Franz, C., Askjaer, P., Antonin, W., Iglesias, C.L., Haselmann, U., Schelder, M., de Marco, A., Wilm, M., Antony, C. and Mattaj, I.W. (2005) Nup155 regulates nuclear envelope and nuclear pore complex formation in nematodes and vertebrates. Embo J, 24, 3519-3531.

Franz, C., Walczak, R., Yavuz, S., Santarella, R., Gentzel, M., Askjaer, P., Galy, V., Hetzer, M., Mattaj, I.W. and Antonin, W. (2007) MEL-28/ELYS is required for the recruitment of nucleoporins to chromatin and postmitotic nuclear pore complex assembly. EMBO Rep, 8, 165-172.

Frey, S. and Gorlich, D. (2007) A saturated FG-repeat hydrogel can reproduce the permeability properties of nuclear pore complexes. Cell, 130, 512-523.

Frey, S., Richter, R.P. and Gorlich, D. (2006) FG-rich repeats of nuclear pore proteins form a three-dimensional meshwork with hydrogel-like properties. Science, 314, 815-817.

Fribourg, S., Braun, I.C., Izaurralde, E. and Conti, E. (2001) Structural basis for the recognition of a nucleoporin FG repeat by the NTF2-like domain of the TAP/p15 mRNA nuclear export factor. Mol Cell, 8, 645-656.

Fried, H. and Kutay, U. (2003) Nucleocytoplasmic transport: taking an inventory. Cell Mol Life Sci, 60, 1659-1688.

Galy, V., Mattaj, I.W. and Askjaer, P. (2003) Caenorhabditis elegans nucleoporins Nup93 and Nup205 determine the limit of nuclear pore complex size exclusion in vivo. Mol Biol Cell, 14, 5104-5115.

Gant, T.M., Goldberg, M.W. and Allen, T.D. (1998) Nuclear envelope and nuclear pore assembly: analysis of assembly intermediates by electron microscopy. Curr Opin Cell Biol, 10, 409-415.

Georgatos, S.D., Pyrpasopoulou, A. and Theodoropoulos, P.A. (1997) Nuclear envelope breakdown in mammalian cells involves stepwise lamina disassembly and microtubule-drive deformation of the nuclear membrane. J Cell Sci, 110 (Pt 17), 2129-2140.

Gerace, L. and Blobel, G. (1980) The nuclear envelope lamina is reversibly depolymerized during mitosis. Cell, 19, 277-287.

Gerace, L., Ottaviano, Y. and Kondor-Koch, C. (1982) Identification of a major polypeptide of the nuclear pore complex. J Cell Biol, 95, 826-837.

Gilchrist, D., Mykytka, B. and Rexach, M. (2002) Accelerating the rate of disassembly of karyopherin.cargo complexes. J Biol Chem, 277, 18161-18172.

Gilchrist, D. and Rexach, M. (2003) Molecular basis for the rapid dissociation of nuclear localization signals from karyopherin alpha in the nucleoplasm. J Biol Chem, 278, 51937-51949.

Glavy, J.S., Krutchinsky, A.N., Cristea, I.M., Berke, I.C., Boehmer, T., Blobel, G. and Chait, B.T. (2007) Cell-cycle-dependent phosphorylation of the nuclear pore Nup107-160 subcomplex. Proc Natl Acad Sci U S A, 104, 3811-3816.

Goldberg, M., Harel, A. and Gruenbaum, Y. (1999) The nuclear lamina: molecular organization and interaction with chromatin. Crit Rev Eukaryot Gene Expr, 9, 285-293.

Goldberg, M.W., Wiese, C., Allen, T.D. and Wilson, K.L. (1997) Dimples, pores, star-rings, and thin rings on growing nuclear envelopes: evidence for structural intermediates in nuclear pore complex assembly. J Cell Sci, 110 (Pt 4), 409-420.

Gonczy, P., Pichler, S., Kirkham, M. and Hyman, A.A. (1999) Cytoplasmic dynein is required for distinct aspects of MTOC positioning, including centrosome separation, in the one cell stage Caenorhabditis elegans embryo. J Cell Biol, 147, 135-150.

Gorlich, D. and Kutay, U. (1999) Transport between the cell nucleus and the cytoplasm. Annu Rev Cell Dev Biol, 15, 607-660.

Grandi, P., Dang, T., Pane, N., Shevchenko, A., Mann, M., Forbes, D. and Hurt, E. (1997) Nup93, a vertebrate homologue of yeast Nic96p, forms a complex with a novel 205-kDa protein and is required for correct nuclear pore assembly. Mol Biol Cell, 8, 2017-2038.

Gruenbaum, Y., Goldman, R.D., Meyuhas, R., Mills, E., Margalit, A., Fridkin, A., Dayani, Y., Prokocimer, M. and Enosh, A. (2003) The nuclear lamina and its functions in the nucleus. Int Rev Cytol, 226, 1-62.

Gruenbaum, Y., Margalit, A., Goldman, R.D., Shumaker, D.K. and Wilson, K.L. (2005) The nuclear lamina comes of age. Nat Rev Mol Cell Biol, 6, 21-31.

Guan, T., Muller, S., Klier, G., Pante, N., Blevitt, J.M., Haner, M., Paschal, B., Aebi, U. and Gerace, L. (1995) Structural analysis of the p62 complex, an assembly of O-linked glycoproteins that localizes near the central gated channel of the nuclear pore complex. Mol Biol Cell, 6, 1591-1603.

Gurdon, J.B. (1976) Injected nuclei in frog oocytes: fate, enlargement, and chromatin dispersal. J Embryol Exp Morphol, 36, 523-540.

Hallberg, E., Wozniak, R.W. and Blobel, G. (1993) An integral membrane protein of the pore membrane domain of the nuclear envelope contains a nucleoporin-like region. J Cell Biol, 122, 513-521.

Handa, N., Kukimoto-Niino, M., Akasaka, R., Kishishita, S., Murayama, K., Terada, T., Inoue, M., Kigawa, T., Kose, S., Imamoto, N., Tanaka, A., Hayashizaki, Y., Shirouzu, M. and Yokoyama, S. (2006) The crystal structure of mouse Nup35 reveals atypical RNP motifs and novel homodimerization of the RRM domain. J Mol Biol, 363, 114-124.

Hanover, J.A., Cohen, C.K., Willingham, M.C. and Park, M.K. (1987) O-linked N-acetylglucosamine is attached to proteins of the nuclear pore. Evidence for cytoplasmic and nucleoplasmic glycoproteins. J Biol Chem, 262, 9887-9894.

Harborth, J., Elbashir, S.M., Bechert, K., Tuschl, T. and Weber, K. (2001) Identification of essential genes in cultured mammalian cells using small interfering RNAs. J Cell Sci, 114, 4557-4565.

Harel, A., Chan, R.C., Lachish-Zalait, A., Zimmerman, E., Elbaum, M. and Forbes, D.J. (2003) Importin beta negatively regulates nuclear membrane fusion and nuclear pore complex assembly. Mol Biol Cell, 14, 4387-4396.

Harel, A., Orjalo, A.V., Vincent, T., Lachish-Zalait, A., Vasu, S., Shah, S., Zimmerman, E., Elbaum, M. and Forbes, D.J. (2003) Removal of a single pore subcomplex results in vertebrate nuclei devoid of nuclear pores. Mol Cell, 11, 853-864.

Hartl, P., Olson, E., Dang, T. and Forbes, D.J. (1994) Nuclear assembly with lambda DNA in fractionated Xenopus egg extracts: an unexpected role for glycogen in formation of a higher order chromatin intermediate. J Cell Biol, 124, 235-248.

Hawryluk-Gara, L.A., Shibuya, E.K. and Wozniak, R.W. (2005) Vertebrate Nup53 interacts with the nuclear lamina and is required for the assembly of a Nup93-containing complex. Mol Biol Cell, 16, 2382-2394.

Hetzer, M., Bilbao-Cortes, D., Walther, T.C., Gruss, O.J. and Mattaj, I.W. (2000) GTP hydrolysis by Ran is required for nuclear envelope assembly. Mol Cell, 5, 1013-1024.

Hetzer, M., Gruss, O.J. and Mattaj, I.W. (2002) The Ran GTPase as a marker of chromosome position in spindle formation and nuclear envelope assembly. Nat Cell Biol, 4, E177-184.

Hetzer, M., Meyer, H.H., Walther, T.C., Bilbao-Cortes, D., Warren, G. and Mattaj, I.W. (2001) Distinct AAA-ATPase p97 complexes function in discrete steps of nuclear assembly. Nat Cell Biol, 3, 1086-1091.

Hetzer, M.W., Walther, T.C. and Mattaj, I.W. (2005) Pushing the envelope: structure, function, and dynamics of the nuclear periphery. Annu Rev Cell Dev Biol, 21, 347-380.

Hinkle, B., Slepchenko, B., Rolls, M.M., Walther, T.C., Stein, P.A., Mehlmann, L.M., Ellenberg, J. and Terasaki, M. (2002) Chromosomal association of Ran during meiotic and mitotic divisions. J Cell Sci, 115, 4685-4693.

Hinshaw, J.E., Carragher, B.O. and Milligan, R.A. (1992) Architecture and design of the nuclear pore complex. Cell, 69, 1133-1141.

Hodel, A.E., Hodel, M.R., Griffis, E.R., Hennig, K.A., Ratner, G.A., Xu, S. and Powers, M.A. (2002) The three-dimensional structure of the autoproteolytic, nuclear pore-targeting domain of the human nucleoporin Nup98. Mol Cell, 10, 347-358.

Holmer, L. and Worman, H.J. (2001) Inner nuclear membrane proteins: functions and targeting. Cell Mol Life Sci, 58, 1741-1747.

Holt, G.D. and Hart, G.W. (1986) The subcellular distribution of terminal N-acetylglucosamine moieties. Localization of a novel protein-saccharide linkage, O-linked GlcNAc. J Biol Chem, 261, 8049-8057.

Holt, G.D., Snow, C.M., Senior, A., Haltiwanger, R.S., Gerace, L. and Hart, G.W. (1987) Nuclear pore complex glycoproteins contain cytoplasmically disposed O-linked N-acetylglucosamine. J Cell Biol, 104, 1157-1164.

Hurwitz, M.E., Strambio-de-Castillia, C. and Blobel, G. (1998) Two yeast nuclear pore complex proteins involved in mRNA export form a cytoplasmically oriented subcomplex. Proc Natl Acad Sci U S A, 95, 11241-11245.

Iouk, T., Kerscher, O., Scott, R.J., Basrai, M.A. and Wozniak, R.W. (2002) The yeast nuclear pore complex functionally interacts with components of the spindle assembly checkpoint. J Cell Biol, 159, 807-819.

Iovine, M.K. and Wente, S.R. (1997) A nuclear export signal in Kap95p is required for both recycling the import factor and interaction with the nucleoporin GLFG repeat regions of Nup116p and Nup100p. J Cell Biol, 137, 797-811.

Isgro, T.A. and Schulten, K. (2005) Binding dynamics of isolated nucleoporin repeat regions to importin-beta. Structure, 13, 1869-1879.

Jarnik, M. and Aebi, U. (1991) Toward a more complete 3-D structure of the nuclear pore complex. J Struct Biol, 107, 291-308.

Joseph, J., Liu, S.T., Jablonski, S.A., Yen, T.J. and Dasso, M. (2004) The RanGAP1-RanBP2 complex is essential for microtubule-kinetochore interactions in vivo. Curr Biol, 14, 611-617.

Joseph, J., Tan, S.H., Karpova, T.S., McNally, J.G. and Dasso, M. (2002) SUMO-1 targets RanGAP1 to kinetochores and mitotic spindles. J Cell Biol, 156, 595-602.

Kalab, P., Weis, K. and Heald, R. (2002) Visualization of a Ran-GTP gradient in interphase and mitotic Xenopus egg extracts. Science, 295, 2452-2456.

Kirchhausen, T. (2000) Three ways to make a vesicle. Nat Rev Mol Cell Biol, 1, 187-198.

Kirchhausen, T. (2000) Clathrin. Annu Rev Biochem, 69, 699-727.

Kiseleva, E., Rutherford, S., Cotter, L.M., Allen, T.D. and Goldberg, M.W. (2001) Steps of nuclear pore complex disassembly and reassembly during mitosis in early Drosophila embryos. J Cell Sci, 114, 3607-3618.

Kondo, H., Rabouille, C., Newman, R., Levine, T.P., Pappin, D., Freemont, P. and Warren, G. (1997) p47 is a cofactor for p97-mediated membrane fusion. Nature, 388, 75-78.

Kose, S., Imamoto, N., Tachibana, T., Shimamoto, T. and Yoneda, Y. (1997) Ran-unassisted nuclear migration of a 97-kD component of nuclear pore-targeting complex. J Cell Biol, 139, 841-849.

Kose, S., Imamoto, N. and Yoneda, Y. (1999) Distinct energy requirement for nuclear import and export of importin beta in living cells. FEBS Lett, 463, 327-330.

Kraemer, D., Wozniak, R.W., Blobel, G. and Radu, A. (1994) The human CAN protein, a putative oncogene product associated with myeloid leukemogenesis, is a nuclear pore complex protein that faces the cytoplasm. Proc Natl Acad Sci U S A, 91, 1519-1523.

Kraemer, D.M., Strambio-de-Castillia, C., Blobel, G. and Rout, M.P. (1995) The essential yeast nucleoporin NUP159 is located on the cytoplasmic side of the nuclear pore complex and serves in karyopherin-mediated binding of transport substrate. J Biol Chem, 270, 19017-19021.

Krull, S., Thyberg, J., Bjorkroth, B., Rackwitz, H.R. and Cordes, V.C. (2004) Nucleoporins as components of the nuclear pore complex core structure and Tpr as the architectural element of the nuclear basket. Mol Biol Cell, 15, 4261-4277.

Lau, C.K., Giddings, T.H., Jr. and Winey, M. (2004) A novel allele of Saccharomyces cerevisiae NDC1 reveals a potential role for the spindle pole body component Ndc1p in nuclear pore assembly. Eukaryot Cell, 3, 447-458.

Lee, M.C., Miller, E.A., Goldberg, J., Orci, L. and Schekman, R. (2004) Bi-directional protein transport between the ER and Golgi. Annu Rev Cell Dev Biol, 20, 87-123.

Lee, S.J., Matsuura, Y., Liu, S.M. and Stewart, M. (2005) Structural basis for nuclear import complex dissociation by RanGTP. Nature, 435, 693-696.

Lim, R.Y., Huang, N.P., Koser, J., Deng, J., Lau, K.H., Schwarz-Herion, K., Fahrenkrog, B. and Aebi, U. (2006) Flexible phenylalanine-glycine nucleoporins as entropic barriers to nucleocytoplasmic transport. Proc Natl Acad Sci U S A, 103, 9512-9517.

Lippincott-Schwartz, J. and Liu, W. (2003) Membrane trafficking: coat control by curvature. Nature, 426, 507-508.

Liu, J., Prunuske, A.J., Fager, A.M. and Ullman, K.S. (2003) The COPI complex functions in nuclear envelope breakdown and is recruited by the nucleoporin Nup153. Dev Cell, 5, 487-498.

Liu, S.M. and Stewart, M. (2005) Structural basis for the high-affinity binding of nucleoporin Nup1p to the Saccharomyces cerevisiae importin-beta homologue, Kap95p. J Mol Biol, 349, 515-525.

Lohka, M.J. and Masui, Y. (1983) Formation in vitro of sperm pronuclei and mitotic chromosomes induced by amphibian ooplasmic components. Science, 220, 719-721.

Loiodice, I., Alves, A., Rabut, G., Van Overbeek, M., Ellenberg, J., Sibarita, J.B. and Doye, V. (2004) The entire Nup107-160 complex, including three new members, is targeted as one entity to kinetochores in mitosis. Mol Biol Cell, 15, 3333-3344.

Lusk, C.P., Makhnevych, T., Marelli, M., Aitchison, J.D. and Wozniak, R.W. (2002) Karyopherins in nuclear pore biogenesis: a role for Kap121p in the assembly of Nup53p into nuclear pore complexes. J Cell Biol, 159, 267-278.

Lusk, C.P., Makhnevych, T. and Wozniak, R.W. (2004) New ways to skin a kap: mechanisms for controlling nuclear transport. Biochem Cell Biol, 82, 618-625.

Lusk, C.P., Waller, D.D., Makhnevych, T., Dienemann, A., Whiteway, M., Thomas, D.Y. and Wozniak, R.W. (2007) Nup53p is a target of two mitotic kinases, Cdk1p and Hrr25p. Traffic, 8, 647-660.

Lutzmann, M., Kunze, R., Stangl, K., Stelter, P., Toth, K.F., Bottcher, B. and Hurt, E. (2005) Reconstitution of Nup157 and Nup145N into the Nup84 complex. J Biol Chem, 280, 18442-18451.

Macara, I.G. (2001) Transport into and out of the nucleus. Microbiol Mol Biol Rev, 65, 570-594, table of contents.

Macaulay, C. and Forbes, D.J. (1996) Assembly of the nuclear pore: biochemically distinct steps revealed with NEM, GTP gamma S, and BAPTA. J Cell Biol, 132, 5-20.

Macaulay, C., Meier, E. and Forbes, D.J. (1995) Differential mitotic phosphorylation of proteins of the nuclear pore complex. J Biol Chem, 270, 254-262.

Madrid, A.S., Mancuso, J., Cande, W.Z. and Weis, K. (2006) The role of the integral membrane nucleoporins Ndc1p and Pom152p in nuclear pore complex assembly and function. J Cell Biol, 173, 361-371.

Mahajan, R., Delphin, C., Guan, T., Gerace, L. and Melchior, F. (1997) A small ubiquitin-related polypeptide involved in targeting RanGAP1 to nuclear pore complex protein RanBP2. Cell, 88, 97-107.

Makhnevych, T., Lusk, C.P., Anderson, A.M., Aitchison, J.D. and Wozniak, R.W. (2003) Cell cycle regulated transport controlled by alterations in the nuclear pore complex. Cell, 115, 813-823.

Makhnevych, T., Ptak, C., Lusk, C.P., Aitchison, J.D. and Wozniak, R.W. (2007) The role of karyopherins in the regulated sumoylation of septins. J Cell Biol, 177, 39-49.

Mansfeld, J., Guttinger, S., Hawryluk-Gara, L.A., Pante, N., Mall, M., Galy, V., Haselmann, U., Muhlhausser, P., Wozniak, R.W., Mattaj, I.W., Kutay, U. and Antonin, W. (2006) The conserved transmembrane nucleoporin NDC1 is required for nuclear pore complex assembly in vertebrate cells. Mol Cell, 22, 93-103.

Marelli, M., Aitchison, J.D. and Wozniak, R.W. (1998) Specific binding of the karyopherin Kap121p to a subunit of the nuclear pore complex containing Nup53p, Nup59p, and Nup170p. J Cell Biol, 143, 1813-1830.

Marelli, M., Lusk, C.P., Chan, H., Aitchison, J.D. and Wozniak, R.W. (2001) A link between the synthesis of nucleoporins and the biogenesis of the nuclear envelope. J Cell Biol, 153, 709-724.

Martin-Lluesma, S., Stucke, V.M. and Nigg, E.A. (2002) Role of Hec1 in spindle checkpoint signaling and kinetochore recruitment of Mad1/Mad2. Science, 297, 2267-2270.

Matsuura, Y. and Stewart, M. (2004) Structural basis for the assembly of a nuclear export complex. Nature, 432, 872-877.

Mattaj, I.W. (2004) Sorting out the nuclear envelope from the endoplasmic reticulum. Nat Rev Mol Cell Biol, 5, 65-69.

Matunis, M.J., Coutavas, E. and Blobel, G. (1996) A novel ubiquitin-like modification modulates the partitioning of the Ran-GTPase-activating protein RanGAP1 between the cytosol and the nuclear pore complex. J Cell Biol, 135, 1457-1470.

Matynia, A., Dimitrov, K., Mueller, U., He, X. and Sazer, S. (1996) Perturbations in the spi1p GTPase cycle of Schizosaccharomyces pombe through its GTPase-activating protein and guanine nucleotide exchange factor components result in similar phenotypic consequences. Mol Cell Biol, 16, 6352-6362.

Maul, G.G., Maul, H.M., Scogna, J.E., Lieberman, M.W., Stein, G.S., Hsu, B.Y. and Borun, T.W. (1972) Time sequence of nuclear pore formation in phytohemagglutinin-stimulated lymphocytes and in HeLa cells during the cell cycle. J Cell Biol, 55, 433-447.

Maul, G.G., Price, J.W. and Lieberman, M.W. (1971) Formation and distribution of nuclear pore complexes in interphase. J Cell Biol, 51, 405-418.

Meyer, H.H., Shorter, J.G., Seemann, J., Pappin, D. and Warren, G. (2000) A complex of mammalian ufd1 and npl4 links the AAA-ATPase, p97, to ubiquitin and nuclear transport pathways. Embo J, 19, 2181-2192.

Miao, M., Ryan, K.J. and Wente, S.R. (2006) The integral membrane protein Pom34p functionally links nucleoporin subcomplexes. Genetics, 172, 1441-1457.

Miyachi, K., Hirano, Y., Horigome, T., Mimori, T., Miyakawa, H., Onozuka, Y., Shibata, M., Hirakata, M., Suwa, A., Hosaka, H., Matsushima, S., Komatsu, T., Matsushima, H., Hankins, R.W. and Fritzler, M.J. (2004) Autoantibodies from primary biliary cirrhosis patients with anti-p95c antibodies bind to recombinant p97/VCP and inhibit in vitro nuclear envelope assembly. Clin Exp Immunol, 136, 568-573.

Moore, W., Zhang, C. and Clarke, P.R. (2002) Targeting of RCC1 to chromosomes is required for proper mitotic spindle assembly in human cells. Curr Biol, 12, 1442-1447.

Nehrbass, U., Rout, M.P., Maguire, S., Blobel, G. and Wozniak, R.W. (1996) The yeast nucleoporin Nup188p interacts genetically and physically with the core structures of the nuclear pore complex. J Cell Biol, 133, 1153-1162.

Nemergut, M.E., Mizzen, C.A., Stukenberg, T., Allis, C.D. and Macara, I.G. (2001) Chromatin docking and exchange activity enhancement of RCC1 by histones H2A and H2B. Science, 292, 1540-1543.

Newport, J. (1987) Nuclear reconstitution in vitro: stages of assembly around protein-free DNA. Cell, 48, 205-217.

Newport, J. and Dunphy, W. (1992) Characterization of the membrane binding and fusion events during nuclear envelope assembly using purified components. J Cell Biol, 116, 295-306.

Newport, J. and Spann, T. (1987) Disassembly of the nucleus in mitotic extracts: membrane vesicularization, lamin disassembly, and chromosome condensation are independent processes. Cell, 48, 219-230.

Newport, J.W. and Forbes, D.J. (1987) The nucleus: structure, function, and dynamics. Annu Rev Biochem, 56, 535-565.

Newport, J.W., Wilson, K.L. and Dunphy, W.G. (1990) A lamin-independent pathway for nuclear envelope assembly. J Cell Biol, 111, 2247-2259.

Nigg, E.A. (1992) Assembly-disassembly of the nuclear lamina. Curr Opin Cell Biol, 4, 105-109.

Nikolakaki, E., Meier, J., Simos, G., Georgatos, S.D. and Giannakouros, T. (1997) Mitotic phosphorylation of the lamin B receptor by a serine/arginine kinase and p34(cdc2). J Biol Chem, 272, 6208-6213.

Ohtsubo, M., Okazaki, H. and Nishimoto, T. (1989) The RCC1 protein, a regulator for the onset of chromosome condensation locates in the nucleus and binds to DNA. J Cell Biol, 109, 1389-1397.

Onischenko, E.A., Gubanova, N.V., Kiseleva, E.V. and Hallberg, E. (2005) Cdk1 and okadaic acid-sensitive phosphatases control assembly of nuclear pore complexes in Drosophila embryos. Mol Biol Cell, 16, 5152-5162.

Orjalo, A.V., Arnaoutov, A., Shen, Z., Boyarchuk, Y., Zeitlin, S.G., Fontoura, B., Briggs, S., Dasso, M. and Forbes, D.J. (2006) The Nup107-160 nucleoporin complex is required for correct bipolar spindle assembly. Mol Biol Cell, 17, 3806-3818.

Panse, V.G., Kuster, B., Gerstberger, T. and Hurt, E. (2003) Unconventional tethering of Ulp1 to the transport channel of the nuclear pore complex by karyopherins. Nat Cell Biol, 5, 21-27.

Pante, N., Bastos, R., McMorrow, I., Burke, B. and Aebi, U. (1994) Interactions and three-dimensional localization of a group of nuclear pore complex proteins. J Cell Biol, 126, 603-617.

Park, M.K., D'Onofrio, M., Willingham, M.C. and Hanover, J.A. (1987) A monoclonal antibody against a family of nuclear pore proteins (nucleoporins): O-linked N-acetylglucosamine is part of the immunodeterminant. Proc Natl Acad Sci U S A, 84, 6462-6466.

Patel, S. and Latterich, M. (1998) The AAA team: related ATPases with diverse functions. Trends Cell Biol, 8, 65-71.

Patel, S.S., Belmont, B.J., Sante, J.M. and Rexach, M.F. (2007) Natively unfolded nucleoporins gate protein diffusion across the nuclear pore complex. Cell, 129, 83-96.

Paweletz, N. and Lang, U. (1988) Fine structural studies of early mitotic stages in untreated and nocodazole-treated HeLa cells. Eur J Cell Biol, 47, 334-345.

Petosa, C., Schoehn, G., Askjaer, P., Bauer, U., Moulin, M., Steuerwald, U., Soler-Lopez, M., Baudin, F., Mattaj, I.W. and Muller, C.W. (2004) Architecture of CRM1/Exportin1 suggests how cooperativity is achieved during formation of a nuclear export complex. Mol Cell, 16, 761-775.

Philpott, A. and Leno, G.H. (1992) Nucleoplasmin remodels sperm chromatin in Xenopus egg extracts. Cell, 69, 759-767.

Pichler, A., Gast, A., Seeler, J.S., Dejean, A. and Melchior, F. (2002) The nucleoporin RanBP2 has SUMO1 E3 ligase activity. Cell, 108, 109-120.

Pichler, A. and Melchior, F. (2002) Ubiquitin-related modifier SUMO1 and nucleocytoplasmic transport. Traffic, 3, 381-387.

Powell, L. and Burke, B. (1990) Internuclear exchange of an inner nuclear membrane protein (p55) in heterokaryons: in vivo evidence for the interaction of p55 with the nuclear lamina. J Cell Biol, 111, 2225-2234.

Powers, M.A., Macaulay, C., Masiarz, F.R. and Forbes, D.J. (1995) Reconstituted nuclei depleted of a vertebrate GLFG nuclear pore protein, p97, import but are defective in nuclear growth and replication. J Cell Biol, 128, 721-736.

Prunuske, A.J. and Ullman, K.S. (2006) The nuclear envelope: form and reformation. Curr Opin Cell Biol, 18, 108-116.

Pyhtila, B. and Rexach, M. (2003) A gradient of affinity for the karyopherin Kap95p along the yeast nuclear pore complex. J Biol Chem, 278, 42699-42709.

Quintyne, N.J., Gill, S.R., Eckley, D.M., Crego, C.L., Compton, D.A. and Schroer, T.A. (1999) Dynactin is required for microtubule anchoring at centrosomes. J Cell Biol, 147, 321-334.

Rabouille, C., Kondo, H., Newman, R., Hui, N., Freemont, P. and Warren, G. (1998) Syntaxin 5 is a common component of the NSF- and p97-mediated reassembly pathways of Golgi cisternae from mitotic Golgi fragments in vitro. Cell, 92, 603-610.

Rabut, G., Doye, V. and Ellenberg, J. (2004) Mapping the dynamic organization of the nuclear pore complex inside single living cells. Nat Cell Biol, 6, 1114-1121.

Rabut, G., Lenart, P. and Ellenberg, J. (2004) Dynamics of nuclear pore complex organization through the cell cycle. Curr Opin Cell Biol, 16, 314-321.

Radu, A., Blobel, G. and Wozniak, R.W. (1993) Nup155 is a novel nuclear pore complex protein that contains neither repetitive sequence motifs nor reacts with WGA. J Cell Biol, 121, 1-9.

Radu, A., Blobel, G. and Wozniak, R.W. (1994) Nup107 is a novel nuclear pore complex protein that contains a leucine zipper. J Biol Chem, 269, 17600-17605.

Reichelt, R., Holzenburg, A., Buhle, E.L., Jr., Jarnik, M., Engel, A. and Aebi, U. (1990) Correlation between structure and mass distribution of the nuclear pore complex and of distinct pore complex components. J Cell Biol, 110, 883-894.

Reinsch, S. and Karsenti, E. (1997) Movement of nuclei along microtubules in Xenopus egg extracts. Curr Biol, 7, 211-214.

Ribbeck, K. and Gorlich, D. (2001) Kinetic analysis of translocation through nuclear pore complexes. Embo J, 20, 1320-1330.

Ribbeck, K. and Gorlich, D. (2002) The permeability barrier of nuclear pore complexes appears to operate via hydrophobic exclusion. Embo J, 21, 2664-2671.

Robbins, E. and Gonatas, N.K. (1964) The Ultrastructure of a Mammalian Cell During the Mitotic Cycle. J Cell Biol, 21, 429-463.

Robinson, J.T., Wojcik, E.J., Sanders, M.A., McGrail, M. and Hays, T.S. (1999) Cytoplasmic dynein is required for the nuclear attachment and migration of centrosomes during mitosis in Drosophila. J Cell Biol, 146, 597-608.

Robinson, M.A., Park, S., Sun, Z.Y., Silver, P.A., Wagner, G. and Hogle, J.M. (2005) Multiple conformations in the ligand-binding site of the yeast nuclear pore-targeting domain of Nup116p. J Biol Chem, 280, 35723-35732.

Roos, U.P. (1973) Light and electron microscopy of rat kangaroo cells in mitosis. II. Kinetochore structure and function. Chromosoma, 41, 195-220.

Rout, M.P., Aitchison, J.D., Magnasco, M.O. and Chait, B.T. (2003) Virtual gating and nuclear transport: the hole picture. Trends Cell Biol, 13, 622-628.

Rout, M.P., Aitchison, J.D., Suprapto, A., Hjertaas, K., Zhao, Y. and Chait, B.T. (2000) The yeast nuclear pore complex: composition, architecture, and transport mechanism. J Cell Biol, 148, 635-651.

Rout, M.P. and Blobel, G. (1993) Isolation of the yeast nuclear pore complex. J Cell Biol, 123, 771-783.

Roy, L., Bergeron, J.J., Lavoie, C., Hendriks, R., Gushue, J., Fazel, A., Pelletier, A., Morre, D.J., Subramaniam, V.N., Hong, W. and Paiement, J. (2000) Role of p97 and syntaxin 5 in the assembly of transitional endoplasmic reticulum. Mol Biol Cell, 11, 2529-2542.

Ryan, K.J., McCaffery, J.M. and Wente, S.R. (2003) The Ran GTPase cycle is required for yeast nuclear pore complex assembly. J Cell Biol, 160, 1041-1053.

Saitoh, H., Pu, R., Cavenagh, M. and Dasso, M. (1997) RanBP2 associates with Ubc9p and a modified form of RanGAP1. Proc Natl Acad Sci U S A, 94, 3736-3741.

Salina, D., Bodoor, K., Eckley, D.M., Schroer, T.A., Rattner, J.B. and Burke, B. (2002) Cytoplasmic dynein as a facilitator of nuclear envelope breakdown. Cell, 108, 97-107.

Salina, D., Bodoor, K., Enarson, P., Raharjo, W.H. and Burke, B. (2001) Nuclear envelope dynamics. Biochem Cell Biol, 79, 533-542.

Salina, D., Enarson, P., Rattner, J.B. and Burke, B. (2003) Nup358 integrates nuclear envelope breakdown with kinetochore assembly. J Cell Biol, 162, 991-1001.

Sasagawa, S., Yamamoto, A., Ichimura, T., Omata, S. and Horigome, T. (1999) In vitro nuclear assembly with affinity-purified nuclear envelope precursor vesicle fractions, PV1 and PV2. Eur J Cell Biol, 78, 593-600.

Schindler, M., Hogan, M., Miller, R. and DeGaetano, D. (1987) A nuclear specific glycoprotein representative of a unique pattern of glycosylation. J Biol Chem, 262, 1254-1260.

Schwartz, T.U. (2005) Modularity within the architecture of the nuclear pore complex. Curr Opin Struct Biol, 15, 221-226.

Schwoebel, E.D., Ho, T.H. and Moore, M.S. (2002) The mechanism of inhibition of Ran-dependent nuclear transport by cellular ATP depletion. J Cell Biol, 157, 963-974.

Schwoebel, E.D., Talcott, B., Cushman, I. and Moore, M.S. (1998) Ran-dependent signal-mediated nuclear import does not require GTP hydrolysis by Ran. J Biol Chem, 273, 35170-35175.

Scott, R.J., Lusk, C.P., Dilworth, D.J., Aitchison, J.D. and Wozniak, R.W. (2005) Interactions between Mad1p and the nuclear transport machinery in the yeast Saccharomyces cerevisiae. Mol Biol Cell, 16, 4362-4374.

Smythe, C., Jenkins, H.E. and Hutchison, C.J. (2000) Incorporation of the nuclear pore basket protein nup153 into nuclear pore structures is dependent upon lamina assembly: evidence from cell-free extracts of Xenopus eggs. Embo J, 19, 3918-3931.

Smythe, C. and Newport, J.W. (1991) Systems for the study of nuclear assembly, DNA replication, and nuclear breakdown in Xenopus laevis egg extracts. Methods Cell Biol, 35, 449-468.

Stavru, F., Hulsmann, B.B., Spang, A., Hartmann, E., Cordes, V.C. and Gorlich, D. (2006) NDC1: a crucial membrane-integral nucleoporin of metazoan nuclear pore complexes. J Cell Biol, 173, 509-519.

Stavru, F., Nautrup-Pedersen, G., Cordes, V.C. and Gorlich, D. (2006) Nuclear pore complex assembly and maintenance in POM121- and gp210-deficient cells. J Cell Biol, 173, 477-483.

Stick, R., Angres, B., Lehner, C.F. and Nigg, E.A. (1988) The fates of chicken nuclear lamin proteins during mitosis: evidence for a reversible redistribution of lamin B2 between inner nuclear membrane and elements of the endoplasmic reticulum. J Cell Biol, 107, 397-406.

Stoffler, D., Fahrenkrog, B. and Aebi, U. (1999) The nuclear pore complex: from molecular architecture to functional dynamics. Curr Opin Cell Biol, 11, 391-401.

Stoffler, D., Feja, B., Fahrenkrog, B., Walz, J., Typke, D. and Aebi, U. (2003) Cryo-electron tomography provides novel insights into nuclear pore architecture: implications for nucleocytoplasmic transport. J Mol Biol, 328, 119-130.

Strambio-de-Castillia, C., Blobel, G. and Rout, M.P. (1999) Proteins connecting the nuclear pore complex with the nuclear interior. J Cell Biol, 144, 839-855.

Strawn, L.A., Shen, T., Shulga, N., Goldfarb, D.S. and Wente, S.R. (2004) Minimal nuclear pore complexes define FG repeat domains essential for transport. Nat Cell Biol, 6, 197-206.

Strom, A.C. and Weis, K. (2001) Importin-beta-like nuclear transport receptors. Genome Biol, 2, REVIEWS3008.

Stukenberg, P.T., Lustig, K.D., McGarry, T.J., King, R.W., Kuang, J. and Kirschner, M.W. (1997) Systematic identification of mitotic phosphoproteins. Curr Biol, 7, 338-348.

Sukegawa, J. and Blobel, G. (1993) A nuclear pore complex protein that contains zinc finger motifs, binds DNA, and faces the nucleoplasm. Cell, 72, 29-38.

Suntharalingam, M. and Wente, S.R. (2003) Peering through the pore: nuclear pore complex structure, assembly, and function. Dev Cell, 4, 775-789.

Tran, E.J. and Wente, S.R. (2006) Dynamic nuclear pore complexes: life on the edge. Cell, 125, 1041-1053.

Ulbert, S., Antonin, W., Platani, M. and Mattaj, I.W. (2006) The inner nuclear membrane protein Lem2 is critical for normal nuclear envelope morphology. FEBS Lett, 580, 6435-6441.

Ulbert, S., Platani, M., Boue, S. and Mattaj, I.W. (2006) Direct membrane protein-DNA interactions required early in nuclear envelope assembly. J Cell Biol, 173, 469-476.

Vassileva, M.T. and Matunis, M.J. (2004) SUMO modification of heterogeneous nuclear ribonucleoproteins. Mol Cell Biol, 24, 3623-3632.

Vasu, S.K. and Forbes, D.J. (2001) Nuclear pores and nuclear assembly. Curr Opin Cell Biol, 13, 363-375.

Vetter, I.R., Arndt, A., Kutay, U., Gorlich, D. and Wittinghofer, A. (1999) Structural view of the Ran-Importin beta interaction at 2.3 A resolution. Cell, 97, 635-646.

Vigers, G.P. and Lohka, M.J. (1991) A distinct vesicle population targets membranes and pore complexes to the nuclear envelope in Xenopus eggs. J Cell Biol, 112, 545-556.

Walther, T.C., Alves, A., Pickersgill, H., Loiodice, I., Hetzer, M., Galy, V., Hulsmann, B.B., Kocher, T., Wilm, M., Allen, T., Mattaj, I.W. and Doye, V. (2003) The conserved Nup107-160 complex is critical for nuclear pore complex assembly. Cell, 113, 195-206.

Walther, T.C., Askjaer, P., Gentzel, M., Habermann, A., Griffiths, G., Wilm, M., Mattaj, I.W. and Hetzer, M. (2003) RanGTP mediates nuclear pore complex assembly. Nature, 424, 689-694.

Walther, T.C., Fornerod, M., Pickersgill, H., Goldberg, M., Allen, T.D. and Mattaj, I.W. (2001) The nucleoporin Nup153 is required for nuclear pore basket formation, nuclear pore complex anchoring and import of a subset of nuclear proteins. Embo J, 20, 5703-5714.

Walther, T.C., Pickersgill, H.S., Cordes, V.C., Goldberg, M.W., Allen, T.D., Mattaj, I.W. and Fornerod, M. (2002) The cytoplasmic filaments of the nuclear pore complex are dispensable for selective nuclear protein import. J Cell Biol, 158, 63-77.

Weirich, C.S., Erzberger, J.P., Berger, J.M. and Weis, K. (2004) The N-terminal domain of Nup159 forms a beta-propeller that functions in mRNA export by tethering the helicase Dbp5 to the nuclear pore. Mol Cell, 16, 749-760.

Weis, K. (2003) Regulating access to the genome: nucleocytoplasmic transport throughout the cell cycle. Cell, 112, 441-451.

Weis, K. (2007) The nuclear pore complex: oily spaghetti or gummy bear? Cell, 130, 405-407.

Wente, S.R. and Blobel, G. (1993) A temperature-sensitive NUP116 null mutant forms a nuclear envelope seal over the yeast nuclear pore complex thereby blocking nucleocytoplasmic traffic. J Cell Biol, 123, 275-284.

Wente, S.R. and Blobel, G. (1994) NUP145 encodes a novel yeast glycine-leucine-phenylalanine-glycine (GLFG) nucleoporin required for nuclear envelope structure. J Cell Biol, 125, 955-969.

Wente, S.R., Rout, M.P. and Blobel, G. (1992) A new family of yeast nuclear pore complex proteins. J Cell Biol, 119, 705-723.

Wilson, K.L. and Newport, J. (1988) A trypsin-sensitive receptor on membrane vesicles is required for nuclear envelope formation in vitro. J Cell Biol, 107, 57-68.

Winey, M., Hoyt, M.A., Chan, C., Goetsch, L., Botstein, D. and Byers, B. (1993) NDC1: a nuclear periphery component required for yeast spindle pole body duplication. J Cell Biol, 122, 743-751.

Worman, H.J. and Courvalin, J.C. (2000) The inner nuclear membrane. J Membr Biol, 177, 1-11.

Worman, H.J. and Courvalin, J.C. (2005) Nuclear envelope, nuclear lamina, and inherited disease. Int Rev Cytol, 246, 231-279.

Wozniak, R.W., Bartnik, E. and Blobel, G. (1989) Primary structure analysis of an integral membrane glycoprotein of the nuclear pore. J Cell Biol, 108, 2083-2092.

Wozniak, R.W. and Blobel, G. (1992) The single transmembrane segment of gp210 is sufficient for sorting to the pore membrane domain of the nuclear envelope. J Cell Biol, 119, 1441-1449.

Wozniak, R.W., Blobel, G. and Rout, M.P. (1994) POM152 is an integral protein of the pore membrane domain of the yeast nuclear envelope. J Cell Biol, 125, 31-42.

Wozniak, R.W. and Lusk, C.P. (2003) Nuclear pore complexes. Curr Biol, 13, R169.

Wozniak, R.W., Rout, M.P. and Aitchison, J.D. (1998) Karyopherins and kissing cousins. Trends Cell Biol, 8, 184-188.

Wu, J., Matunis, M.J., Kraemer, D., Blobel, G. and Coutavas, E. (1995) Nup358, a cytoplasmically exposed nucleoporin with peptide repeats, Ran-GTP binding sites, zinc fingers, a cyclophilin A homologous domain, and a leucine-rich region. J Biol Chem, 270, 14209-14213.

Yang, L., Guan, T. and Gerace, L. (1997) Integral membrane proteins of the nuclear envelope are dispersed throughout the endoplasmic reticulum during mitosis. J Cell Biol, 137, 1199-1210.

Yang, Q., Rout, M.P. and Akey, C.W. (1998) Three-dimensional architecture of the isolated yeast nuclear pore complex: functional and evolutionary implications. Mol Cell, 1, 223-234.

Ye, Q., Callebaut, I., Pezhman, A., Courvalin, J.C. and Worman, H.J. (1997) Domain-specific interactions of human HP1-type chromodomain proteins and inner nuclear membrane protein LBR. J Biol Chem, 272, 14983-14989.

Yoshida, K. and Blobel, G. (2001) The karyopherin Kap142p/Msn5p mediates nuclear import and nuclear export of different cargo proteins. J Cell Biol, 152, 729-740.

Zeitler, B. and Weis, K. (2004) The FG-repeat asymmetry of the nuclear pore complex is dispensable for bulk nucleocytoplasmic transport in vivo. J Cell Biol, 167, 583-590.

Zeligs, J.D. and Wollman, S.H. (1979) Mitosis in rat thyroid epithelial cells in vivo. I. Ultrastructural changes in cytoplasmic organelles during the mitotic cycle. J Ultrastruct Res, 66, 53-77.

Zhang, C. and Clarke, P.R. (2000) Chromatin-independent nuclear envelope assembly induced by Ran GTPase in Xenopus egg extracts. Science, 288, 1429-1432.

Zhang, C. and Clarke, P.R. (2001) Roles of Ran-GTP and Ran-GDP in precursor vesicle recruitment and fusion during nuclear envelope assembly in a human cell-free system. Curr Biol, 11, 208-212.

Zhang, C., Goldberg, M.W., Moore, W.J., Allen, T.D. and Clarke, P.R. (2002) Concentration of Ran on chromatin induces decondensation, nuclear envelope formation and nuclear pore complex assembly. Eur J Cell Biol, 81, 623-633.

Zhang, C., Hughes, M. and Clarke, P.R. (1999) Ran-GTP stabilises microtubule asters and inhibits nuclear assembly in Xenopus egg extracts. J Cell Sci, 112 (Pt 14), 2453-2461.

Zhang, C., Hutchins, J.R., Muhlhausser, P., Kutay, U. and Clarke, P.R. (2002) Role of importin-beta in the control of nuclear envelope assembly by Ran. Curr Biol, 12, 498-502.

Zhang, H., Saitoh, H. and Matunis, M.J. (2002) Enzymes of the SUMO modification pathway localize to filaments of the nuclear pore complex. Mol Cell Biol, 22, 6498-6508.

Zuccolo, M., Alves, A., Galy, V., Bolhy, S., Formstecher, E., Racine, V., Sibarita, J.B., Fukagawa, T., Shiekhattar, R., Yen, T. and Doye, V. (2007) The human Nup107-160 nuclear pore subcomplex contributes to proper kinetochore functions. Embo J, 26, 1853-1864.

Chapter VII: *Appendix*

This Appendix contains a number of experiments that are either unpublished or in the process of being assembled for publication. While they do not directly fit with the continuity of the results sections of the previous chapters, they will be a resource for future members of the laboratory involved with this project and aid in the discussion presented in Chapter VI.

Figure 7-1. Phosphorylation of vertebrate Nup53.
(A) Vertebrate Nup53 is phosphorylated in mitosis. Lysates from either asynchronous or nocodazole arrested HeLa cells were treated with phosphatase. The phosphorylation state of endogenous Nup53 was monitored by Western blot with Nup53 antibodies. (B) Phosphorylated Nup53 is localized in the cytoplasm. The localization of endogenous Nup53 in an M-phase cell of an asynchronous population was analyzed by immunofluorescence with Nup53 antibodies and confocal microscopy. (C) Phosphorylated and unphosphorylated Nup53 are enriched in cytoplasmic and membrane fractions, respectively. Cytosol and membrane fractions of nocodazole arrested HeLa cells that were lysed in either the presence or absence of phosphatase inhibitors were separated by SDS-PAGE and the phosphorylation state of endogenous Nup53 was monitored as in (A). (D) GFP-Nup53 is not phosphoryated to the same extent as endogenous Nup53. HeLa cells that were stably expressing GFP-Nup53 were arrested in nocodazole and the ability of this fusion to be phoshphorylated was determined using antibodies directed against GFP. (E) GFP-Nup53 is partially localized to the ER. The localization of GFP-Nup53 was analyzed by confocal microscopy in live, nocodazole arrested HeLa cells that were co-stained with either DAPI (blue), or ER-tracker (red).

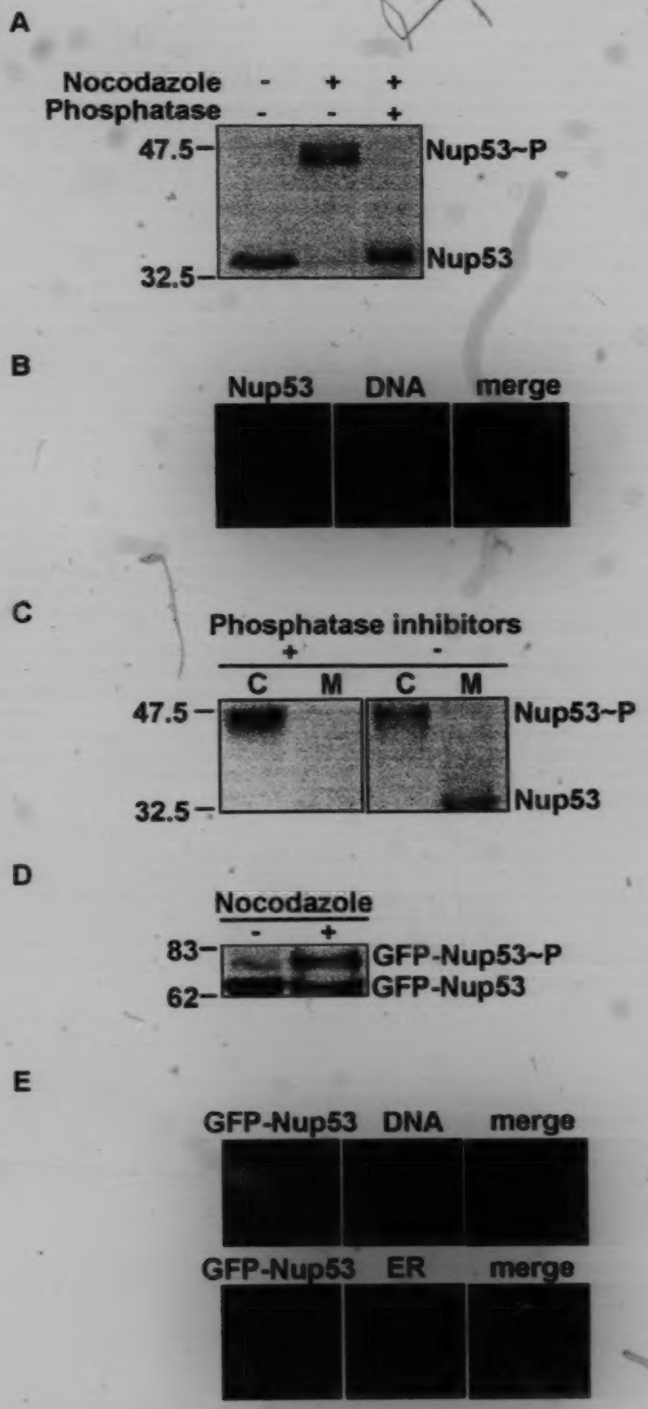
A
Nocodazole - + +
Phosphatase - - +
47.5
32.5
Nup53~P
Nup53
B
Nup53
DNA
merge
C
Phosphatase inhibitors
+
-
C
M
C
M
47.5
32.5
Nup53~P
Nup53
D
Nocodazole
-
+
83
62
GFP-Nup53~P
GFP-Nup53
E
GFP-Nup53
DNA
merge
GFP-Nup53
ER
merge

Figure 7-1. The phosphorylation of human Nup53

Figure 7-2. Nup53 interacts with ss- and dsDNA.
(A) Purified recombinant Nup53, Nup53$^{1\text{-}143}$, Nup53$^{167\text{-}252}$, Nup53$^{1\text{-}143}$, and Nup53$^{204\text{-}326,}$ along with Nup93 were incubated with 20 µg of ssDNA crosslinked to cellulose. Following binding and washing, bound (B) proteins were eluted off the column by boiling in SDS-PAGE sample buffer, separated by SDS-PAGE, detected with Coomassie Blue staining, and compared to load (L) and unbound (UB) fractions. (B)/(C) Mapping of Nup53 RRM residues critical for ssDNA and dsDNA binding. Purified recombinant Nup53 RRM point mutants were incubated with 20 µg of ss- or dsDNA crosslinked to cellulose. Following extensive washing, the column bound protein was eluted by boiling in SDS-PAGE sample buffer, separated by SDS-PAGE and detected by Coomassie Blue staining. Point mutations positioned on the α-helical interface (Nup53^{S187Q} and Nup53^{K223Q}) do not affect Nup53 binding to nucleic acid. Conversely, a double mutation of two residues on the β-sheet interfaces (Nup53$^{F179A/W210A}$) results in a reduction of Nup53 nucleic acid binding.

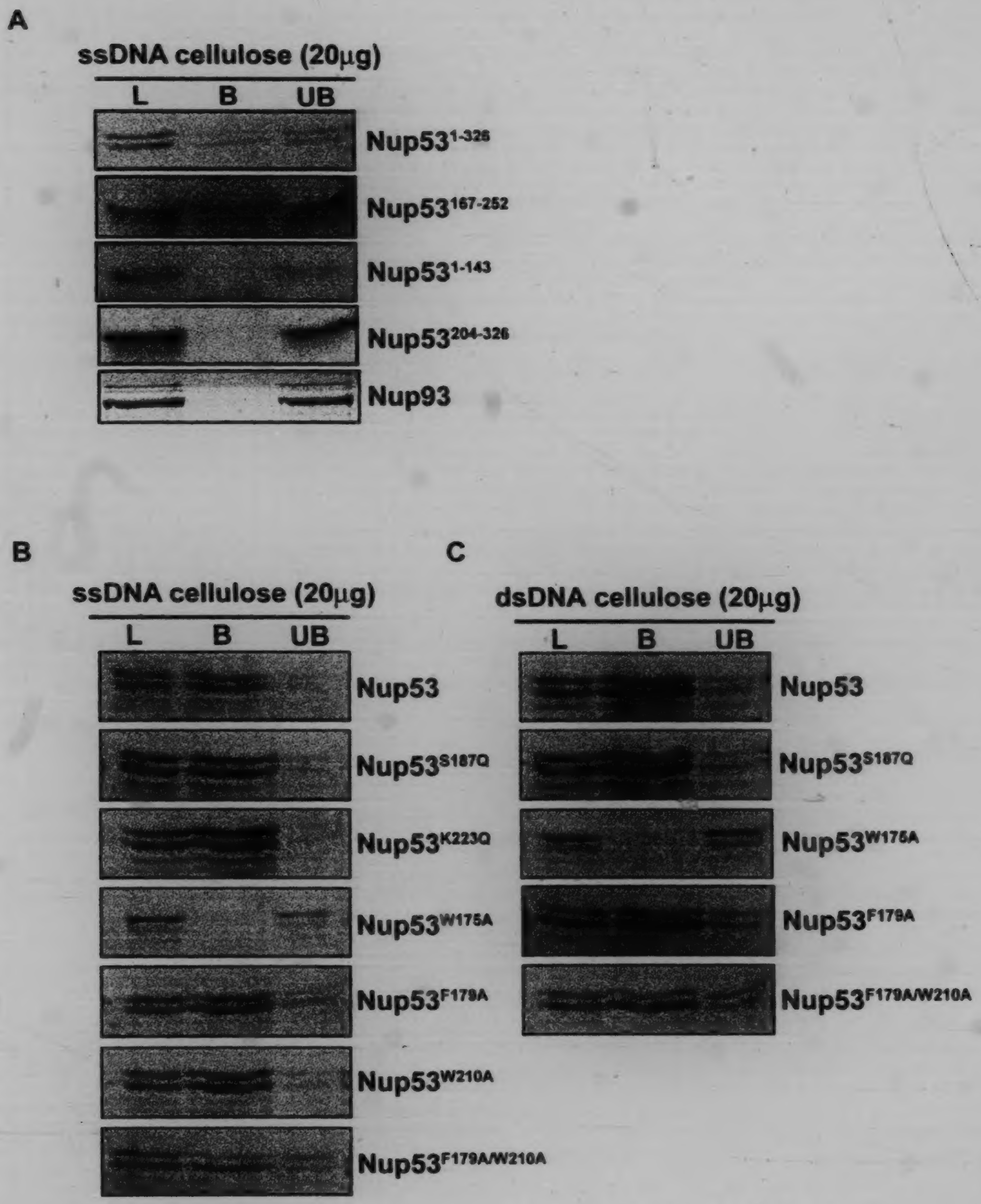
A
ssDNA cellulose (20μg)
L
B
UB
Nup53$^{1-326}$
Nup53$^{167-252}$
Nup53$^{1-143}$
Nup53$^{204-326}$
Nup93
B
ssDNA cellulose (20μg)
L
B
UB
Nup53
Nup53^{S187Q}
Nup53^{K223Q}
Nup53^{W175A}
Nup53^{F179A}
Nup53^{W210A}
Nup53$^{F179A/W210A}$
C
dsDNA cellulose (20μg)
L
B
UB
Nup53
Nup53^{S187Q}
Nup53^{W175A}
Nup53^{F179A}
Nup53$^{F179A/W210A}$

Figure 7-2. Nup53 interacts with ss- and dsDNA.

Figure 7-3. Characterization of the Nup53 RRM.
(A) The Nup53 RRM does not interact with either Nup155 or Nup93. Purified recombinant Nup53 RRM containing fragments (GST-Nup53$^{167-252}$ and GST-Nup53$^{144-265)}$ were immobilized on glutathione Sepharose beads. Identical GST-pulldown assays to those presented in Fig. 3-3, 4-1, and 4-3 were performed. SS-silver stain, WB-Western blot. Positions of mass markers in kilodaltons are indicated. (B) The Nup53 RRM does not appear to have a dominant negative effect on NE formation. Mock depletions identical to those presented in Fig. 4-5, 4-6, 4-7, 4-8, 4-9, and 4-10 were performed here with the exception that Nup53$^{144-265}$ was added in excess (bottom panel).

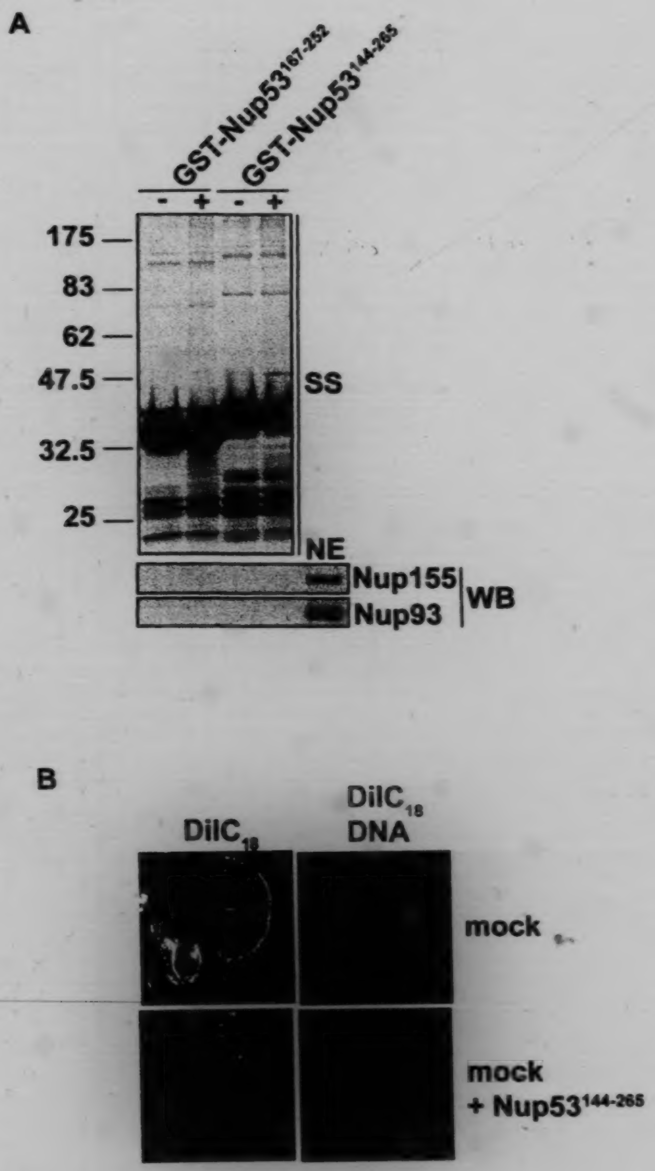
A
GST-Nup53167-252
GST-Nup53144-265
-
+
-
+
175
83
62
47.5
32.5
25
SS
NE
Nup155
Nup93
WB
B
DiIC18
DiIC18
DNA
mock
mock
+ Nup53144-265

Figure 7-3. Characterization of the Nup53 RRM.